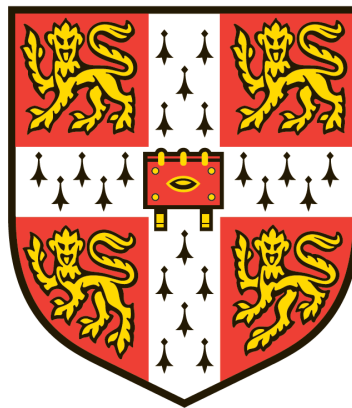


# Characterisation of new regulators and neural plasticity of the O<sub>2</sub>-sensing circuit in *Caenorhabditis elegans*



This dissertation is submitted for the degree of  
*Doctor of Philosophy* in Biological Science

**Giulio Valperga**

Trinity Hall  
University of Cambridge

Cell Biology Division  
MRC Laboratory of Molecular Biology

March 2019



*"Rain pourin' down, I swing my hammer  
My hands are rough from working on a dream,  
From working on a dream"*

Bruce Springsteen, *Working on a Dream*, 2009

*To my family, old and new.*



## **Declaration**

This dissertation is the result of my own work and includes nothing which is the outcome of work done in collaboration except as declared in the Statement of Contribution. All the work described in this dissertation was carried out in the Cell Biology Division of the Medical Research Council Laboratory of Molecular Biology, under the supervision of Dr. Mario de Bono. It is not substantially the same as any that I have submitted, or, is being concurrently submitted for a degree or diploma or other qualification at the University of Cambridge or any other University or similar institution. I further state that no substantial part of my dissertation has already been submitted, or, is being concurrently submitted for any such degree, diploma or other qualification at the University of Cambridge or any other University or similar institution. It does not exceed 60,000 words, excluding figures, tables, appendices and bibliography, as specified by the Degree Committee.



## Statement of contribution

Due to the collaborative nature of this project some of the experiments carried out for this thesis have been done in collaboration with other people who are listed below. Above all other contributors, the work presented in this thesis is the result of a collaboration with my supervisor **Mario de Bono** who help me design and perform the initial experiments, discussed results and provided helpful insights into the biological consequences of my work. Chapter 5 is the result of a shared collaboration with **Isabel Beets**. We designed and performed the experiments together as well as discussing the results.

**Chapter 3:** The genetic screens on N2 reference strain and *flp-21* were performed by previous member of the de Bono Lab **Gemma Brown** and **Merav Cohen** up to the isolation of aggregating mutant strains. **Mario de Bono** helped and performed some of the crosses for 3-point mapping of aggregating mutants. **Paula Freire-Pritchett** and **Tim Stevens** developed the pipeline to analyse whole-genome sequencing data.

**Chapter 4:** **Tim Steven** developed the algorithms and performed the analysis to build the phylogenetic tree for QUI-1 and identify its homologues in other species. **José David Moniño Sánchez** performed some of the experiments for the characterisation of ADL increased neurosecretion.

**Chapter 5:** O<sub>2</sub>-sensing neurons isolation as well as library preparation were performed in collaboration with **Isabel Beets**. **Paula Freire-Pritchett** and **Alastair Crisp** developed the pipelines used to analyse RNA-sequencing data.



## Abstract

Oxygen is the main sensory stimulus that promotes aggregation and elicits O<sub>2</sub>-escape behaviour in *C. elegans*. It also constitutes a salient cue for this nematode that reprograms its behavioural strategies as well as physiology after prolonged oxygen experience. However, it is not known how other sensory modalities affect O<sub>2</sub>-escape behaviour. Moreover, the molecular details of how oxygen alters *C. elegans* behavioural preferences are elusive. Wild isolates of *C. elegans* aggregate and avoid oxygen at high concentrations, whereas both behaviours are suppressed in the N2 reference strain by a gain of function mutation in the neuropeptide receptor 1 (*npr-1*). This mutation, among other things, sculpts the flow of information in the O<sub>2</sub>-circuit and prevents O<sub>2</sub>-evoked Ca<sup>2+</sup> responses in the sensory neuron ADL. Here, we perform a forward genetic screen to isolate mutants that confer O<sub>2</sub>-escape behaviour on N2 animals. Using whole-genome sequencing and genetic mapping, we identify several conserved genes not previously shown to regulate aggregation. Among these, we characterise mutants that do not show defects in O<sub>2</sub>-evoked Ca<sup>2+</sup> responses in URX and RMG, but show increased secretion of dense-core vesicles from ADL, which could be rescued cell specifically for at least one mutant. Furthermore, we demonstrate that this increased neurosecretion is likely to result from sensitisation of ADL neurons to incoming activity from the O<sub>2</sub>-circuit. In fact, while N2 does not modulate ADL neurosecretion according to ambient oxygen levels, mutants with enhanced ADL neurosecretion acquire this feature. These mutants also display defects for other sensory modalities, including pheromone-evoked Ca<sup>2+</sup> responses in ADL. These data provide a link between defective sensory perception and O<sub>2</sub>-escape behaviour. Reminiscent of how sensory deprivation induces homeostatic plasticity, we propose that, in sensory defective mutants, similar mechanisms might sensitise ADL to incoming activity from the O<sub>2</sub>-circuit and promote O<sub>2</sub>-escape behaviour. Moreover, we also investigate the extent to which prolonged oxygen exposure reprograms the O<sub>2</sub>-circuit. These results shed light on how changes in one sensory modality reprograms responses to other sensory modalities.



## Acknowledgments

The work described in this thesis has been for me transformative. Although, it has been painful at times and came with a high dose of uncertainty that I did not foresee, I enjoyed every minute of it. This has been possible thanks to a number of people.

I am grateful to my supervisor Mario de Bono to show me the ins and outs of *C. elegans* research, to show me what a powerful tool genetics is and for interesting insights into how to do science. Even more, its joyous and carefree approach to everyday science has been an inspiration for me.

I realised early on during my PhD, that I was not capable of coming up with a valid idea unless I discussed it with someone. For this reason I am very grateful to Lorenz Fenk and Isabel Beets for extremely interesting scientific discussions.

I am also extremely lucky to work in the nice environment that is the de Bono Lab and I am grateful to present and past member of the lab for that. Especially I would like to thank Sean Flynn and Isabel Beets for useful comments on this thesis.

I would like to thank the MRC for generous funding and the MRC Laboratory of Molecular Biology and especially the Cell Biology Division for providing people with the tools to do great science.

I would not have enjoyed my PhD half as much without Stefano Giandomenico, Patrick Hofmann, Lorenz Fenk and Changchun Chen. I would like to thank them for their support.

I am extremely grateful to Laura Masullo for her continuous support, endless scientific arguments and injecting a high dose of fun in my life. I am also extremely grateful for invaluable help on this thesis.

Finally, I want to thank, Rita Tieppo, Michele Valperga and Bianca Valperga. Thanks to two of them, I have been lucky enough to do what I love, but thanks to the third, I am continuously pushing myself to do more.





# Table of contents

<b>1. Introduction</b>	<b>16</b>
1.1. Genetic investigation of behaviours; an historic perspective .....	16
1.2. Genes and behaviour .....	17
1.3. Gene expression and behaviour .....	20
1.4. Plasticity in the nervous system .....	22
1.5. Aggregation and O <sub>2</sub> -escape behaviour in <i>C.elegans</i> : Genes, Neural Circuits and Behaviour ... 29	
1.6. Aims of this work .....	38
<b>2. Material and Methods</b>	<b>39</b>
<b>3. A forward genetic screen for novel regulators of aggregation and O<sub>2</sub>-escape behaviour in <i>C. elegans</i></b>	<b>45</b>
3.1. Design of the genetic screen.....	45
3.2. Most aggregating mutants exhibit increased O <sub>2</sub> -escape behaviour.....	48
3.3. Seven aggregating strains harbour <i>npr-1</i> mutations, validating the screen .....	48
3.4. Mapping mutants by whole-genome sequencing.....	49
3.5. The diacylglycerol kinase <i>dgk-1</i> inhibits O <sub>2</sub> -escape behaviour.....	51
3.6. <i>dgk-1</i> mutants reduce O <sub>2</sub> -evoked Ca <sup>2+</sup> responses in URX, but increase overall synaptic output.....	53
3.7. Two alleles are likely to confer O <sub>2</sub> -escape behaviour by increasing RMG activity.....	54
3.8. Mapping of <i>db1221</i> allele .....	55
3.9. The thrombospondin FIG-1 is a glial protein inhibiting O <sub>2</sub> -escape behaviour.....	57
3.10. A glial signalling ligand of the Warthog family, WRT-6, suppresses O <sub>2</sub> -escape behaviour without changing O <sub>2</sub> -circuit activity .....	59
3.11. The hyperactive mutant <i>db1220</i> is mapped to a small region on Chromosome V .....	61
3.12. Summary .....	63
<b>4. QUI-1, a NACHT/WD domains containing protein homologous to human NWD1, inhibits O<sub>2</sub>-escape behaviour and it is required for sensory perception</b>	<b>65</b>
4.1. Disrupting QUI-1 confers O <sub>2</sub> -escape behaviour.....	65
4.2. QUI-1 is a NACHT/WD40 domain containing protein, homologous to human NWD1.....	65
4.3. QUI-1 acts down-stream of neurons integrating O <sub>2</sub> -stimuli.....	68
4.4. QUI-1 is required in sensory neurons that sense avoidance cues and promote aggregation...69	
4.5. <i>qui-1</i> acts in the same genetic pathway as <i>npr-1</i> .....	72

4.6. QUI-1 is required for pheromone sensing .....	72
4.7. qui-1 mutant show enhanced dense core vesicles release from ADL neurons .....	73
4.8. Removing qui-1 recruits ADL in the O2-circuit.....	75
4.9. bbs mutants also exhibit increased O2-escape behaviour.....	76
4.10. High levels of neurosecretion are observed in several aggregating mutants.....	77
4.11. Impairing sensory inputs confers O2-evoked neurosecretion on ADL sensory neurons .....	78
4.12. Summary .....	79
<b>5. Oxygen-experience reprograms the expression profile of O2-sensing neurons</b>	<b>81</b>
5.1. A transgenic reporter line combined with FACS allows to isolate and profile AQR, PQR and URX O2-sensing neurons.....	81
5.2. AQR, PQR and URX neurons are highly peptidergic.....	84
5.3. O2-experience reprograms peptidergic properties of O2-sensing neurons.....	86
5.4. O2-evoked activity regulates expression of distinct groups of genes at high and low oxygen....	89
5.5. O2-evoked activity drives expression of distinct sets of neuropeptides at high and low oxygen... 92	
5.6. Summary.....	93
<b>6. Discussion and future directions</b>	<b>95</b>
6.1. Novel regulators of O2-escape behaviour .....	95
6.2. qui-1 is a conserved protein homologous to NWD1 .....	98
6.3. Absence of qui-1 redirects the flow of information in the O2-circuit .....	99
6.4. Absence of sensory inputs sensitises C. elegans sensory neurons to incoming activity .....	100
6.5. Oxygen experience reprograms neuropeptide expression in AQR, PQR and URX.....	103
6.6. Concluding remarks.....	106
Bibliography .....	108
<b>Appendix 1 - 3-point mapping sequencing data</b>	<b>120</b>
<b>Appendix 2 - EMS induced SNPs</b>	<b>132</b>
<b>Appendix 3 - QUI-1 homology</b>	<b>139</b>
<b>Appendix 4 - Neuropeptides expressed in AQR, PQR and URX</b>	<b>142</b>
<b>Appendix 5 - Neuropeptide receptors expressed in AQR, PQR and URX</b>	<b>144</b>
<b>Appendix 6 -Strain list</b>	<b>146</b>



# 1. Introduction

## 1.1. Genetic investigation of behaviours; an historic perspective

Behaviour can be defined as a range of actions made by individuals, organisms, systems, in conjunction with their environment (Bendesky and Bargmann, 2011). In humans, a single behaviour is implemented by the brain as a combined response to external stimuli, internal motivational states, and prior experiences (Bendesky and Bargmann, 2011). Above all, behaviour is exceptionally interesting for scientific investigation, as its biological importance is apparent; animals meet their most basic needs of feeding, mating and reproduction through behavioural patterns. However, the sheer complexity of behavioural patterns and an incomplete understanding of the principles governing the nervous system, make understanding behaviour an extremely complex problem to approach.

During the late 1960s two molecular biologists Sydney Brenner and Seymour Benzer proposed to start tackling the problem using genetics (Benzer, 1971; Brenner, 1973). Brenner argued when setting out his plan to approach the problem: "*In principle, it should be possible to dissect the genetic specification of behaviour much in the same way as was done for biosynthetic pathways in bacteria or for bacteriophage assembly*" (Brenner, 1973). Both he and Benzer mutagenised animals, the first using *C. elegans*, the latter *Drosophila melanogaster*, and isolated several behavioural mutants, which initiated a long collective effort that provided insight into aspects of animal behaviours such as circadian rhythms (Konopka and Benzer, 1971), learning (Dudai et al., 1976) as well as cell fate determination (Horvitz and Sulston, 1980) and sex determination (Hodgkin and Brenner, 1977). Despite Brenner's bold intuition, initial attempts at isolating genes were rather slow due to technical limitations (Hodgkin, 1989). In fact, they all shared a similar framework, where mutants were isolated, complementation groups were formed to distinguish alleles of the same gene, and finally, if other mutants involved in the same phenotype were already available, double mutants were built to group genes into genetic pathways (Greenwald, 2012). This whole process was accelerated first by the introduction of molecular cloning and the generation of genetic physical maps for *C. elegans* and *Drosophila* genomes (Coulson et al., 1986; Sidenkiamos et al., 1990), followed some years later by the publication of *C. elegans*, *Drosophila*, mouse and human entire genome sequences (Adams et al., 2000; Consortium,

1998; Lander et al., 2001; Venter et al., 2001; Waterston et al., 2002). In particular the publication of the mouse genome extended the study of behavioural genes to mammals. Due to their large genomes, long life cycles and reduced brood size, it is impractical to perform genetic screens in mammals. However, the availability of the complete genomic sequence of the mouse, made it possible to query its genome in search of homologues of genes already implicated in behaviour in other species, and vice versa (Allada et al., 1998; King et al., 1997). Once a candidate gene was identified through analysis of its sequence, gene knockout strategies allowed the precise disruption of a gene to investigate its function. This in turn paved the way for reverse genetics. These approaches were further refined by the introduction of conditional knockout strategies, which allowed to probe genetic contribution in specific cell types or precise times points. Recently new sequencing technologies and a decrease in sequencing cost, have again transformed the framework for studying behavioural genetics. In model systems where genetic screens are feasible, identifying genes by examining recurring genetic lesions in a large population of mutants by high-throughput next-generation sequencing is now the protocol of choice (Zuryn et al., 2010).

The old endeavour of understanding the genetics of behaviour is far from being over. Recent technological advancements have the potential to greatly stimulate the field and break new ground in the understanding of genetic components of poorly understood molecular mechanisms of the brain such as neural identity determination and function of neuropeptide signalling pathways (Sudhof, 2017). Moreover, by applying these new technologies to the study of gene expression it is now possible to address if certain genetically determined concepts, such as identity and physiological properties of neurons, are in fact dynamic and susceptible to experience. It is now easier than ever before to address the molecular basis of complex behaviours.

## **1.2. Genes and behaviour**

Historic advancements in the study of genetic components of behaviour paved the way for a genetic and molecular understanding of a multitude of behaviours. It will be impractical to discuss too many examples, instead I will focus on few key examples necessary to discuss (1) the genetic control of behaviour, (2) considerations over the nature of behavioural genes, (3) the unit of behavioural regulation and (4) introduce themes recurrent in this thesis.

## **Behavioural genes are involved in different functions within the nervous system**

A remarkable example of how genetic screens were instrumental to pinpoint the genetic basis of behaviour is given by the study of circadian rhythms in *Drosophila* (Sokolowski, 2001). Flies show two main behaviours which follow day-night cycles: pupae eclosion, where flies emerge from their pupal case when expecting dawn, and activity-rest cycles, where adult flies tend to show locomotory activity during the day and rest at night (Panda et al., 2002). The first mutants isolated for defects in these two behaviours were mapped to a single locus, *per*, which alone was able to regulate lengthening, shortening and arrhythmic of both eclosion and activity-rest cycles, thus suggesting this gene orchestrates circadian behaviours (Konopka and Benzer, 1971). Further genes involved in control of day-night activity were identified, including *tim*, *cycle* and *clock* for which mutations resulted in arrhythmia and extended period of daylight activity (Allada et al., 1998; Rutila et al., 1998; Sehgal et al., 1994). Moreover, molecular and biochemical characterisation of these genes revealed how they are crucial in forming a master biological clock that coordinates behaviours according to circadian cycles (Panda et al., 2002). The effect that mutations in each one of these genes has on eclosion and activity-rest cycles exemplifies the powerful control that genes have on behaviour.

The example of *per* in *Drosophila* elegantly shows how one gene is able to control many aspects of multiple behaviours. However, this is an extreme example. Despite a multitude of behavioural mutants being isolated over the years, the large majority of them led to the identification of genes that, rather than actively controlling behaviour, were involved in the development or function of parts of the nervous system necessary for executing behaviour (Sokolowski, 2001). For example, the study of behaviour in *C. elegans* identified a large number of genes involved in olfaction and sensory perception, as nematodes initiate several behaviours, including avoidance, attraction and entry into an alternative developmental stage, in response to chemical signals from the environment. Nematodes detect the majority of environmental chemicals using specialised sensory neurons which localise chemical receptors to the tip of their dendrites using a microtubule-based structure called cilium (Inglis et al., 2007). Sensory neurons detect environmental signals through the sensory channels, openings in the nematode head generated by glial cells in which sensory cilia are in direct contact with the exterior of the animal (Bargmann, 2006). These structures are necessary for sensory perception, and, accordingly, mutations in genes regulating either the formation of cilia, like X-box transcription factor *daf-19* (Swoboda et al., 2000), the trafficking of chemoreceptors to the dendritic tips, like *odr-4* (Chen et al., 2014; Dwyer et al., 1998), or encoding

for specific chemical receptors, like the GPCR ODR-10 (Sengupta et al., 1996), all result in behavioural defects. This strong correlation between genetic lesion and behaviour has allowed for a detailed characterisation of how sensory stimuli are transformed into neural activity in *C. elegans* sensory neurons (Bargmann, 2006).

Neurons are not the only cell type involved in behaviour. Glia cells are necessary for essential neural function such as synaptogenesis, induction of synaptic activity and synaptic pruning. Therefore, it is not surprising that genes involved in glial functions affect behaviour as well (Zuchero and Barres, 2015). Evidences for glia function in behaviour, have been gathered from studies in *C. elegans* where ablating glia cells suppressed the animal's attraction to benzaldehyde, avoidance of 1-octanol and glycerol-evoked  $Ca^{2+}$ -responses (Bacaj et al., 2008). Furthermore, mutating Patched containing protein *daf-6* or a NEMO/MAP kinase homolog *lit-1*, resulted in similar behavioural defects (Oikonomou et al., 2011; Perens and Shaham, 2005; Perkins et al., 1986). Both genes are active in glia cells and their absence results in gross abnormalities in the sensory channel, suggesting glia actively contribute to its formation (Oikonomou and Shaham, 2011). Since absence of sensory channels prevents the nematode sensory neurons from detecting external chemicals, the behavioural phenotypes observed in glial mutants resulted from failing to detect sensory stimuli (Bacaj et al., 2008).

### **Natural variation results in different behavioural strategies**

Genes regulating behaviours are often under evolutionary pressure from natural selection as behaviours are able to provide individuals with evolutionary advantages. Therefore, it is not surprising that multiple alleles of a gene are present in a population and regulate opposing behaviours in the wild. The first example of natural variation in behavioural genes was the *for* gene in *Drosophila*. Wild fruit fly larvae show two separate foraging strategies; either they travel long distances and explore multiple food patches, a behaviour known as “rover”, or they leave the food patch less frequently, a behaviour known as “sitter” (Bendesky and Bargmann, 2011). These two behaviours are regulated by two natural variants of the *for* gene, which encodes for a conserved cGMP-dependent protein kinase (PKG) (Debelle and Sokolowski, 1987; Osborne et al., 1997). The natural variants differ both in the activity and levels of the *for* gene such that rovers show higher expression and activity compared to sitters (Osborne et al., 1997). The PKG protein encoded by *for* has been shown to regulate behaviour in other species as well (Hong et al., 2008b). PKG's ability to control behaviour extends over different time scales, and its temporal regulation as well as overall gene expression level seems to be crucial. In honeybees PKG levels are higher in old bees, specialised in foraging tasks,

compared to young bees, which instead nurse the hive. Increasing PKG activity in young flies promotes foraging behaviours, suggesting that PKG expression levels coordinate foraging behaviours (Ben-Shahar et al., 2002). Also in another insect species, such as the red harvester ant, levels of PKG have been associated with food-seeking behaviours. Forager ants display low expression levels of the ant orthologue of *for* (*Pbfor*), whereas expression of this gene is much higher in ants tasked with working in the hive (Ingram et al., 2005).

Gene expression levels are not the only genetic substrate controlling behaviour. Variations in the protein sequence of behavioural genes can lead to strikingly different behaviours. One example is a single amino acid substitution that changes a phenylalanine (215F) to a valine (215V) in the neuropeptide receptor 1 (NPR-1) in the *C. elegans* laboratory strain (N2) (de Bono and Bargmann, 1998). This change is responsible for the “solitary” behaviour of N2 animals. While strains bearing the 215F allele form aggregates while feeding, strains carrying the 215V allele do not form aggregates and disperse while feeding. These opposing behaviours are the result of a single amino acid substitution which increases the activity of NPR-1 and suppresses aggregation behaviour.

### **1.3. Gene expression and behaviour**

It is clear from the findings considered above that genes play a crucial role in shaping animal behaviour. However, if genes were the sole determinant of behaviour, which would render behaviours fixed, animals would be unlikely to survive natural selection. In fact, animal behaviours are not fixed, and they can be modulated by environmental conditions, internal motivational states of the animal, and previous experiences (Bendesky and Bargmann, 2011). For example, the nematode *C. elegans* lays eggs at regular temporal intervals, yet, in the presence of unfavourable conditions such as food scarcity or high levels of CO<sub>2</sub>, egg-laying is delayed or inhibited respectively (Fenk and de Bono, 2015; Taghert and Nitabach, 2012). Genes are nevertheless crucial for behavioural modulation as they encode molecules involved in detection and processing of sensory cues that modulate behaviour. Yet, behavioural plasticity can also exploit the same behavioural gene that exert a tight control over behaviour. It has been proposed that regulation of their expression levels, expression pattern or their expression over time is an additional mechanism that allows behavioural plasticity (Sokolowski, 2001). In the next section, I will discuss this mechanism more in details.

## Gene expression regulates behaviour

Rover and sitter behaviours in *Drosophila* offer again a useful example to discuss the molecular mechanism underlying behavioural flexibility. In fact, neither rover nor sitter behaviours are fixed and short food deprivation induces flies with rover alleles to behave like sitter (Graf and Sokolowski, 1989). Moreover, PKG expression levels change during development and the natural variant of *for* actually alter the expression levels of PKG in rover and sitter (Ben-Shahar et al., 2002; Osborne et al., 1997). This indicates that PKG expression levels, rather than the presence of PKG alone, are responsible for these two natural behaviours and lead to a model where dosage rather than the presence or absence of genes coordinates behaviour (Sokolowski, 2001). If gene levels are in fact crucial, then restricting gene expression is likely to be also important in shaping behaviour. In fact, the arginine vasopressin (AVP) neuropeptide shapes social behaviour in mammals because of the specific expression pattern of its cognate receptor. In two related species, monogamous prairie voles and polygamous montane voles, differences in social behaviours have been associated with the neuropeptide AVP (Young et al., 1999). The coding sequence of both AVP and its cognate receptor, vasopressin V1a receptor (V1aR) are indistinguishable between the two species. Nonetheless expression levels differ in that only monogamous voles express V1aR in a region of the brain involved in signalling reward, the ventral pallidum (Insel et al., 1994). Strikingly, over-expressing V1aR in the ventral pallidum of polygamous voles was sufficient for the acquisition of social behavioural traits similar to that of monogamous voles (Lim et al., 2004).

Gene expression levels of behavioural genes are also crucial for shaping the activity of neurons required to initiate behaviour. In fact several genes contribute to neural activity and changes in their expression reprograms the intensity, frequency and dynamic of neural activity (O'Leary et al., 2013). Flies, like many other animals, can learn to avoid certain concentrations of odour. When asked to discriminate between noxious and benign concentrations of the same odour, flies take time to make a decision based on the difficulty of the task (DasGupta et al., 2014). The time required for *Drosophila* to decide whether or not to avoid a certain odour concentration can be extended by mutating the Forkhead box transcription factor *FoxP* (DasGupta et al., 2014). *FoxP* is required in  $\alpha\beta_C$  Kenyon cells (KCs), a small population of third-order olfactory neurons in the mushroom body. These cells increase decision times when hyper-polarised, suggesting *FoxP* facilitate neural activation (DasGupta et al., 2014). This strong correlation between the *FoxP* gene and decision-making in flies, was recently shown to rely on elevated expression

levels of the voltage-gated potassium channel *Shal* ( $K_v4$ ) in  $\alpha\beta_C$  KC, consistent with a model where absence of *FoxP* increases *Shal* levels, which decreases  $\alpha\beta_C$  KC activity and inflates the time flies need to make a decision (Groschner et al., 2018).

At a time when the genetic of behaviour was not understood, Sydney Brenner and Seymour Benzer suggested to approach the problem by isolating behavioural mutants. This strategy was largely successful and led to the isolation of genes directly involved in shaping behaviour, as well as genes involved in the development and function of molecular and cellular structures necessary for behaviour. However, technologies available at the time did not permit a deep understanding of the molecular mechanisms underlying this control. Further studies, of which a few examples have been described in this Introduction, suggest that gene expression levels or gene expression patterns are also important in shaping behaviour. Consequently, although genes are necessary for behaviour, the unit on which selective pressure is applied to control behaviour is likely to be gene regulatory elements. By coordinating gene expression in different neurons, these regulatory elements are able to promote or inhibit different behaviours (Sokolowski, 2001). This is far from being an isolated case and it does not apply exclusively to behaviour. This is in fact a more general principle of evolution. Many novel functions that span the entirety of an organism's biology have emerged through an evolution process that restricted or expanded a gene's expression pattern or changed its expression level.

## **1.4. Plasticity in the nervous system**

Despite being genetically determined, behaviours are dynamic and retain the capacity to adapt to previous experiences. What are the cellular and molecular underpinnings of such behavioural plasticity? Since the nervous system is responsible for behavioural adaptation, do its unitary components (neurons) also adapt under the same conditions? Furthermore, if gene expression is crucial for regulating behaviour, then it might not be unreasonable to speculate that, when behavioural adaptation takes place due to experience, gene levels might change to promote this adaptation. I will describe in more detail examples that illustrate the extent to which neurons can adapt to different experiences, and how they can regulate gene expression in response to these experiences.

## Activity-dependent changes in transcription

Changing gene expression is a common strategy that cells, in many organisms, use to adapt to perturbation in environmental conditions. To this end neurons have evolved sophisticated mechanisms to regulate gene levels, which underlie experience-driven adaptation. Experience is already known to modify neural physiology, allowing neurons to store information and animals to learn and form memories (Kandel et al., 2014). Brief experiences usually promote changes through mechanisms that do not require either transcription or protein synthesis, while prolonged or repeated experiences promote alterations through induction of transcription and protein synthesis (Nicoll, 2017; Zucker and Regehr, 2002). To promote such changes neurons in principal need a mechanism that perceives changes in animals experience and couples that with changes in transcription. One possibility is that neurons are able to perceive changes in their activation state and use that as a proxy of experience. The first observation of such a model showed that a persistent increase in neural activity could induce transcription of neuropeptide processing enzymes (Zigmond and Ben-Ari, 1977). Later, the molecular details of activity-dependent gene expression have been thoroughly investigated for a different class of genes known as immediate-early genes (IEGs), in particular for the proto-oncogene *c-fos*. IEGs are induced by an increase in neural activation and their transcription does not require protein synthesis (Flavell and Greenberg, 2008). These observation showed that neurons are in fact able to adjust gene expression in response to changes in activity, yet several questions remained. How can neurons sense alterations in activity and how do they couple these changes with refinement of gene expression? The first question has been addressed by investigating signalling pathways promoting neural activation in neurons (Flavell and Greenberg, 2008). Activation of *c-fos* has been found to rely on increases in cytoplasmic calcium, which can be mediated by glutamate ionotropic receptors (AMPA and NMDA), calcium release from intracellular storage sites or L-type voltage-gated calcium channels, with the latter being the major source of calcium for activity-dependent regulation (West et al., 2001). An increase in intracellular calcium levels stimulate several independent signalling pathways (Yap and Greenberg, 2018), resulting in nuclear activation of cyclic adenosine monophosphate (cAMP)-responsive element binding protein (CREB) and histone modification enzyme CREB binding protein (CBP) (Flavell and Greenberg, 2008). Since these pathways are most likely recruited with different kinetics, it has been proposed that neurons signal prolonged activity by activating multiple activity-dependent pathways. The simultaneous activation of several pathways activates nuclear factors such as CREB and CBP (Yap and Greenberg, 2018). Such a system would require a certain threshold to be exceeded for neural activity to promote a change in transcription (Deisseroth et al., 1996).

Activity-dependent pathways are essential for the correct development and functioning of an healthy brain. As such, it is not surprising that many intellectual disorders are linked to mutations in genes involved in activity-dependent transcription (Ebert and Greenberg, 2013). These studies show that neurons sense changes in activity using multiple independent activity-sensing pathways, but it is poorly understood how this is coupled to extensive changes in gene transcription. It has been observed that several IEGs have sequences in their promoters which are bound by CREB and CBP transcription factors (Flavell and Greenberg, 2008), thus linking neural activation with transcriptional induction of these genes. Following this first wave of expression, IEGs such as transcription factors *fos* and *jun* form the activator protein 1 (AP-1) which has binding sites for a large number of late-response genes (LRGs) (Yap and Greenberg, 2018). These genes are also induced upon neural activation, yet their expression requires protein synthesis, suggesting they are part of second wave of transcription promoted by IEGs. By using activity-dependent transcription factors and IEGs, neurons can effectively couple changes in neural activity with changes in transcription. Furthermore, several studies also demonstrated that similar activity-dependent mechanisms regulating gene expression are elicited *in vivo* by presenting mice with multiple salient sensory experiences (Cheadle et al., 2018; Mukherjee et al., 2018), thus confirming that previous experiences trigger activity-dependent transcription.

### **Experience-dependent genes**

Much evidence confirms neurons are able to regulate gene expression levels depending on an animal previous experience. However, animals respond differently to exposure to distinct salient experiences; for instance *Drosophila* shows appetitive responses toward sugar but avoids vinegar. So is it the case that genes induced in a fly brain by exposure to sugar are different from genes induced after exposure to vinegar? To address whether different experiences induce expression of different genes Mukherjee *et al.* presented mice with multiple sensory experiences. Some were simple, such as sucrose or cocaine administration, while other were complex, such as feeding after starvation and cocaine administration after abstinence. They showed that each experience induces a unique combination of IEGs which was used to create a specific signature for each experience. These signatures were shown to be predictive, thus enabling the correct prediction of a mouse's recent experience by analysing expression of IEGs (Mukherjee et al., 2018). These experience-dependent differences in gene induction might be due to different neurons contributing to the sensing of each experience.

Additional studies have identified unique activity-dependent genes in several neural types such as excitatory and inhibitory neurons (Spiegel et al., 2014) and, among inhibitory neurons, between parvalbumin-, somatostatin-, and vaso active peptide-expressing neurons (Mardinly et al., 2016). Although these studies provide evidences that different neural types induce expression of different genes, it is unlikely that they account for the difference observed by Mukherjee *et al.*. In fact, it is improbable that each sensory experience they used elicits activity in a different neural type, as experiences such as feeding after starvation and cocaine administration after abstinence are likely to activate many different neural types. Moreover, mimicking increased activity in the entire brain of *Drosophila* by using three distinct activation paradigms (channelrhodopsin activation, temperature-sensitive cation channel activation and potassium chloride) induces distinct sets of genes with little overlap between paradigms, suggesting different activation paradigms elicit expression of different genes. Although no work has addressed this issue, it is tempting to speculate that differences observed in Mukherjee *et al.* are due to different neural circuits being recruited when mice experience sugar consumption compared to more complex experiences such as cocaine administration after abstinence.

For sensory experiences to modulate behaviour at least two events must coexist in neurons: (1) they must be able to detect brief or prolonged experiences, and (2) they must promote changes in their biophysical properties resulting in an altered behavioural output. Neurons detect brief and prolonged experiences through changes in activity, but how are their biophysical properties changed? If gene expression is truly crucial to control behaviour it must change biophysical properties of neurons as well, as neurons and neural circuits are ultimately responsible for executing behaviour. While these questions have been addressed in details in the context of learning and memory (Kandel et al., 2014), less is known about how prolonged exposure to specific sensory experiences changes the properties of neurons. In this context, homeostatic plasticity is the best known form of plasticity which depends on previous sensory experiences.

### **Homeostatic plasticity**

Homeostatic plasticity allows neural circuits to adjust to perturbations and maintain a constant level of overall activity. It has been proposed that neurons achieve this regulation by detecting internal activity and adjust it by implementing a series of molecular changes which counteract excessive or diminished internal activity (Turrigiano, 2008). This form of plasticity was first discovered by observing that tonic firing of stomatogastric neurons in lobsters changes from tonic to bursting

after neurons were isolated and maintained in culture for days (Turrigiano et al., 1994). This suggests that neurons adjust to different conditions by changing their biophysical properties and that recent history of activation might promote these changes (Turrigiano et al., 1994). In a further study, silencing mouse inhibitory cortical neurons in culture showed an initial decrease in circuit activity which over time returned to a set value, suggesting neurons adjust their neural properties after perturbation to meet target level of activity (Turrigiano et al., 1998). As neurons seem to have a notion of which levels of activity they are supposed to experience, at times they counter intuitively increase their responses in the absence of stimuli. When rats were deprived of visual inputs by monocular deprivation, a technique which abolishes evoked-activity in neurons of the visual cortex responsive to one eye, studies demonstrated that cortical neurons showed larger miniature excitatory post-synaptic currents (mEPSCs) due to an increase in synaptic strength (Desai et al., 2002). These findings suggest that neurons adjust to sensory deprivation by increasing synaptic activity.

There are several distinct components of neural activity. Hence neurons, in principle, can adjust their overall activity by changing their post-synaptic responses, membrane excitability or synaptic release. Homeostatic plasticity has been showed to change both post-synaptic responses and membrane excitability (Maffei and Turrigiano, 2008; Turrigiano et al., 1998). In the first instance, homeostatic plasticity regulates trafficking of AMPA glutamate receptors to post-synaptic terminals which enhances mEPSC, thus increasing synaptic strength (Turrigiano et al., 1998). Moreover, sensory deprivation by monocular deprivation has been observed to change intrinsic excitability as well as synaptic strength of visual cortical neurons, suggesting that after sensory deprivation homeostatic plasticity also drives changes in neural intrinsic excitability (Desai et al., 2002; Maffei and Turrigiano, 2008).

Although the molecular players which implement these plastic changes in excitability are not well known (Turrigiano, 2008), a few observations suggest that changes in neural activity are sensed by some of the molecular pathways involved in activity-dependent transcription (Yap and Greenberg, 2018). Sensory deprivation results in a reduction in calcium influx which neurons detect largely by decreased activity of calcium/calmodulin-dependent protein kinase type IV (CAMKIV), and an increase in transcription (Ibata et al., 2008). This suggests that in addition to synaptic remodelling, homeostatic plasticity could also be mediated by changes in transcription.

Homeostatic plasticity can also be initiated by release of secreted growth factors and cytokines, such as BDNF and tumour necrosis factor alpha (TNF $\alpha$ ). BDNF is a critical factor for many forms of plasticity and it has been shown to block homeostatic plasticity (Rutherford et al., 1997), while TNF $\alpha$  is secreted from glia increasing the trafficking of AMPA receptors to the membrane (Stellwagen and Malenka, 2006). Interestingly, BDNF is also a late-response gene induced by neural activity, and its transcription is regulated through a CREB binding site in its promoter, which regulates activity-dependent transcription of the gene, but does not affect its basal levels (Hong et al., 2008a). Mice in which this regulatory element was mutated displayed a reduction in strength of inhibitory synapses, suggesting activity-dependent gene expression of BDNF is required for controlling inhibitory synapses and circuit refinement (Hong et al., 2008a). Since neurons working in concert within a circuit need to adjust their neural properties in accordance to one another to maintain balance, it is not surprising that secreted molecules can contribute to homeostatic plasticity. However, the hypothesis that BDNF or TNF $\alpha$  are released upon the sensing of an initial change in activity in order to promote homeostatic plasticity in the rest of the circuit, has been postulated but not tested.

### **Neuropeptide as modulators of behaviour**

The examples of TNF $\alpha$  and BDNF in homeostatic plasticity offer an opportunity to further discuss the role of secreted protein in coordinating neural plasticity. In fact, although neurons are plastic and can adapt their biophysical properties to experience, they do not work alone in coordinating behaviour. Recent work has highlighted a role for neuropeptides, a class of neuromodulators, as a group of genes regulated by experience in the context of memory formation (Lakhina et al., 2015). In *C. elegans* neuropeptide genes have been shown to be the target of the experience-dependent transcription factor CREB in the context of memory formation (Lakhina et al., 2015). Moreover, neuropeptides are also necessary for the formation of olfactory associative learning in flies (Knapek et al., 2013). Neuropeptides ability to modulate behaviour by affecting neural properties (Nusbaum et al., 2017) is of particular interest. They are a class of neuromodulators composed of small secreted peptides which bind, mainly, to G protein coupled receptors (GPCRs) and, through G protein effectors, affect neural activity (Frooninckx et al., 2012). In the case of egg-laying in nematodes, the neuropeptide FLP-1, is responsible for food-related modulation, as *flp-1* mutants do not change the pace of egg-laying in the presence or absence of food (Waggoner et al., 2000). Neuropeptides are released from neurons and mediate neural communication similarly to neurotransmitters. However, they differ in that they modulate activity

and they activate receptors extra-synaptically, thus forming a suitable molecular substrate to coordinate the response of multiple neurons. This feature is critical for their role as behavioural modulators since behaviour is not regulated by single neurons, but by multiple neurons connected together into neural circuits.

In *C. elegans*, observations that neuropeptide receptors seem to modulate chemical and electrical synapses, and evidences that neurons can be recruited or excluded from neural circuits by neuropeptides, led to the conclusion that neuropeptides are able to control the flow of information within a neural circuit (Bargmann, 2012). In fact, multiple neuropeptide systems shape the flow of information by changing the gain of sensory neurons, thus shaping the salience with which the nervous system process sensory inputs (Taghert and Nitabach, 2012). One example of such a process has been studied in *Drosophila* where starvation elevates food search efficiency by sharpening the detection of food. This increase in efficiency requires the facilitation of synaptic outputs from Or42b olfactory receptor neurons (ORNs) and suppression of Or85s ORNs synaptic outputs, thus re-directing the flow of information (Ko et al., 2015; Root et al., 2011). These changes in synaptic strength are mediated respectively by sNPF and tachykinin, a neuropeptide relate to substance P (Kim et al., 2017). When flies are starved, a reduction in insulin levels induces the transcription of sNPF and tachykinin receptors in Or42b and Or85a respectively which allows sNPF and tachykinin neuropeptides to remodel the synaptic strength of the two sensory neurons. This adjust the flow of information in the circuit, and change the animal foraging strategy (Ko et al., 2015; Root et al., 2011).

From studies discussed so far it is clear that neurons alter gene expression levels according to specific sensory experiences. They also adapt their neural properties to compensate for changes in activity. The specificity of activity-dependent genes for sensory experiences might underline the need of neurons to adjust their neural properties according to specific sensory experiences. If we consider the model described in previous paragraphs stating that regulation of genes, rather than genes themselves, is the unit of control for behaviour, then it might seem reasonable to ask whether genes regulated by one sensory experience are implicated in a behavioural response to that experience. As some of the experience-dependent genes involved in homeostatic plasticity adjust neurons to high or low activity, they might also confer on neural circuits the ability to compensate for changes in overall activity, thus possibly contributing to behavioural adaptation. Similarly, neuropeptides, because of their ability to coordinate neural activity in ensemble of neurons, might be targets of experience-dependent mechanisms, thus allowing experience to shape neural circuits.

However, to my knowledge none of these hypothesis have been tested yet. In fact, understanding the function of experience-dependent genes in the context of behaviour is challenging (Yap and Greenberg, 2018). This is in part because, for many of the sensory experiences used to elicit experience-dependent transcription, the neural circuit underlining their perception are not very well understood, and in part because the experience paradigms routinely used to elicit transcription are very different from experience in natural behaviours (Yap and Greenberg, 2018).

## **1.5. Aggregation and O<sub>2</sub>-escape behaviour in *C.elegans*: Genes, Neural Circuits and Behaviour**

### **Advantages of studying innate behaviours**

Innate escape behaviours are one example of genetically determined behaviours that can be implemented by individuals without the requirement for any element of learning, yet modulated by the environment, an animal's motivational states and experience (Evans et al., 2019; Kim et al., 2017). Animals' ability to recognise a predator is genetically determined from birth by the formation of a "hard-wired" neural circuit which allows detection of peril, and implementation of a defensive motor reflex (Evans et al., 2019). Mice and rats reared in laboratory conditions and kept away from any natural predators still avoid feline urine upon first encounter. The evolutionary advantage of a predisposition to avoid danger is clear. However, many escape behaviours are not simply reflexes and can take into account other sensory cues to thoroughly assess the environment before deploying defensive mechanisms. Escape behaviours are energetically expensive and furthermore they can impede other essential aspects of animal life such as feeding and mating, thus they need to be carefully regulated (Lima and Dill, 1990). Water striders insects delay escape initiation when in large groups of conspecific compared to small groups (Dill and Ydenberg, 1987). Global animal states such as hunger can alter defensive mechanisms as well, such that starved individuals suppress defensive mechanisms in search of food. While aquatic dragonflies larvae seek refuge from predators among aquatic plant leafs, hunger prompts them to leave the safeness of leafs and be more susceptible to predation (Wellborn and Robinson, 1987). Defensive mechanisms, such as the gill-withdraw reflex in *Aplysia*, can also be altered by previous experience (Pinsker et al., 1970; Pinsker et al., 1973).

Due to the robustness of their behavioural responses, innate escape behaviours and reflexes have been extremely amenable to the isolation of genetic, cellular and circuitry components of behaviour. For the same reason, I argue, they might be

crucial to address outstanding questions in the field. In fact, the molecular details of how neural circuit underlying escape behaviour modulate other sensory modalities are not known. Moreover, although several studies have identified major molecular pathways involved in signalling experience-dependent changes in neurons, less is known about the molecular machinery which implements such changes and how they shape behaviour (Carlezon et al., 2005; Flavell and Greenberg, 2008; Kandel et al., 2014).

### **Aggregation is an innate behaviour modulated by sensory experiences in *C. elegans***

The nematode *Caenorhabditis elegans* is a favourable model system to study genetic and molecular contributions to innate behaviours and behavioural plasticity (Bargmann, 1998; Brenner, 1973), due to its compact nervous system of 302 uniquely identifiable neurons (White et al., 1986), due to its powerful genetics (Bargmann, 1998; Brenner, 1974; Hobert, 2013), and due to the presence of a wiring diagram listing all the chemical and electrical connections between its neurons (Cook et al., 2019; Jarrell et al., 2012; White et al., 1986). This particular feature of *C. elegans* has allowed for a deep understanding of how an ensemble of neurons function within several neural circuits to generate multiple behaviours.

*C. elegans* are free-living nematodes which live burrowed inside rotting fruits, where they feed on bacteria (Schulenburg and Felix, 2017). Like any other organism they have evolved a sophisticated repertoire of behaviours that allow them to feed, explore surroundings and reproduce. In the wild *C. elegans* escapes from high oxygen concentrations (>12%) (Dusenbery, 1980). It has been proposed that this behaviour has evolved to protect animals from prolonged exposure to their habitat surface. In fact, increasing oxygen concentrations could signal approaching the surface where *C. elegans* are at risk of desiccation and predation. In laboratory conditions, wild animals escape atmospheric oxygen by collectively forming clumps on the edges of the bacterial lawn where they feed (Rogers et al., 2006). By forming these aggregates, wild animals dampen oxygen within an aggregate to create more favourable concentrations (7%-11%) (Rogers et al., 2006). If not inside a clump, animals dwell on the edge of the bacterial lawn, where bacteria are thicker and the oxygen concentration is lower (Gray et al., 2004). Rearing animals at low oxygen concentrations abolishes any form of aggregation and bordering, confirming oxygen is the main driver of both behaviours (Gray et al., 2004).

Aggregation is a complex behaviour, but it is driven by a simple avoidance reflex toward oxygen (Busch et al., 2012; Laurent et al., 2015). In fact, when presented

with 21% oxygen, *C. elegans* elicits an O<sub>2</sub>-escape behaviour where animals first reverse, a reflex shared by many avoidance reflexes, and subsequently increase their locomotory speed (Rogers et al., 2006). This increase in locomotion can be sustained for long periods of time, but it ceases as soon as animals return to low oxygen concentrations (Busch et al., 2012). When animals experience prolonged exposure to atmospheric oxygen, O<sub>2</sub>-escape behaviour drives the cooperation with conspecific to form aggregates.

Aggregation and O<sub>2</sub>-escape responses are examples of innate behaviours. However, both behaviours have a built in propensity for plasticity which is manifested in the ability of *C. elegans* to adjust these behaviours to previous oxygen experience (Cheung et al., 2005 and Mario de Bono, unpublished data). Prolonged exposure to hypoxia reduces aggregation and bordering. This effect can be reverted by growing animals in atmospheric oxygen (Cheung et al., 2005). Interestingly, prolonged exposure to hypoxia also shifts animals' oxygen preference. Since this switch is contingent on the presence of food, it has been proposed that *C. elegans* can form an appetitive association of low oxygen concentrations and food availability (Cheung et al., 2005).

Previous experience of different oxygen concentration can also reprogram other avoidance behaviours in *C.elegans*. Animals avoid CO<sub>2</sub> at 7% oxygen but at atmospheric concentrations this behaviour is suppressed (Carrillo et al., 2013). If animals are exposed to low oxygen (7%) for long periods of time (more than 30min), a memory of previous oxygen experience is formed and animals do not suppress CO<sub>2</sub> avoidance when exposed again to 21% (Fenk and de Bono, 2017). A more drastic experience-dependent change is observed in pheromone attraction. *C. elegans* is attracted or repelled by certain ascarosides pheromones (Ludewig and Schroeder, 2012). Aggregating animals have been isolated that avoid ascarosides (Jang et al., 2012). Interestingly, their avoidance behaviour can be shaped by previous oxygen experience such that animals pre-exposed to 7% oxygen reverted their pheromone preferences from repulsion to attraction (Fenk and de Bono, 2017)

### **The genetics of aggregation behaviour**

What makes aggregation and O<sub>2</sub>-escape behaviour in *C.elegans* attractive paradigms to investigate the genetics of behaviour, is the existence of a large body of work uncovering multiple genetic pathways controlling these behaviours (Fig 1.1).

The first gene involved in aggregations was isolated following the observation that wild isolates of *C. elegans* aggregate in laboratory condition, whereas the N2 reference does not (de Bono and Bargmann, 1998). In fact, as mentioned previously in this Introduction, N2 shows a “solitary” behaviour by dispersing over the bacterial lawn and does not display O<sub>2</sub>-escape behaviour. This striking behavioural difference involves a single amino-acid change in the neuropeptide receptor 1 (NPR-1) a GPCR of the RFamide receptor class. The N2 reference strains harboured, as a result of domestication, a gain of function mutation (215V) which increases NPR-1 activity (Rogers et al., 2003). Consistently with this observation, loss of function mutations of *npr-1* restore aggregation and O<sub>2</sub>-escape behaviour in N2 animals.

Further studies isolated *flp-21* and *flp-18*, two ligands of *npr-1* also involved in aggregation (Rogers et al., 2003). More *npr-1* ligands are likely required to inhibit aggregation as *flp-21;flp-18* double mutants are still solitary. Both FLP-21 and FLP-18 are expressed in several sensory neurons that perceive hyperosmolarity, nose touch, volatile chemical repellent and pheromones, but the stimuli which triggers their release are still unknown.

Upon ligand binding NPR-1 activates heterotrimeric G proteins and initiates signalling transduction (Rogers et al., 2003). In neurons G proteins can be loosely divided into G proteins promoting (G<sub>q</sub>/G<sub>s</sub>) and G proteins inhibiting neural activity (G<sub>i</sub>/G<sub>o</sub>). Hindering genes inhibiting G<sub>i/o</sub> signalling or impairing genes that mediates G<sub>i/o</sub> signalling, both result in increased aggregation and O<sub>2</sub>-responses, thus suggesting G<sub>i/o</sub> signalling is crucial for NPR-1 inhibition of aggregation (Laurent et al., 2015). *npr-1* is expressed in a large sub-set of neurons, but much of its effect on aggregation and O<sub>2</sub>-escape behaviour relies on its activity in RMG interneurons (Macosko et al., 2009). Over-expressing the highly active NPR-1 215V isoform in RMG transforms aggregating *npr-1* mutants into solitary animals and suppresses high locomotory activity at 21% oxygen (Macosko et al., 2009). The effect of NPR-1 on RMG neural properties are not completely understood. Rather than shaping stimulus-evoked calcium activity, NPR-1 seems to modulate neural communication downstream of Ca<sup>2+</sup> entry (Laurent et al., 2015). In fact, activating RMG using optogenetics elicits behavioural responses in *npr-1* mutants but not in N2 reference strains, suggesting hyperactive NPR-1 blocks neural communication regardless of evoked activity (Laurent et al., 2015).

*C. elegans* uses aggregation and O<sub>2</sub>-escape behaviour to avoid atmospheric oxygen. Like all animals, they perceive environmental signals by means of

molecular receptors which couples binding of a ligand to an increase in neural activity. To detect oxygen *C. elegans* employs two guanylyl cyclases, GCY-35 and GCY-36, which couple the binding of oxygen with an increase in production of cGMP (Cheung et al., 2004; Gray et al., 2004). These receptors are active in AQR, PQR and URX which are the main O<sub>2</sub>-sensing neurons in *C. elegans*. A rise in cGMP levels opens cyclic nucleotide-gated channels which depolarise neurons by mediating a Ca<sup>2+</sup> influx (Persson et al., 2009; Zimmer et al., 2009). This first small depolarisation is propagated by the opening of voltage-gated calcium channels, inositol-1,4,5-trisphosphate (IP<sub>3</sub>) receptors and ryanodine receptors, which facilitate further influx of Ca<sup>2+</sup> from extracellular domains and endoplasmic reticulum reserves respectively (Arellano-Carbajal et al., 2011; Busch et al., 2012). Consistent with this model, genetic deletion of soluble guanylyl cyclases *gcy-35* or *gcy-36*, cyclic nucleotide-gated channels *tax-2* or *tax-4* and voltage-gated channels *egl-19* all suppress neural activity evoked by oxygen in O<sub>2</sub>-sensing neurons and abolish aggregation and O<sub>2</sub>-escape behaviour.

Although oxygen is the main driver of aggregation, it is not the only environmental cue involved in this behaviour. *C. elegans* aggregates exclusively in the presence of food which promotes aggregation through unknown sensory neurons (de Bono et al., 2002). Moreover, many genes involved in sensory perception are involved in promoting aggregation. Two genes related to mammalian cation channels TRPV1/*osm-9* and TRPV4/*ocr-2* are required for aggregation in *npr-1* mutants (de Bono et al., 2002). They localise to the cilia of sensory neurons where they promote evoked activity and they are required in ASH and ADL sensory neurons for aggregation (de Bono et al., 2002). Similarly, two other genes involved in sensory perception, *odr-4* and *odr-8*, promotes aggregation. A conserved tail-anchored ER protein ODR-4 together with Ufm1 specific protease 2(UfSP2)/ODR-8 direct trafficking of GPCR from the ER to the plasma membrane (Chen et al., 2014). As expected, *odr-4* and *odr-8* mutants are olfactory and sensory defective mutants, and, suppress the aggregation of *npr-1* mutants.

*C. elegans* is capable of increasing and maintaining high locomotory activity for long periods of time in its search for optimal oxygen concentrations. Disrupting *C. elegans* homologues of Interleukin 17 (IL-17) and IL-17 receptors, *ilc-17.1*, *ilcr-1* and *ilcr-2* respectively, alters the ability of animals to sustain O<sub>2</sub>-responses for long periods of time (Chen et al., 2017). *ilc-17.1*, *ilcr-1* and *ilcr-2* mutants do show O<sub>2</sub>-escape responses, but the behaviour cannot be sustained and their speed quickly returns to baseline levels (Chen et al., 2017). Looking for the same inability to

sustain O<sub>2</sub>-escape behaviour, Chen *et al.* isolated additional genes involved in the same molecular pathway, Act1/*actl-1*, Interleukin-1 receptor-associated kinase/*pik-1* and Inhibitor of  $\kappa$ B/*nfk-1*. The IL-17 pathway shapes the ability of RMG interneurons to reach correct levels of O<sub>2</sub>-evoked activity. In absence of either ligand or receptors RMG does not achieve proper O<sub>2</sub>-evoked activity, whereas over-expressing *ilc-17.1* heightens RMG O<sub>2</sub>-evoked activity. This work further illustrates the extent to which O<sub>2</sub>-escape behaviour is subject to modulation. Nevertheless, a major outstanding question is which environmental cue is responsible for regulating physiological levels of interleukin signalling in *C. elegans*.

Studies on aggregation have also implicated genes crucial for development as behavioural regulators. The *C. elegans* orthologue of TGF- $\beta$ , DAF-7, is secreted from ASI peptidergic neurons and controls a large number of processes such as dauer development, fat storage and ageing (Gumienny and Savage-Dunn, 2013). Genetic ablation of *daf-7* and other genes involved in TGF- $\beta$  signalling in *C. elegans* all confer aggregation to the N2 reference strain (de Bono *et al.*, 2002). Likewise, *daf-7* mutants show preferences for low oxygen concentration in aereotaxis experiments regardless of food availability (Chang *et al.*, 2006). Importantly, genetic analysis showed that *daf-7* and *npr-1* are part of two distinct pathways inhibiting aggregation (de Bono *et al.*, 2002). However, very little is known of the molecular changes occurring in *daf-7* mutants that could explain their aggregation behaviour.

One additional genetic pathway inhibiting aggregation behaviour has been isolated. We have previously discussed that *ocr-2*, *osm-9* and *odr-4* act in in ASH and ADL sensory neurons to promote aggregation. In fact, aggregation behaviour can be restored in mutants for these genes by mutating *C. elegans* homodimeric kinesin/*osm-3* (de Bono *et al.*, 2002). This suggests there is an additional *npr-1* independent genetic pathway inhibiting aggregation. OSM-3 is required for formation of distal cilia in 26 neurons in *C. elegans* and *osm-3* mutants consequently show gross defects in cilia formation and sensory detection (Perkins *et al.*, 1986). Mutating *osm-3* abolishes ASH and ADL stimulation of aggregation, but at the same time disrupts an additional negative regulator such that double mutants with *ocr-2*, *osm-9* and *odr-4* show restored aggregation behaviour (de Bono *et al.*, 2002). This additional genetic pathway has not been identified to this date and it is unlikely to coincide with *daf-7* as ASI, which regulates secretion of DAF-7 upon detecting food, requires cilia formation to properly detect environmental stimuli.

### **Aggregation and O<sub>2</sub>-escape behaviour are controlled by the O<sub>2</sub>-circuit**

As discussed in previous paragraphs aggregation and O<sub>2</sub>-avoidance are innate behaviours and yet shaped by sensory modalities as well as past experiences. To fully understand the molecular mechanisms that are crucial for this regulation one has to understand how neural circuits interact with one another and how they are altered by previous experiences. Although many important biological discoveries have been carried out on the molecular and cell biological changes underlying plasticity mechanisms such as learning, short-term and long-term memory (Kandel, 2012), less is known about how neural circuits adapt to different global states or how experience can regulate cross sensory plasticity. Aggregation and O<sub>2</sub>-escape behaviour offer an attractive system in which to study the molecular, cellular and circuitry mechanisms underpinning such phenomena. Both behaviours are ultimately controlled by the O<sub>2</sub>-circuit, a tonic neural circuit which senses up and down shifts in oxygen concentrations and drives escape from 21% oxygen as well as controlling animal global state (Busch et al., 2012; Laurent et al., 2015; Zimmer et al., 2009) (Fig 1.1). The circuit is coordinated by a hub-and-spoke network, where a central hub, RMG interneurons, is connected to several spokes through mainly electrical synapses (Macosko et al., 2009). When *C. elegans* encounter high oxygen levels, AQR, PQR and URX become depolarised and signal to RMG, via chemical and electrical synapses, to drive O<sub>2</sub>-escape behaviour (Busch et al., 2012; Laurent et al., 2015; Macosko et al., 2009). Communication between URX and RMG is sufficient to promote O<sub>2</sub>-escape behaviour. URX O<sub>2</sub>-evoked activity is sufficient to drive O<sub>2</sub>-escape behaviour, when O<sub>2</sub>-evoked activity from AQR and PQR is abolished (Laurent et al., 2015). Moreover, activating RMG using optogenetics increases animal locomotory activity both at 7% and 21% oxygen, and impairing its synaptic connection by expressing tetanus toxin or by abolishing peptidergic maturation by knocking down carboxipeptidase/*egl-21*, both suppress O<sub>2</sub>-escape behaviour (Laurent et al., 2015). These data support a model where URX and RMG are the main constituents of an O<sub>2</sub>-circuit driving O<sub>2</sub>-escape behaviour. The neural circuit driving aggregation is likely to include additional neurons as expressing tetanus toxin in URX, RMG or both neurons does not completely abolish aggregation (Macosko et al., 2009).

Several studies have dissected in even greater details the contribution of each type of RMG synapses to aggregation. Impairing RMG electrical or chemical synapses reduces aggregation and high locomotory activity at 21% oxygen, but does not completely abolish either behaviours suggesting some level of redundancy between electrical and chemical synapses exists (Jang et al., 2017; Macosko et al., 2009). Similarly, also impairing either chemical or electrical URX synapses does not affect aggregation (Jang et al., 2017; Macosko et al., 2009). Synapses of other

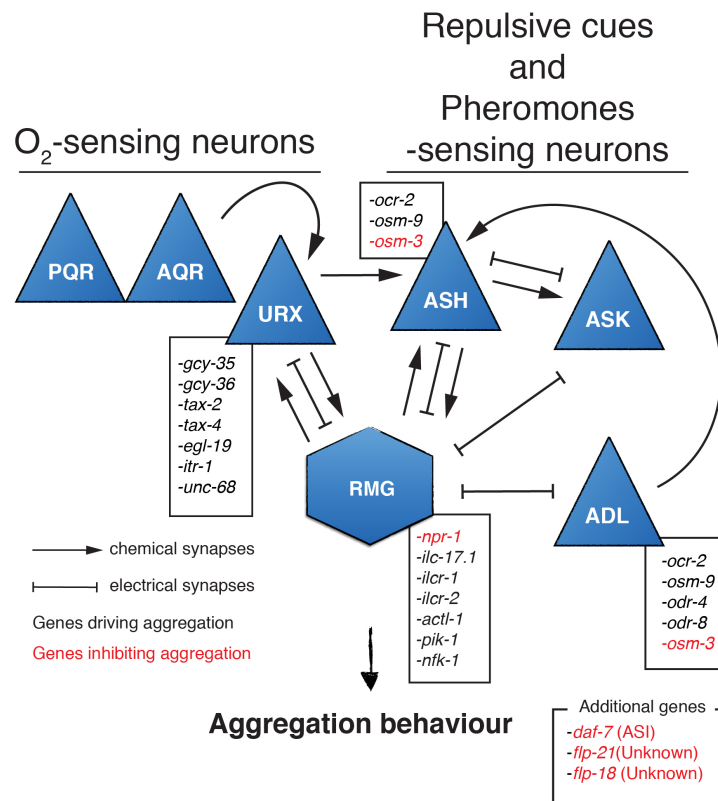


**Figure 1.1 O<sub>2</sub>-sensing neural circuit and its genes**

Schematic representation of O<sub>2</sub>-circuit that controls aggregation and O<sub>2</sub>-escape behaviour. Each box contains genes that promote or inhibit aggregation or O<sub>2</sub>-escape behaviour. Genes grouped together in one box are active in the same neuron.

components of the hub-and-spoke circuit have been tested as well. Blocking electrical synapses from ASH and ADL neuron does not affect aggregation (Jang et al., 2017). Moreover, disrupting synaptic release in both neurons does not completely suppress O<sub>2</sub>-escape behaviour, and, if both neurons are ablated, optogenetical activation of RMG is still able to induce O<sub>2</sub>-escape responses, suggesting ASH and ADL initiate the behaviour upstream of RMG (Laurent et al., 2015).

Aggregation offers an ideal model system to study cross-talk plasticity between distinct sensory modalities. Manipulating connections in the hub-and-spoke circuit, either through molecular or genetic manipulation of electrical and chemical synapses, alters *C. elegans* avoidance behaviours. This effect is perhaps reflected in the design of the hub-and-spoke circuit that allows RMG to modulate evoked responses of its pre-synaptic inputs according to O<sub>2</sub>-circuit activity. In fact,

modulating RMG outputs by removing *npr-1* sensitises ASK and ADL for pheromone-evoked activity (Jang et al., 2012; Macosko et al., 2009). Also manipulating electrical synapses in the circuit shapes ADL evoked responses. Blocking electrical synapses in URX, RMG and ADL changes ADL pheromone-evoked activity as well as suppressing ADL mediated pheromone avoidance (Jang et al., 2017). The molecular mechanism by which *npr-1* loss of function sensitises animals to pheromone avoidance is not clear. It has been proposed that NPR-1 controls opening and closing of specific electric synapses so that impairing *npr-1* enhances electrical coupling of RMG with ASK and ADL (Jang et al., 2017; Macosko et al., 2009). This re-organisation of electrical coupling could render neurons connected to RMG more sensitive to O<sub>2</sub>-evoked activity. In fact, ADL neurons became responsive to oxygen in *npr-1* mutants, and their O<sub>2</sub>-evoked activity has been show to be dependent on GCY-35 activity in URX (Fenk and de Bono, 2017). ADL O<sub>2</sub>-evoked activity in *npr-1* could in part explain differences in ADL pheromone-evoked activity between *npr-1* mutants and N2 reference strain. Although compelling evidences suggest NPR-1 activity modulates sensory modalities pre-synaptic to RMG, whether these effects are dependent on NPR-1 function in RMG has not been investigated in details.

*C. elegans* shapes pheromone avoidance according to O<sub>2</sub>-circuit activity, and it is likely to take advantage of the RMG hub-and-spoke circuit to regulate cross talk between oxygen and pheromone sensing circuits. Recent work from Fenk *et al.* showed that *C. elegans* retains a memory of previous oxygen experience that modifies pheromone avoidance. They propose animals exposed to low oxygen re-program the hub-and-spoke circuit. In fact, although *npr-1* mutants normally avoid ascarosides, this behaviour is reversed by prolonged exposure to 7% oxygen (Fenk and de Bono, 2017). Moreover, prolonged exposure to low oxygen sensitises ASK and ADL sensory neurons to pheromone-evoked activity (Fenk and de Bono, 2017). Despite both neurons forming electrical synapses with RMG in the hub-and-spoke circuit, neuropeptide release from RMG seem to be crucial for experience-dependent changes in the circuit. In fact, both ASK sensitisation and experience-dependent change of pheromone valence are contingent on RMG peptidergic secretion (Fenk and de Bono, 2017). Persistent changes in pheromone avoidance are likely to be dependent on O<sub>2</sub>-circuit activity. Fenk *et al.* show that prolonged exposure of *npr-1* mutants to low oxygen reprograms neural properties of the O<sub>2</sub>-circuit. Both URX and RMG neurons heighten their O<sub>2</sub>-evoked responses after sustained exposure to 21% but not 7% oxygen. In the case of RMG, this effect is mediated by neuropeptide release. One model predicts that RMG hub-and-spoke electrical synapses are required for cross-talk between the O<sub>2</sub>-circuit and

pheromone-sensing neurons, whereas neuropeptides are crucial to sustain modulation after prolonged exposure to oxygen.

Neuropeptide release regulates an additional experience-dependent behaviour in *C. elegans*. I have previously discussed how prolonged exposure to high oxygen suppresses CO<sub>2</sub>-avoidance. RMG contributes to this suppression by releasing neuropeptides; disrupting neuropeptide maturation or expressing a high activity allele of *npr-1* in RMG, both restore CO<sub>2</sub>-avoidance in *npr-1* mutants (Fenk and de Bono, 2017).

## 1.6. Aims of this work

The work reviewed in this Introduction points out a few interesting biological questions worth pursuing. In particular, cross-talk between sensory modalities is critical to coordinate animal global state responses. However, molecular underpinnings of such plasticity are not well understood. The O<sub>2</sub>-circuit in *C. elegans* offers an excellent model to investigate them. Understanding how neurons alter gene expression levels in response to prolonged experience in the context of behaviour is challenging. Moreover, how genes modulated by experience are capable of altering neural properties has not been fully investigated. Oxygen experience in *C. elegans* is a useful paradigm to investigate these questions, due to the possibility of genetically labelling O<sub>2</sub>-sensing neurons and a deep understanding of their genetics.

This study has two goals. (1) I aim to identify novel and conserved genetic regulators of aggregation and O<sub>2</sub>-escape behaviour in *C. elegans* with the intention to unravel conserved functions of the nervous system for which we do not have a complete molecular understanding. (2) By studying the effects of oxygen experience on AQR, PQR and URX, O<sub>2</sub>-sensing neurons in *C. elegans*, I plan to identify a set of experience-dependent genes. These genes will help shed light on the molecular remodelling undergoing in O<sub>2</sub>-sensing neurons during prolonged oxygen experience. Since oxygen experience reprograms many aspects of *C. elegans* behaviour and physiology, such genes might help us understand how these alterations are brought about.

## 2. Material and Methods

*Strains:* All strain strains were grown at controlled room temperature under standard condition (Brenner, 1974). All assay used less than 1 day old adults. Transgenic animals were obtain microinjecting 20-40ng/uL of expression construct or fosmid and 20-40 ng/uL of co-injection marker (*unc-122p:gf*). A list of all strains used in provided in Appendix 6

*Mutagenesis assay:*Animals at the L4 stage were treated with a 50mM solution of EMS in M9 buffer as per standard protocol (Brenner, 1974). To isolate aggregating mutants a strategy was devised where, in the centre of a thin bacterial lawn, a small drop of concentrated thick OP50 was spotted. Upon sensing food, non aggregating strain stop, whereas aggregating strain search for optimal oxygen concentration where bacteria are thicker. Mutants were place on the plate and after 60 minutes, animals dwelling in the thicker spot were picked, self-fertilise and the progeny was tested for aggregation behaviour.

### Behavioural assay

*Aggregation assay:* The assay was performed as perviously described (de Bono and Bargmann, 1998). 60 young adults were picked onto assay plates seeded with 200uL OP50 2 days before. Animals were left undisturbed for 3 hours before counting. Animals in clumps were scored as 3 or more animals in contact with more than 50% of their body length, and animals in borders were counted as the number of animals dwelling approximately within 2 mm of the edges of the bacterial lawn. Scoring was performed blindly. For each biological replicate the percent of animals in clumps was calculated as follow:

$$\% \text{ Animals in clumps} = \frac{\text{number animals in clumps}}{\text{total number animals}} * 100$$

while the percentage of animals in the border was calculated as follow:

$$\% \text{ Animals in border} = \frac{\text{number animals in border}}{\text{total number animals}} * 100$$

*Locomotion assay:* NGM plate with low peptone (0.13% of peptone) were seeded with 60uL of OP50 bacteria 2 days prior the assay. On the day of the assay, test plates were prepared by cutting the edge of the bacterial lawn using a rubber stamp. Around 20 young adults were picked onto test plates and they were left undisturbed for 10 minutes before starting the assay. If transgenic animals were used, young adults displaying a fluorescent marker were picked on the day of the assay, firstly on fresh plates and then, together with the non-transgenic strains, onto test plates. To deliver the correct O<sub>2</sub> concentration, a PDMS chamber was put on top of the bacterial lawn. Worms were left to adapt to 7% O<sub>2</sub> for 2 minutes before the recording was started. Worms were recorded for a total of 9 minutes while oxygen concentration were changed from 7% to 21% every 2 minutes. Recordings were taken at 2 frame per second (fps) with Point Grey Grasshopper camera mounted on stereo-microscope. Videos were analysed and the speed of the worms was plotted using a custom-written Matlab software (*Zentracker*: <https://github.com/wormtracker/zentracker> and *Metaverage*). Bar graphs showing O<sub>2</sub>-evoked speed change use average speed values extracted using *Metaverage* a custom-written Matlab software. The average speed 30s before the end of the first 21% oxygen stimulus was divided for the average speed 30s before the first 21% oxygen stimulus (baseline) to obtain a fold change value. This value was computed for all biological replicates (independent assays) and they were computed into Prism to perform statistical analysis.

## **Molecular Biology**

*Genomic DNA extraction:* For genotyping 1-5 crowded plates were washed with M9 buffer. Animals were left precipitate, supernatant removed and animals were washed again. This step was repeated twice to remove OP50. Worms were frozen at -80°C at least overnight to soften the cuticle. Animals were then thawed and genomic DNA was extracted using DNeasy Blood and Tissue Kit. Samples were left in Lysis buffer (Buffer AL) for 3h at 56°C. The rest of the protocol was followed according to procedure “Purification of Total DNA from Animal Blood or Cells (Spin-Column Protocol)”. For genomic DNA isolation of samples for whole-genome sequencing, the same procedure was followed, but 5-10 crowded plates were used.

*Sequencing *npr-1* gene:* The *npr-1* locus was amplified using PCR standard condition. The PCR product was purified using the QIAquick PCR Purification Kit. The DNA obtained by the purification was sent for sequencing multiple times using a total of 16 primers covering each an interval of 300bps on both strands.

*Library preparation:* Genomic libraries for whole-genome sequencing were prepared using Nextera XT DNA Library from Illumina following manufacturer's instruction and using purified genomic DNA. The quality of the libraries was checked on a Bionalyser using a Agilent High Sensitivity Gel. Libraries concentration was assessed using KAPA Library Quantification Kits for Illumina and submitted for high-throughput sequencing.

For RNA-sequencing a protocol from Picelli et al. was adapted (Picelli et al., 2014). Briefly, FACsorted neurons were dissociated in 10uL of Triton X-100 0.2% (vol/vol) and the steps from Picelli et al. of reverse transcription was followed while reaction volumes were adjusted to a 10uL input. To synthesise cDNA oligodT primers were used to enrich for polyadenylated transcripts. In the PCR pre-amplification step 18 cycles were used to amplify cDNA. 50 uL PCR product from pre-amplification step were purified using 50 uL of Ampure XP beads, and after purification pre-amplified cDNA was resuspended in 35uL of EB solution. purified cDNA from the pre-amplification step was used as input for library preparation using Nextera XT DNA Kit at a concentration of 0.2 ng/uL, total volume = 5uL. For the rest of the library preparation protocol, the instruction from the manufacturer were followed. Quality of RNA-seq libraries was assessed on a Bionalyser using a Agilent High Sensitivity Gel. Libraries concentration was assessed using KAPA Library Quantification Kits for Illumina and submitted for high-throughput sequencing.

## **Calcium imaging**

*Calcium imaging of URX activity:* All aggregating mutants were assayed in the same condition. L4 animals expressing the YC2.60 Ca<sup>2+</sup> sensor were picked 24 h before imaging. On the day of the assay 5 – 10 worms were glued to agarose pads (2% in M9 buffer, 1 mM CaCl<sub>2</sub>), using Dermabond tissue adhesive, with their body immersed in OP50 washed off from a seeded plate using M9. The animals were quickly covered with a PDMS microfluidic chamber and 7% O<sub>2</sub> pumped into the chamber for 2 min before imaging, to allow animals to adjust to the new conditions. Neural activity was recorded for 6 minutes with switches in O<sub>2</sub> concentration every 2 minutes. Imaging was on an AZ100 microscope (Nikon) bearing a TwinCam adaptor (Cairn Research), two ORCAFlash4.0 V2 digital cameras (Hamamatsu), and an AZ Plan Fluor 2× lens with 2× zoom. Recordings were at 2Hz. Excitation light from a Lambda LS xenon arc lamp (Sutter) was passed through a 438/24 nm filter and a dichroic (Semrock). Emitted light was passed to a dichroic filter in the TwinCam adaptor cube and then filtered using a 483/32 nm filter (CFP), or 542/27 nm filter (YFP) before collection on the cameras. Recordings were analysed using

Neuron Analyser, a customwritten Matlab program available at <https://github.com/neuronanalyser/neuronanalyser>.

*Calcium imaging of RMG activity:* Experimental procedure was the same as reported for URX and all strains were selected 24h in advance by picking L4 with expressing if the YC2.60 reporter. *db104* mutants were imaged on a different calcium image set-up to increase the YC2.60 signal. *db104* mutants were picked, immobilised and placed under a PDMS chamber as detailed for URX calcium imaging, but calcium imaging was performed on a inverted microscope (Axiovert, Zeiss), with a 40Å~ C-Apochromat lens. Acquisition was at 2Hz and exposure time of 100 ms. To reduce photobleaching an optical density filter 2.0 or 1.5 was used. Excitation light (Lambda DG-4, Sutter Interments) was passed through an excitation filter (Chroma) for the cyan channel, a dichroic filter for yellow cameleon (Semrock) and a beam splitter (Optical Insights) was used to separate the cyan and yellow emission light using a dichroic filter for 483/32-55 nm (CFP) and 542/27-25 nm (GFP)(Semrock). Recording were acquired using a EMCCD Evolve 512 Delta camera (Photometrics). Recordings were analysed using Neuron Analyser, a custom-written Matlab program available at <https://github.com/neuronanalyser/neuronanalyser>.

*Calcium imaging of ADL activity:* To image young adults, L4 animals expressing the GCaMP3 Ca<sup>2+</sup> sensor were picked 24 h before imaging. On the day animals were immobilised using olfactory chips (Microkosmos) as described in (Chronis et al., 2007). Animals were kept under constant flow of M13 buffer and after 2min stimulated for 20s with C9 pheromone (10nM in M13 buffer). Calcium imaging was performed on a inverted microscope (Axiovert, Zeiss), with a 40Å~ C-Apochromat lens. Acquisition was at 2Hz and exposure time of 100 ms. To reduce photobleaching an optical density filter 2.0 or 1.5 was used. Excitation light (Lambda DG-4, Sutter Interments) was passed through an excitation filter (AmCyan,Chroma), a dichroic filter for GCaMP and RFP, and a beam splitter (Optical Insights) was used to separate the GCaMP and RFP signal using a dichroic filter 514/30-25 nm (GFP) and 641 nm (RFP) (Semrock). Recording were acquired using a EMCCD Evolve 512 Delta camera (Photometrics). Recordings were analysed using Neuron Analyser, a customwritten Matlab program available at <https://github.com/neuronanalyser/neuronanalyser>.

Bar graphs showing  $\frac{\Delta R}{R_0}$  (%) used YFP/CFP values extracted using Metaverage a

custom-written Matlab software. YFP/CFP value 30s before the first 21% oxygen stimulus (baseline) were subtracted from YFP/CFP value 30s before the end of the first 21% oxygen stimulus (stimulus). This ratio was normalised by dividing for the

baseline. This value was calculated for all biological replicates (independent assays) and computed into Prism to perform statistical analysis. For GCaMP3 imaging (ADL pheromone stimulation) the same analysis was performed but intensity values were used instead to calculate  $\frac{\Delta F}{F_0}$  (%).

## Cell isolation and FACS

*Neuron isolation:* Transgenic animals were grown on 90cm NGM plate with 3 times the normal amount of peptone, and seeded with OP50 3 day in advance. 4 days after picking, 10 large 90cm plates per genotypes which contained adult animals were washed (*npr-1* and *npr-1;gcy-35;gcy-36*) in M9 buffer and aliquot into two separate eppendorf tube (critical for bleaching the correct amount of worms). Worms were left sink and supernatant was aspirated until a final volume of 500 uL was reached. 250uL of Bleach Mix (Sodium hypochlorite 10-15%, 1.6M Sodium hydroxide) were added to the 500uL solution of worms and incubated for exactly 4min. Bleaching was stopped by adding 800uL of M9 buffer and worms were quickly washed 3 times. A solution of synchronised eggs, resulting from the bleaching protocol, was spotted on 55cm plates (1000-1500 eggs per plate) seeded with OP50 3 days in advance. For each genotype half of the plates was grown for 4 days in an oxygen-controlled incubation chamber at 7% oxygen, while the other half was grown at atmospheric oxygen, by placing the plates outside of the chamber. To dissociate GFP positive neurons initially worms were washed from plates and collected in tubes. Animals were washed and spin down 5 time to limit food contamination (10sec at 2500rpm). Their cuticle was softened by incubating them in Lysis Buffer (200mM DTT, 0.25% SDS, 20mM HEPES, 3% sucrose) for 6.5min. Worms were again washed 5 times to reduce Lysis Buffer contamination. 500uL of 20 mg/uL Pronase was used to dissociate worms into single cells solution by mechanical dissociation pipetting up and down. The reaction was stopped by adding FBS 2% in PBS and adding 1mL of PBS. Cells were filtered (5uM) to removed clumps. GFP positive cells were sorted into Triton X-100 0.2% (vol/vol).

## Imaging ADL neurosecretion

*ADL neurosecretion assay:* The DAF-28-mCherry fusion protein is released from ADL and accumulate in coelomocytes, so imaging coelomocytes function as a good proxy of neural secretion. Animals were picked 24h before the assay. The first pair of coelomocytes were imaged on a TE-2000 (Nikon) inverted microscope using a 10X air lens. Z-stack images were taken at sub-saturating exposure. Analysis was performed using ImageJ. Coelomocytes boundaries were delineated using the GFP

signal driven by the *unc-122* promoter and measurement were taken of the same area in the mCherry channel. Values were plotted in Prism as arbitrary units of intensity.

## **Analysis**

*Whole-genome sequencing:* Analysis of whole-genome data was performed using a customised python script: `cross_filter` ([https://github.com/lmb-seq/cross\\_filter](https://github.com/lmb-seq/cross_filter)). Briefly, reads were checked for quality filters and aligned to the *C. elegans* reference genome. To subtract common background mutations, a list of mutations present in multiple strain was compiled. List of mutations for each sequenced line was cross-referenced with the list of background mutation to remove mutations present in both lists.

*RNA-sequencing:* Analysis of RNA-sequencing, including computation of differentially expressed genes, transcript per million (tpm) and PCA analysis was performed using a customised python script: PRAGUI (<https://github.com/lmb-seq/PRAGUI>). Briefly, reads were checked for quality and aligned to the *C.elegans* genome. Despite library preparation protocol enriched for polyadenylated transcript a large number of reads aligned to ribosomal RNA and they were therefore removed. To confront our data set with published data, a list of genes expressed in our data set based in tpm values (all transcript with  $\text{tpm} \geq 5$  were considered expressed) was generated and confronted with published data using the web-based software Venn Diagram (<http://bioinformatics.psb.ugent.be/webtools/Venn/>). Analysis of differentially expressed genes was performed using customised R script: PEAT (<https://github.com/lmb-seq/PEAT>). Lists of differentially expressed genes were filtered for expression levels by applying a cut-off value of 50 (normalised reads count), so that genes which expression in both conditions was lower that 50 were excluded. PEAT was also used to obtain union, intersection and symmetric differences of list of genes.

*Tissue enrichment analysis and GO enrichment analysis:* Enrichment analysis were performed using the web-based softwares Enrichment Analysis (<https://www.wormbase.org/tools/enrichment/tea/tea.cgi>) (Angeles-Albores et al., 2016). Enrichment fold data were extracted and plotted using Prism 7.

*Statistics:* Statistics was performed using Prism 7. In all the bar graphs, when shown, error bars represent standard mean error (SEM). Statistics per each experiment is shown in figures legends.

### **3. A forward genetic screen for novel regulators of aggregation and O<sub>2</sub>-escape behaviour in *C. elegans***

#### **3.1. Design of the genetic screen**

Wild isolate of *C. elegans* avoid and escape ambient (21%) oxygen. One consequence of this behaviour is that under laboratory conditions these animals form aggregates on the edges of the bacterial lawn where the oxygen concentrations are lower. To investigate genetic and molecular pathways that inhibit this O<sub>2</sub>-escape behaviour we studied two collections of aggregating mutants already available in the lab. The first collection was generated by a previous member of the lab, Gemma Brown, by mutagenising the laboratory strain N2 (Bristol) using the chemical mutagen ethyl methanesulfonate (EMS) (Fig 3.1). N2 carries a gain-of-function allele (215V) of the *npr-1* gene which leads to solitary behaviour. The second mutant collection, generated by Merav Cohen, used the same procedure (Fig 3.1) but was obtained mutagenising animals defective for *flp-21*. The FMRFamide neuropeptide FLP-21 activates NPR-1, however its absence alone is not sufficient to restore aggregation behaviour. A *flp-21* mutant background may, however, provide a sensitised background to identify enhancers of aggregation behaviour.

Potential mutants showing aggregation behaviour were identified by picking animals that, like *npr-1* mutants, accumulated where the bacterial food lawn was thickest (Fig 3.1). Worms from the two parental lines, N2 and *flp-21*, were incubated in 50mM EMS at the L4 stage. Animals were retrieved and allowed to lay eggs. At this point 2500 heterozygous F<sub>1</sub> were picked and divided into 50 90mm NGM plates. From each of these plates, the F<sub>2</sub> progeny was washed off, food deprived briefly and worms were placed outside a large, thin bacterial lawn on a 90 mm NGM plate that contained at its centre a small patch of thicker food. Under standard conditions of atmospheric oxygen, N2 worms stop upon encountering the thin food whereas aggregating mutants do not stop until they reach the thicker food at the centre. Mutagenised animals were screened for their preference for thicker food, and animals dwelling in the thick food patch at the centre of the plate were individually picked. From each of these selective plates only one mutant line was isolated to avoid characterising identical mutants originating from the same F<sub>1</sub>. Approximately 5,000 genomes (2500 F<sub>1</sub>) were screened from the mutagenised N2 strain, whereas, unfortunately, we did not recover data regarding the depth of

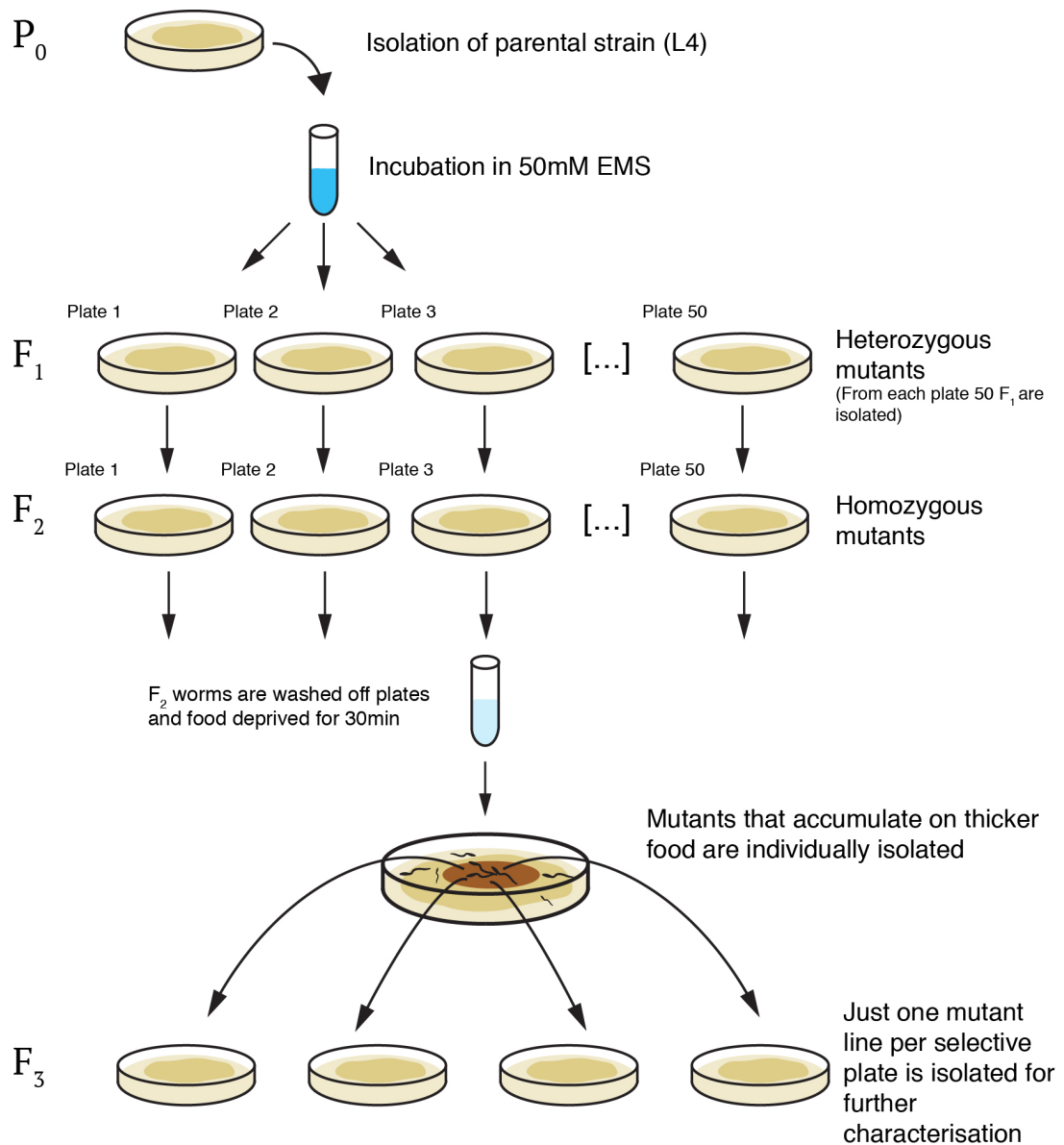


**Figure 3.1 Genetic screen for the isolation of aggregating mutants**

Schematic representation of the design used for the isolation of aggregating mutants. Animals at the L4 stage were treated with a 50mM EMS. Heterozygous mutants were let throw progeny and 50 F<sub>1</sub> were re-picked on new plates. Aggregating mutants (F<sub>2</sub>) were washed off plates and placed on a assay plate. After 60 minutes, mutants dwelling in the thicker spot were picked, self-fertilised and the progeny was tested for aggregation behaviour. Light coloured spots on plates represent thin OP50 lawns, while dark coloured spots represent thick OP50 lawns.

mutagenesis for the *flp-21* strain. Since, EMS produces around 1 mutation every 2,000 bps under the condition used in the two mutagenesis assay (50mM, See Material and Methods), screening 5,000 genomes is sufficient to isolate multiple independent mutants. Using this protocol 22 mutants were isolated from the N2 parental strain and 17 mutants from the *flp-21* parental strain. We retrieved 7 mutants from the first collection and all 17 from the second.

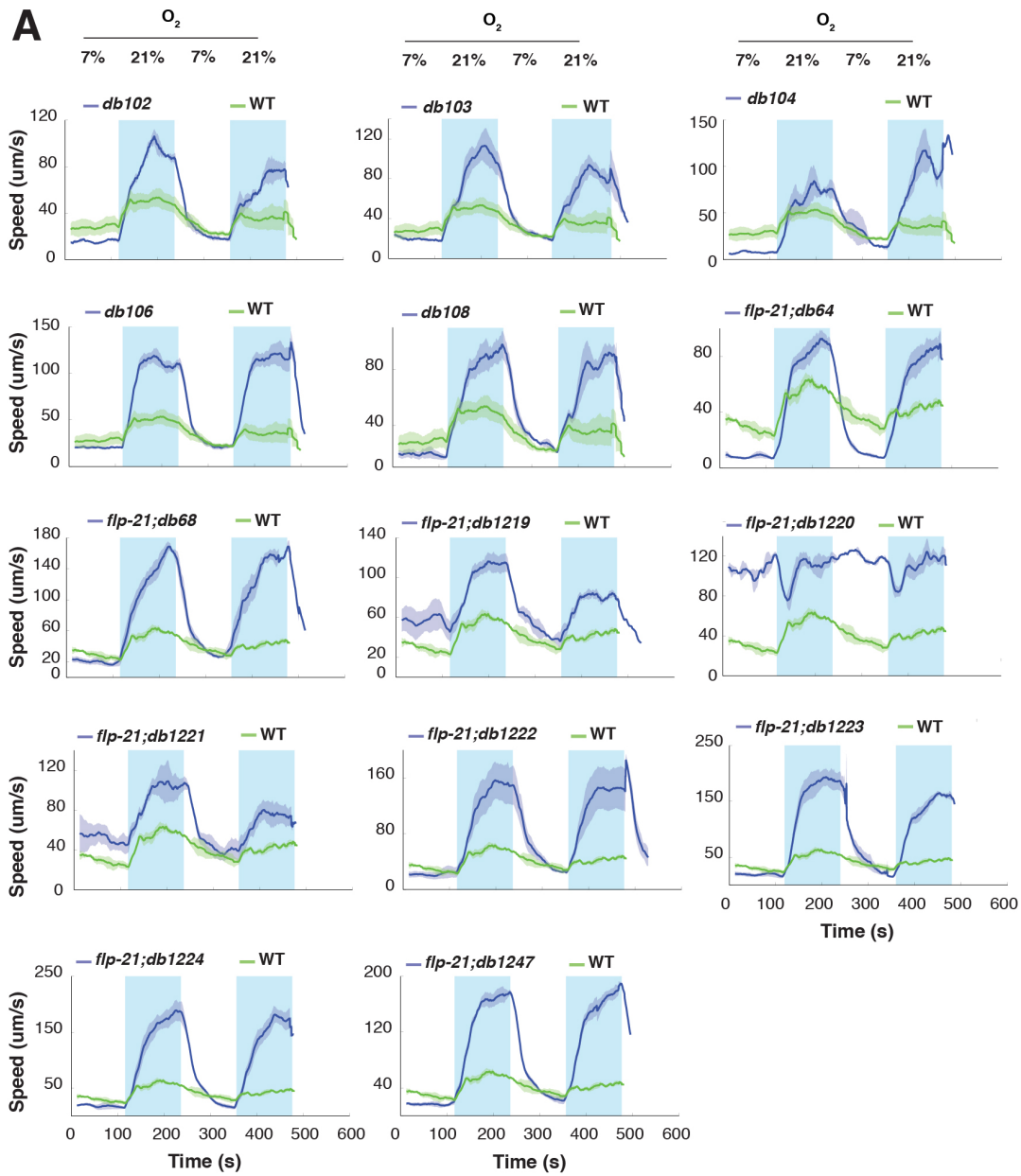


**Figure 3.2 O<sub>2</sub>-escape behaviour of aggregating mutants**

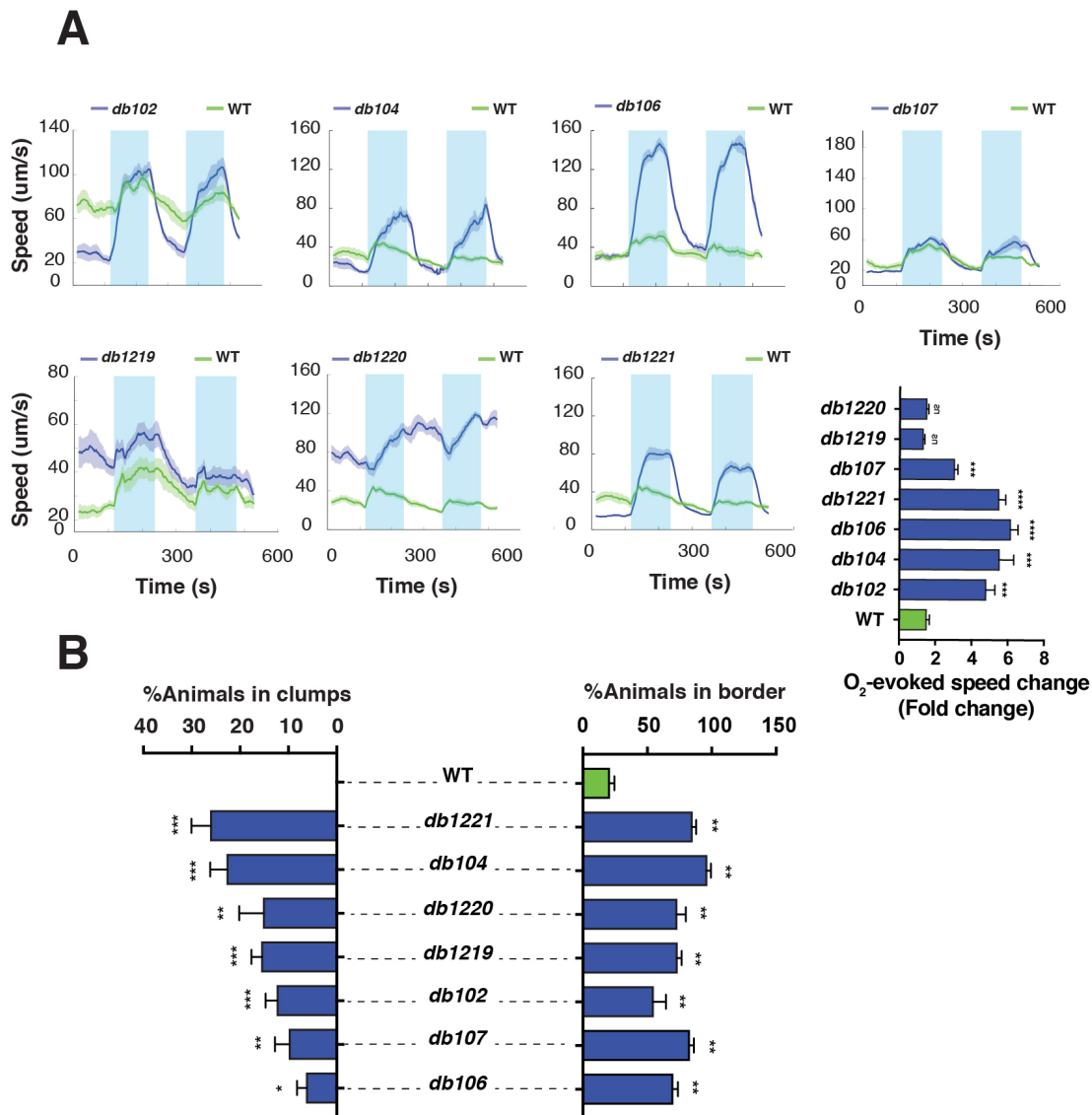
**(A)** Average speed of animal stimulated with 7% and 21% oxygen (blue rectangles). N= 4 assay. **(B)** Schematic cartoon of the *npr-1* locus. All seven alleles are shown.

### 3.2. Most aggregating mutants exhibit increased O<sub>2</sub>-escape behaviour

To confirm the aggregation phenotype of these mutants we grew animals on plates in triplicates and quantified their phenotype by visual inspection. 14 mutants showed various degrees of aggregation behaviour. Feeding *npr-1* animals aggregate to avoid 21% oxygen: when they experience an increase in O<sub>2</sub> from 7% to 21% they initially reverse and then, if O<sub>2</sub> levels remain at 21%, switch to rapid continuous movement. The laboratory strain N2 (WT) responds weakly to this stimulus, with a only small increase in speed. To test how the new aggregating mutants respond to oxygen we assayed their O<sub>2</sub>-escape behaviour. 14 mutants responded more strongly than wild type to changes in oxygen concentrations (Fig 3.2A). The aggregation behaviour and the O<sub>2</sub>-escape phenotypes for 9 additional mutants were weak, and we therefore excluded these from further analysis. All but one strain that showed strong O<sub>2</sub>-escape behaviour also showed aggregation. The exception was the *db103* mutant that failed to aggregate despite strongly avoiding 21%O<sub>2</sub>. Conversely, one strain, *db107*, showed aggregation behaviour despite only weakly avoiding 21%O<sub>2</sub>. Unfortunately, the absence of significant aggregation made it cumbersome to isolate the *db103* mutation, so we did not characterise the mutant further. In summary, phenotypic analyses led to isolate 14 mutants for further study.

### 3.3. Seven aggregating strains harbour *npr-1* mutations, validating the screen

Only a handful of genes are known to confer aggregation and O<sub>2</sub>-escape behaviour when mutated. Among these, *npr-1* confers the strongest phenotype. As some of the mutants showed a strong aggregation phenotype characteristic of *npr-1* mutants, we sequenced the *npr-1* locus for each strain. To identify any possible mutation that would change NPR-1 function, we sequenced the entire *npr-1* coding region plus 616 bps upstream of the 5'UTR and 309 bps downstream its 3' UTR. Seven strains carried 4 different alleles of *npr-1* (Fig 3.2B). 3 alleles, *db64*(Q164Stop) *db1223*(Q266Stop) and *db1224*(W182Stop), introduced an early stop codon and are therefore likely to be strong loss of function mutants. The remaining 4 mutants, *db68*, *db108*, *db1222*, and *db1227*, all harboured the same missense mutation which leads to the codon encoding cysteine 210 to encode a tyrosine. This particular residue has been shown in other GPCRs to be important for G-protein activation and the resulting NPR-1 protein is likely to be non functional. We therefore focused our attention on mutants that, despite showing robust O<sub>2</sub>-responses, did not show lesions in *npr-1*.



### 3.4. Mapping mutants by whole-genome sequencing.

Mutants isolated from mutagenesis screens harbour a high number of mutations. To isolate causal mutations conferring O<sub>2</sub>-escape behaviour, we extensively outcrossed each mutant for a total of 4 to 6 generations. Although not exactly the same behaviour, aggregation and O<sub>2</sub>-escape behaviour are closely linked and many genes regulates both. Aggregation, however, it is much simpler to score as it can be reliably scored by visual inspection. We decided to follow the mutations

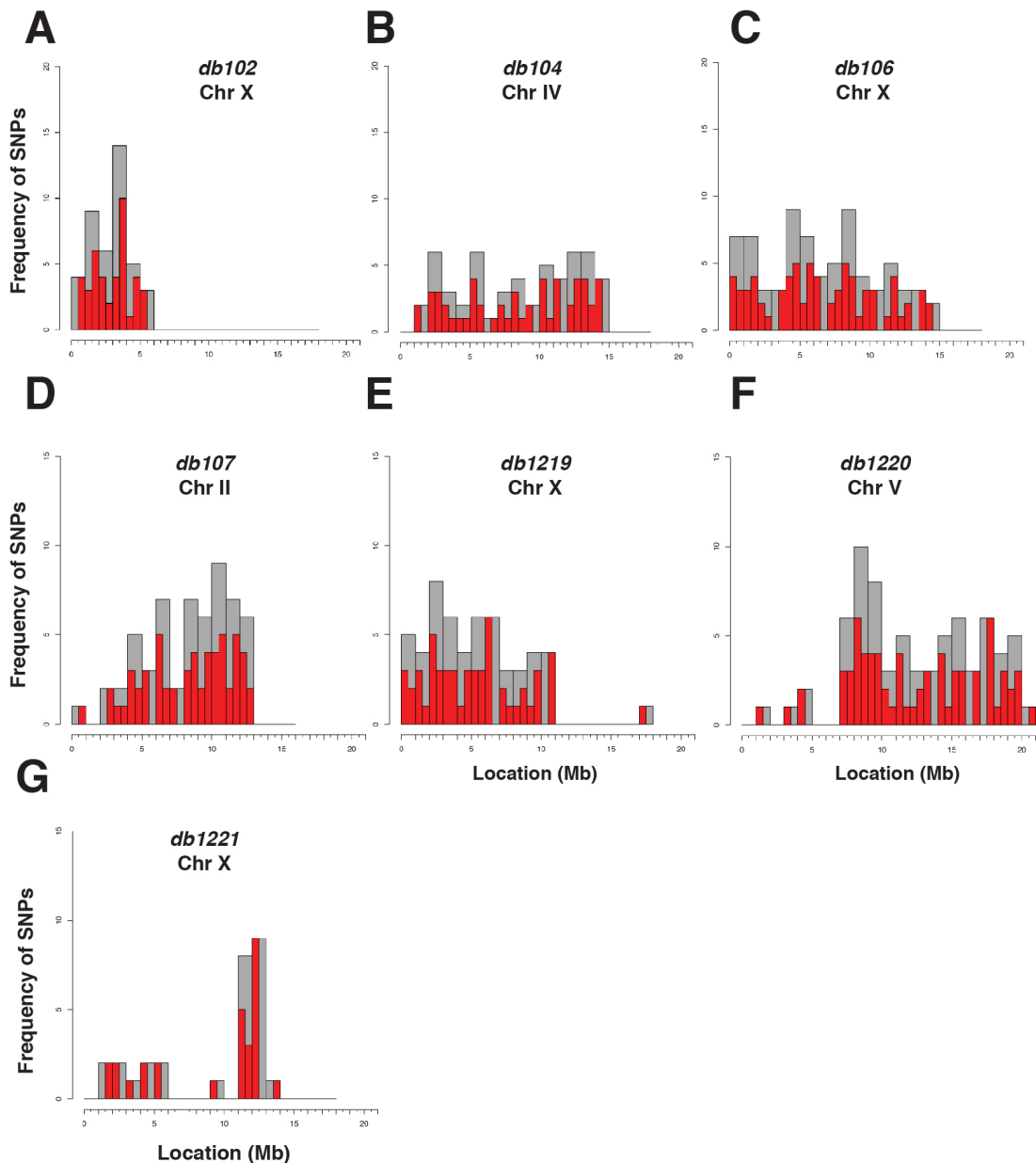


**Figure 3.4 Clusters of EMS-induced SNPs map the causal mutation to a chromosome**

(A-G) Plots show the frequency of SNPs generated by EMS mutagenesis over the length of chromosomes. Only outcrossed lines submitted for whole-genome sequencing are shown. Only the chromosomes harbouring a large EMS-cluster are shown. This interval is where the causal mutation is most likely to be.

responsible for the  $O_2$ -escape behaviour by using aggregation as a proxy. This allowed us to follow many mutations at once and sped up the process of outcrossing each mutant. To confirm that the outcrossed mutants showed a similar phenotype to the original, we tested their  $O_2$ -escape behaviour (Fig 3.3A). All but two mutants retained their original avoidance to 21%  $O_2$ . We will discuss the reason why *db106* differs from the originals more in details in later paragraphs. We also quantified the aggregation phenotype of the outcrossed mutants (Fig 3.3B). Every

mutant that showed a significantly higher O<sub>2</sub>-response than wild type, also showed aggregation. On the contrary, 2 mutants, *db1219* and *db1220*, showed aggregation despite lacking an O<sub>2</sub>-escape behaviour significantly higher than wild type. The strength of both phenotypes gave us confidence we could move forward and identify genes responsible for O<sub>2</sub>-escape behaviour.

For each mutant we isolated multiple independent outcrossed lines, isolated DNA from these lines, and submitted the DNA for whole-genome sequencing. To identify the chromosomal interval harbouring the mutation causing aggregation we examined the distribution of EMS-induced mutation in the outcrossed lines. Each time a mutant line is outcrossed it loses 50% of the randomly distributed EMS-induced mutations. However, mutations are more frequently co-inherited when they are in close proximity on one chromosome. As expected, EMS-induced mutations clustered on 5-15 Mb large intervals on one chromosome per mutant, while all other chromosomes showed little mutations (Fig 3.4A-G and Appendix 2). To further reduce this interval we compared independent outcrossed lines. Each independent line inherited a slightly different set of *de novo* mutations due to recombination events with the homologous wild type chromosome. We further reduce the EMS-mutated intervals to 5-7 Mb. Within this interval we used whole-genome sequencing data to identify candidate mutations. We prioritised mutations affecting protein-coding genes, mutations likely to disrupt protein function and mutations affecting genes expressed in the nervous system.

### **3.5. The diacylglycerol kinase *dgk-1* inhibits O<sub>2</sub>-escape behaviour**

Diacylglycerol kinase 1 phosphorylates diacylglycerol (DAG) to phosphatidic acid (PA) in neurons, and thus reduces neurotransmission by counteracting G-protein activated pathways (Miller et al., 1999). However, *dgk-1* has not been implicated in the regulation of O<sub>2</sub>-escape behaviour. We identified a mutation in the coding region of the *dgk-1* gene. The mutation, *db106*, affects a conserved Proline in an accessory kinase domain of DGK-1 (Fig 3.5A). Expressing a wild type copy of *dgk-1* completely rescued *db106* O<sub>2</sub>-escape behaviour, confirming *db106* is an allele of *dgk-1* (Fig 3.5B).

Despite being completely rescued by *dgk-1*, the *db106* mutation behaved differently after being outcrossed, as mentioned in previous paragraphs. Expressing a wild type copy of *dgk-1* failed to rescue the original *db106* mutant (Fig 3.5C). To investigate this inconsistency we compared the original *db106* with the outcrossed mutant. Their O<sub>2</sub>-escape behaviour differed significantly and in particular, the original mutant showed a much stronger phenotype, raising the possibility that the outcrossing reduced the intensity of the phenotype (Fig 3.5D). By re-mapping the



### Figure 3.5 DGK-1 inhibits O<sub>2</sub>-escape behaviour

(A) Schematic representation illustrates the *dgk-1* locus and the location of *db106* allele. Sequences from orthologues of *dgk-1* are used to highlight the conservation of the residue P814, which in the *db106* allele is mutated to a Lysine. (B) A wild type copy of *dgk-1* rescues the *db106* mutant. (C) A wild type copy of *dgk-1* does not rescue the original unoutcrossed *db106* mutant. (D) *dgk-1(db106)* and the original unoutcrossed *db106* mutant differ in the intensity of their O<sub>2</sub>-escape behaviour. (B-C-D) Average speed of animal stimulated with 7% and 21% oxygen (blue rectangles). N= 6-9 assay. Bar graph shows quantification of O<sub>2</sub>-evoked speed change defined as the fold change between average speed at 21% oxygen and average speed at 7% oxygen (See Methods). Statistical comparison between samples was performed using Mann-Whitney *U* test. If not differently specified each sample was tested against WT. \*=*p* value <0.05, \*\*=*p* value <0.01, \*\*\*=*p* value <0.001, ns=not significant.

original *db106* we isolated two distinct alleles. One proved to be *db106*, as confirmed by PCR sequencing (Data not shown) and the other one was an additional allele which we termed *db1239* and added to our collection of aggregating mutants.

### 3.6. *dgk-1* mutants reduce O<sub>2</sub>-evoked Ca<sup>2+</sup> responses in URX, but increase overall synaptic output

DGK-1 is expressed throughout the nervous system in *C. elegans*, including the O<sub>2</sub>-sensory neurons URX, AQR and PQR. To investigate the role of DGK-1 in oxygen perception, we measured neural activity of the O<sub>2</sub>-sensory neurons URX in *dgk-1* mutants. Mutants showed significantly reduced responses to upwards shifts in oxygen concentration, as well as overall levels of Ca<sup>2+</sup> at 21%O<sub>2</sub>, when compared to wild type (Fig 3.6A,B).

Synaptic release is facilitated by high levels of DAG and, consequently, by a faulty DGK-1. To investigate if DGK-1 affected synaptic communication of URX with the rest of the O<sub>2</sub>-circuit, we measured neural activity in RMG neurons, a pair of interneurons which forms chemical and electrical synapses with URX. RMG O<sub>2</sub>-evoked Ca<sup>2+</sup> responses were indistinguishable between *dgk-1* mutants and wild types (Fig 3.6C). Comparison of URX and RMG O<sub>2</sub>-evoked Ca<sup>2+</sup> responses suggests *dgk-1* mutants show enhanced synaptic release in the O<sub>2</sub>-circuit, thus increasing O<sub>2</sub>-escape behaviour.

Further experiments are needed to address the extent of *dgk-1* contribution to O<sub>2</sub>-escape behaviour, including in which neurons DGK-1 expression is sufficient to inhibit O<sub>2</sub>-responses. However, the aim of our work was to focus on novel and unknown genes and the effects of *dgk-1* on neural communication has been nicely

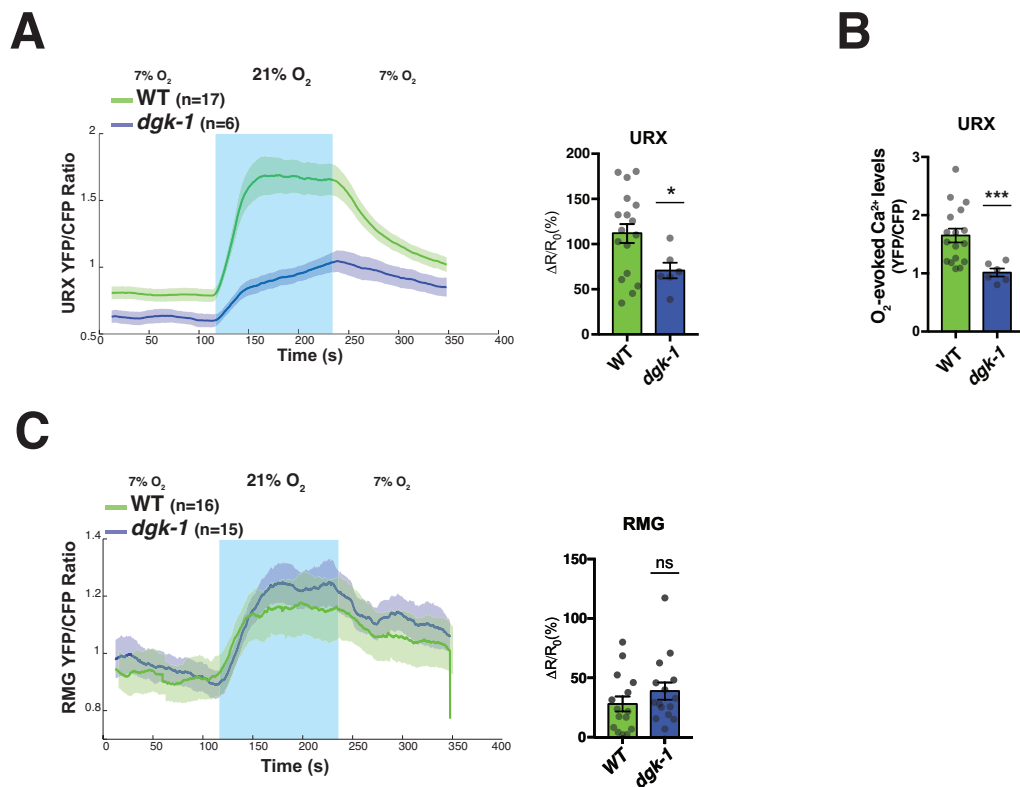


**Figure 3.6 DGK-1 reduce synaptic output in URX and RMG O<sub>2</sub>-sensing neurons**

**(A)** *dgk-1* mutants dampen O<sub>2</sub>-evoked Ca<sup>2+</sup> response for URX. Plot shows average Ca<sup>2+</sup> response in URX upon 21% oxygen stimulation. Bar graph quantifies O<sub>2</sub>-evoked Ca<sup>2+</sup> responses. n=number of animals as reported in figure **(B)** Bar graph shows intensity of O<sub>2</sub>-evoked Ca<sup>2+</sup> levels for URX. n=number of animals as reported in figure. **(C)** *dgk-1* mutants do not affect RMG O<sub>2</sub>-evoked Ca<sup>2+</sup> responses. Plot shows average Ca<sup>2+</sup> response for RMG upon 21% oxygen stimulation. Bar graph quantifies O<sub>2</sub>-evoked Ca<sup>2+</sup> responses. n=number of animals as reported in figure. (A,C) ΔR/R<sub>0</sub> is calculated using an interval of 30s before and during stimulation (See methods). Statistics: Statistical comparison between samples was performed using Mann-Whitney U test. If not differently specified each sample was tested against WT. \* = p value < 0.05, \*\*\*\* = p value < 0.0001, ns = not significant

shown by previous work in *C. elegans* (Miller et al., 1999; Nurrish et al., 1999). Therefore we decided to focus our effort on other less known genes.

### 3.7. Two alleles are likely to confer O<sub>2</sub>-escape behaviour by increasing RMG activity

O<sub>2</sub>-escape behaviour is controlled by the O<sub>2</sub>-circuit. Within the circuit, RMG interneurons function by integrating activity from O<sub>2</sub>-sensing neurons with that from other circuits to drive behavioural outputs. We reasoned that mutations conferring O<sub>2</sub>-escape behaviour might affect the overall activity of the circuit and, in particular, that of RMG. To investigate this hypothesis, we measured neural activity in URX and RMG neurons for all the aggregating mutants. Two mutants, *db107* and *db1221*, showed an enhanced RMG O<sub>2</sub>-evoked activity compared to wild type (Fig

3.7B,D). RMG is not able to detect oxygen cell autonomously and its responses are dependent on URX (Laurent et al., 2015). To test if URX responses were also enhanced in these mutants, we measured *db107* and *db1221* URX O<sub>2</sub>-evoked activity. Neither of the mutants showed differences compared to wild type (Fig 3.7A,C) confirming that enhanced RMG activity is not dependent on URX O<sub>2</sub>-evoked responses.

Since RMG is an essential regulator of O<sub>2</sub>-escape behaviour, we decided to try and identify the two alleles. Looking for *de novo* mutations from whole-genome sequences did not identify a likely candidate mutation. We decided, therefore, to map further the two mutants using a 3-point mapping strategy. Unfortunately, 3-point mapping relies on reference mutations which provide phenotypic markers for the chromosomes one wants to map. In the case of *db107*, the causal mutation was likely to be on Chromosome II which has been proven hard to map in the past (Fig 3.4D, Appendix 2.4 and Mario de Bono, personal communication). We decided to tackle the *db1221* first and leave the isolation of *db107* for a later time.

### **3.8. Mapping of *db1221* allele**

Analysis of *db1221* whole-genome sequences showed an EMS cluster on Chromosome X between 11Mb and 14 Mb. To map the candidate mutation in this interval we chose a *dpy-6(e14);lin15A(n76ts)* line, since the distance between the two genes contains the EMS-cluster. We screened recombinant individuals and identified 11 out of 20 aggregating recombinants linked to *lin-15A* mutation and 2 out of 20 aggregating recombinants linked to *dpy-6* mutation (Appendix Table 1,2). Based on this information we placed the mutation between 9.2 Mb and 11.3 Mb on Chromosome X. To map the mutation to a smaller interval we used a modified version of single nucleotide polymorphism (SNP)-mapping. Using whole-genome data from *db1221*, we selected seven mutations sparse along the 3 Mb interval, and sequenced them in all 40 recombinants (Appendix Table 1,2). Unfortunately, the data did not look clear enough to identify the causal mutation.

There are several reasons why 3-point mapping might fail. Chiefly, if the causal mutation is not on the chromosome under examination, mapping will fail. To test if *db1221* was on Chromosome X, we designed a strategy to outcross only autosomal chromosomes of *db1221* mutant, thus excluding any contribution from Chromosome X. If the causal mutation is on the X, none of the cross progeny would aggregate. Briefly, we mated *db1221* male mutants with N2 reference strain and used male cross-progeny to cross again with N2. *C. elegans* males are XO, so male cross-progeny inherits only maternal X chromosome. We isolated two independent

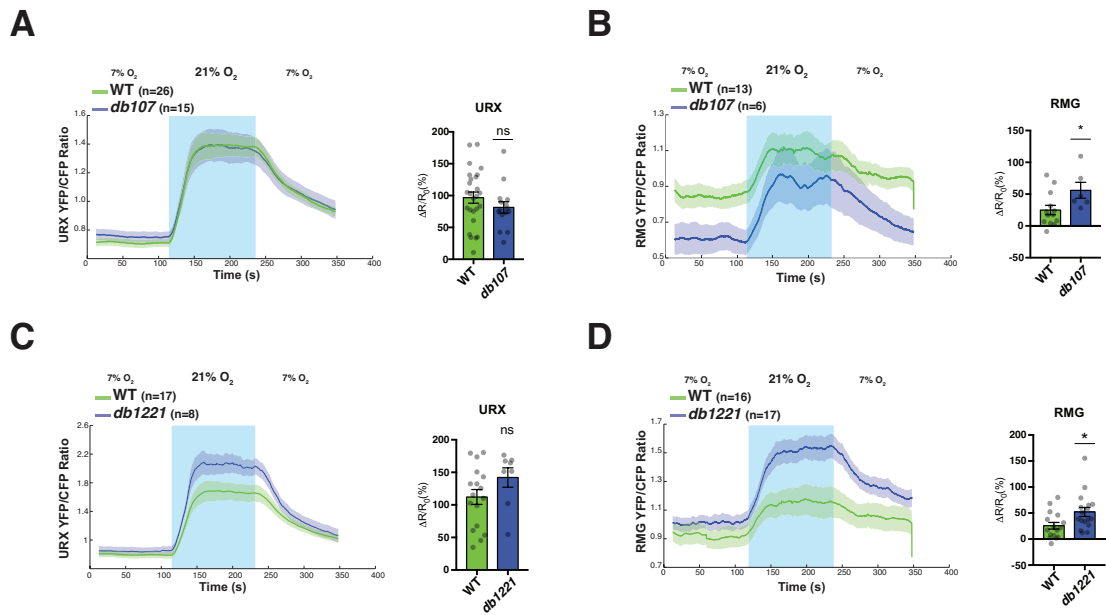


**Figure 3.7 Two mutants show enhanced  $\text{Ca}^{2+}$  activity in RMG  $\text{O}_2$ -sensing neuron**

**(A)** *db107* mutants do not affect URX  $\text{O}_2$ -evoked  $\text{Ca}^{2+}$  response. **(B)** *db107* mutants increase RMG  $\text{O}_2$ -evoked  $\text{Ca}^{2+}$  response. **(C)** *db1221* does not significantly increase URX  $\text{O}_2$ -evoked  $\text{Ca}^{2+}$  responses. **(D)** *db1221* mutants increase RMG  $\text{O}_2$ -evoked  $\text{Ca}^{2+}$  response. (A,C) Plot shows average  $\text{Ca}^{2+}$  response for URX upon 21% oxygen. Bar graph quantifies  $\text{O}_2$ -evoked  $\text{Ca}^{2+}$  responses.  $n$ =number of animals as reported in figure. (B,D) Plot shows average  $\text{Ca}^{2+}$  response for RMG upon 21% oxygen. Bar graph quantifies  $\text{O}_2$ -evoked  $\text{Ca}^{2+}$  responses.  $n$ =number of animals as reported in figure. (A-D)  $\Delta R/R_0$  is calculated using an interval of 30s before and during stimulation (See methods). Statistical comparison between samples was performed using Mann-Whitney  $U$  test. If not differently specified each sample was tested against WT. \*= $p$  value <0.05, \*\*\*\*= $p$  value <0.0001, ns=not significant

aggregating lines, confirming the *db1221* mutation is not on Chromosome X (Data not shown). To confirm which chromosome *db1221* is linked to, we used a 2-point mapping strategy. We chose three available transgenic lines where chromosome II, IV or V had integrated exogenous arrays encoding for a fluorescent marker. *db1221* showed the highest linkage to fluorescent marker on chromosome II in three independent lines compare to IV and V (Appendix Table 3-7). Although contrasting with previous results, we decided to map this linkage further. We again used 3-point mapping and selected a number of phenotypic markers on chromosome II. We chose 3 pair of markers that covered the majority of chromosome II: *sqt-2(sc3)l;lin-31(n301)*, *lin-31(n301);unc-4(e120)* and *sqt-1(sc13);unc-52(e444)*. Since *unc-4*, *unc-52* and *sqt-2* homozygous mutants do not aggregate, we tested the linkage to the other three genes. We isolated 3 out of 12 aggregating lines from recombinants of *sqt-2(sc3)l;lin-31(n301)*, 3 out of 12 aggregating lines from

*lin-31(n301);unc-4(e120)* and 1 out of 12 aggregating lines from *sqt-1(sc13);unc-52(e444)* (Appendix Tables 8-10). Unfortunately, each of these results pointed to the causal mutation being on a different region of chromosome II. Moreover, the ratio of aggregating lines over the total number of lines was very close to 1/4. That is what you would expect if the *db1221* was not linked to chromosome II. All these data taken together pointed to *db1221* not being linked to chromosome II.

Several attempts to isolate *db1221* gave contrasting results. Although we cannot exclude trivial mistakes in the mapping procedures, we think *db1221* might be a more complicated locus than previously thought. However, this diminished our confidence to successfully isolate *db107* since it has an even weaker phenotype than *db1221*. Other genes proved easier to identify, so we turn our attention to them.

### **3.9. The thrombospondin FIG-1 is a glial protein inhibiting O<sub>2</sub>-escape behaviour**

During the isolation of *db106*, we noticed that the original mutant harboured two mutations able to confer O<sub>2</sub>-escape behaviour (Fig 3.5C). We named the second allele *db1239*. To test if *db1239* conferred O<sub>2</sub>-escape behaviour regardless of *dgk-1*, we isolated *db1239* from the original mutant and outcrossed it four times with the N2 reference strain. When stimulated with 21% O<sub>2</sub> *db1239* showed a greater O<sub>2</sub>-evoked speed response compared to wild type (Fig 3.8A). Mutants showed aggregation and bordering phenotypes as well (Fig 3.8B). We next isolated independent outcrossed lines, and submit genomic DNA for whole-genome sequencing. Analysis of the data revealed a large EMS-cluster on chromosome V (Fig 3.8C). The interval did not contain mutations likely to disrupt protein function, so we could not identify candidate genes. We, therefore, decided to pursue *db1239* by additional mapping.

To further map *db1239* on Chromosome V, we choose phenotypic markers covering different portions of the EMS-cluster (Fig 3.8C). We first used a *dpy-11(e224);unc-76(e911)* line to map the EMS-cluster between 6.5 Mb (*dpy-11*) and 15Mb (*unc-76*). We identified 8 out of 13 aggregating recombinants linked to *dpy-11*, thus placing the causal mutation around 11.7Mb (Appendix Table 11). We selected five additional *de novo* mutations spread around 11.7 Mb and sequenced them in 13 recombinants. Results highlighted a region of the mutant chromosome, between 10.2 Mb and 11.2 Mb, that was present in all the aggregating mutants and absent from all solitary recombinants. To further reduce the interval, we selected

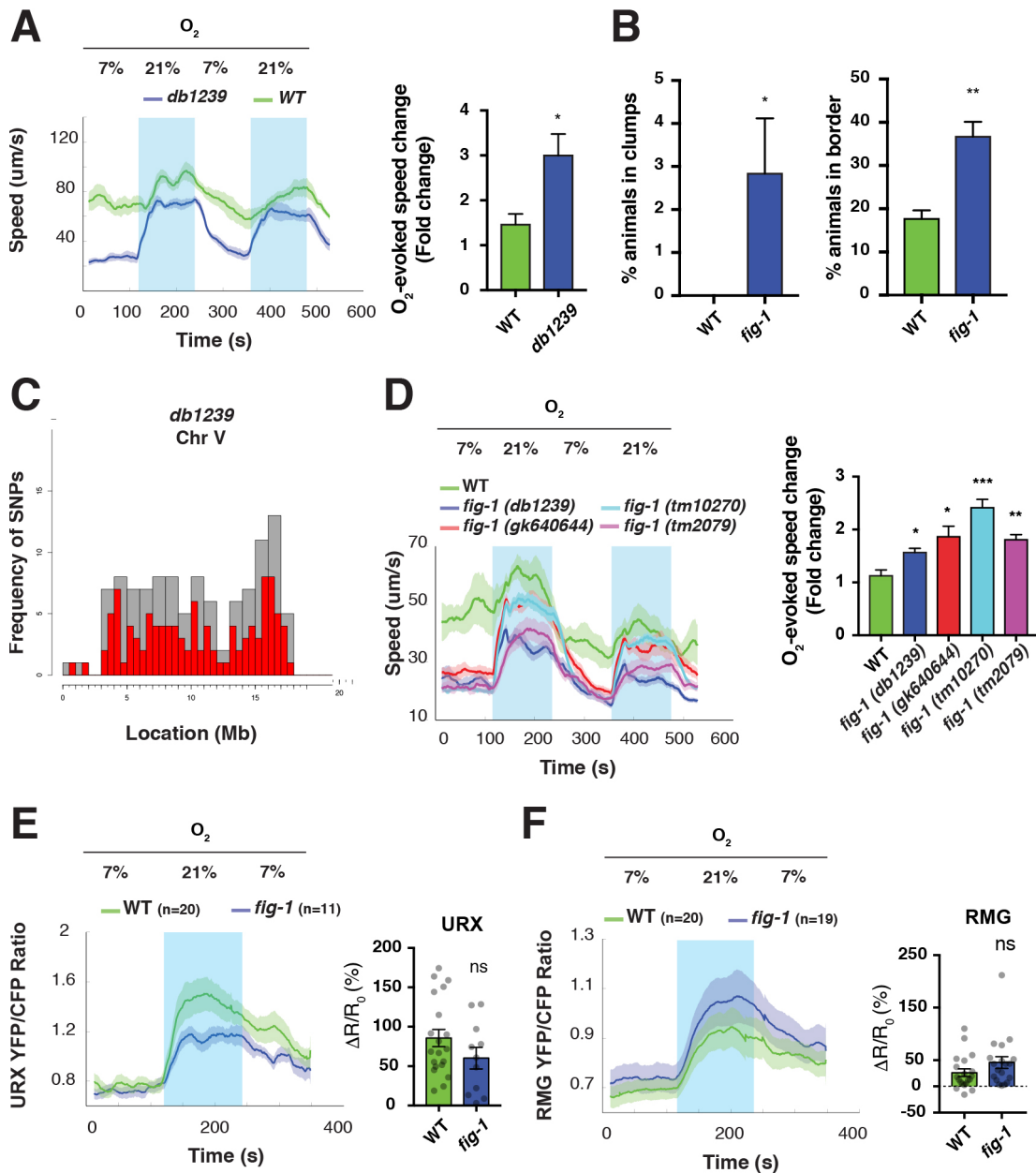


**Figure 3.8 FIG-1 inhibits  $O_2$ -escape behaviour without affecting URX or RMG activity**

**(A)** Speed plot shows *db1239* mutants display  $O_2$ -escape behaviour. Bar graph quantifies  $O_2$ -evoked speed change. **(B)** *db1239* show aggregation and bordering phenotypes. **(C)** Cluster of EMS-induced mutation in *db1239* mutants. **(D)** Multiple independent alleles of *fig-1* confer  $O_2$ -escape behaviour. Average speed of animal stimulated with 7% and 21% oxygen (blue rectangles). N= 6-9 assay. Bar graph shows quantification of  $O_2$ -evoked speed change defined as the fold change between average speed at 21% oxygen and average speed at 7% oxygen (See Methods). **(E,F)** *fig-1* does not affect URX or RMG  $O_2$ -evoked  $Ca^{2+}$  activity. Plot shows average  $Ca^{2+}$  response for URX or RMG upon 21% oxygen. Bar graph quantifies  $O_2$ -evoked  $Ca^{2+}$  responses. n=number of animals as reported in figure. (E,F)  $\Delta R/R_0$  is calculated using an interval of 30s before and during stimulation (See methods). Statistical comparison between samples was performed using Mann-Whitney *U* test. If not differently specified each sample was tested against WT. \*=*p* value <0.05, \*\*=*p* value <0.01, \*\*\*=*p* value <0.001, ns=not significant.

two further mutation within the 10.2-11.2 Mb interval and repeated the 3-point mapping experiment, selecting 96 recombinants. From all 96 recombinants we sequenced mutations at the edges of the interval (9Mb and 13.2Mb) (Appendix Table 12). We selected all lines where we detected a recombination event, and further sequenced within the interval (10.2Mb,11.2Mb and 11.8Mb) (Appendix Table 12). Finally, four lines were sequenced for mutations within 10.1-11.2 Mb interval, narrowing the interval to 0.5Mb. The mapped region comprised just one protein-coding mutation, a missense mutation in the *fig-1* gene. The gene encodes for a thrombospondin containing protein with several cysteine-rich (C6) domains. The mutation changed a cysteine part of a C6 domain into a tyrosine (C1951Y).

To confirm that *fig-1* was the causal mutation, we tested O<sub>2</sub>-escape responses in multiple independent alleles of *fig-1*. We selected three alleles likely to be loss of function (Fig 3.8D). All *fig-1* alleles showed O<sub>2</sub>-response, confirming *fig-1* is inhibiting O<sub>2</sub>-escape behaviour. We also injected *db1239* mutants with a wild type copy of *fig-1* to test if we could rescue the phenotype. However, wild type *fig-1* failed to rescue O<sub>2</sub>-escape behaviour (Data not shown). Taking all data together, we hypothesises the rescue failed because appropriate protein levels are necessary for FIG-1 correct function.

Thrombospondin proteins are secreted from glia in the nervous system and regulate synaptic formation. To test if *fig-1* affects the ability of the O<sub>2</sub>-circuit to perceive oxygen, we measured URX O<sub>2</sub>-evoked activity. We did not measure a disparity of O<sub>2</sub>-evoked activity between *fig-1* and wild type (Fig 3.8E).

Several sensory neurons communicate with the O<sub>2</sub>-circuit and their activity is integrated with that of the O<sub>2</sub>-sensing neurons. *fig-1* might affect other sensory modalities, thus changing the O<sub>2</sub>-circuit by affecting RMG O<sub>2</sub>-responses. To test this hypothesis, we probed *fig-1* mutants for RMG O<sub>2</sub>-evoked responses. Wild type and *fig-1* animals did not show statistically different O<sub>2</sub>-evoked activity in RMG (Fig 3.8F). We concluded that *fig-1* is likely to affect the O<sub>2</sub>-circuit downstream of RMG interneurons.

### **3.10. A glial signalling ligand of the Warthog family, WRT-6, suppresses O<sub>2</sub>-escape behaviour without changing O<sub>2</sub>-circuit activity**

Isolation of *fig-1* through extensive mapping gave us confidence to tackle other mutants that did not show good candidate genes in the EMS-cluster. We focus our attention on *db102* because of its strong phenotype (Fig 3.3A,B). Whole-genome sequencing showed a cluster of mutations on Chromosome X (Fig 3.4A).

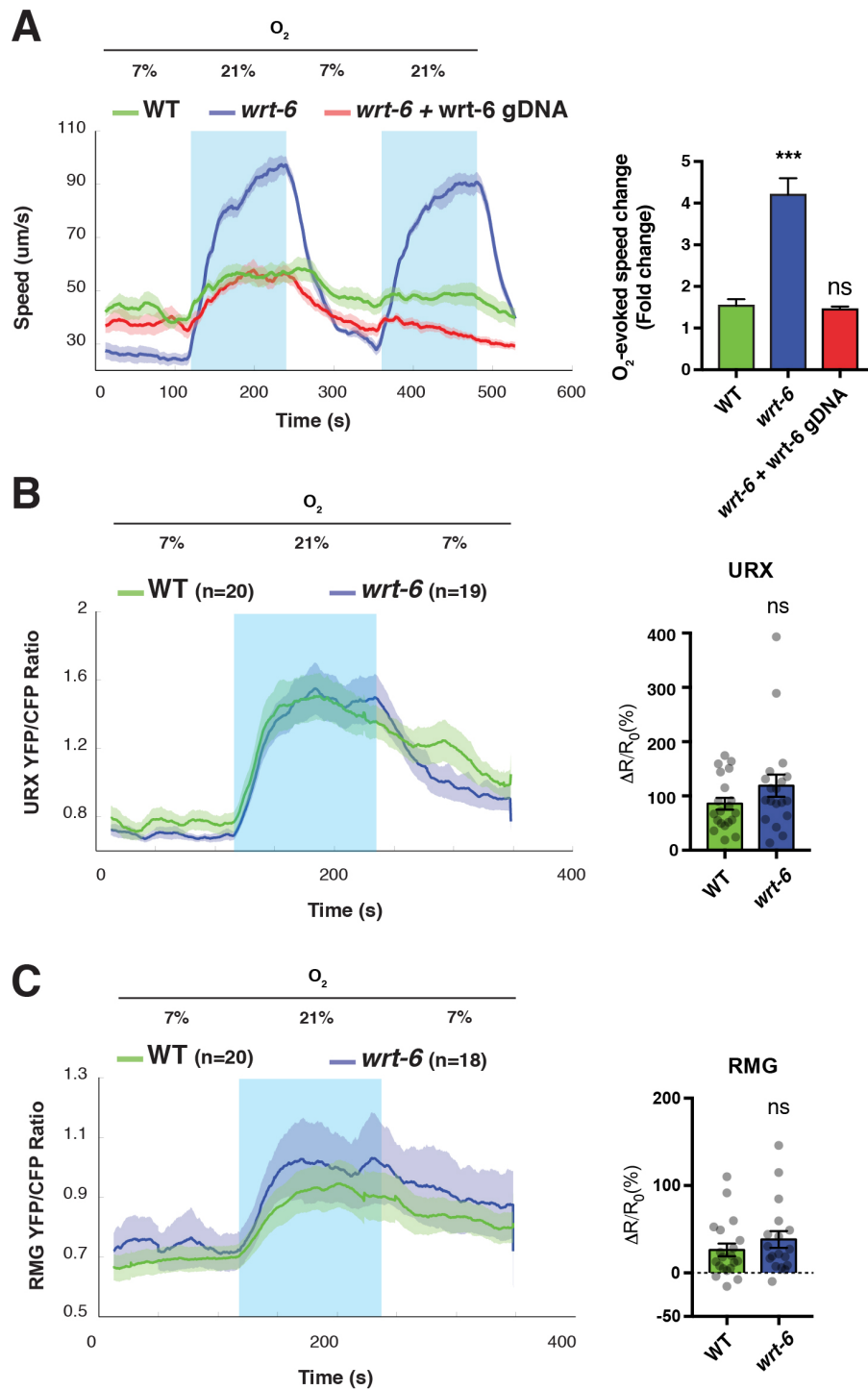


**Figure 3.9 WRT-6 inhibits O<sub>2</sub>-escape behaviour but does not affect URX or RMG O<sub>2</sub>-evoked activity**

**(A)** Speed plot shows *wrt-6* mutants display O<sub>2</sub>-escape behaviour. Bar graph quantifies O<sub>2</sub>-evoked speed change. Average speed of animal stimulated with 7% and 21% oxygen (blue rectangles). N= 6-9 assay. Bar graph shows quantification of O<sub>2</sub>-evoked speed change defined as the fold change between average speed at 21% oxygen and average speed at 7% oxygen (See Methods). **(B,C)** *wrt-6* shows wild types URX or RMG O<sub>2</sub>-evoked Ca<sup>2+</sup> activity. Plot shows average Ca<sup>2+</sup> response for URX or RMG upon 21% oxygen. Bar graph quantifies O<sub>2</sub>-evoked Ca<sup>2+</sup> responses. n=number of animals as reported in figure. (E,F) ΔR/R<sub>0</sub> is calculated using an interval of 30s before and during stimulation (See methods). Statistical comparison between samples was performed using Mann-Whitney *U* test. If not differently specified each sample was tested against WT. \*\*\*=p value <0.001, ns=not significant.

Comparing independent outcrossed lines narrowed the EMS-cluster to an interval between 0.5Mb and 5.5Mb. To map *db102*, we chose an *unc-2(e55);lon-2(e678)* line which covered the 2.7Mb-4.7Mb interval. We screen recombinant and found 4 out of 10 aggregating recombinant lines linked to *lon-2*. This positioned the causal mutation around 3.9Mb. To increase mapping resolution, we selected 5 protein-coding mutations around the interval and sequenced them in the 10 recombinant lines (Appendix Table 13). Due to small size of the interval, we did not identified enough recombination events. We repeated the mapping selecting 40 recombinants. We sequenced the five protein-coding mutations and we selected lines where a recombination event had occurred within the interval (Appendix Table 14). By scoring the aggregation phenotype of these lines, we identified a *db102* genomic region between 3.4Mb and 3.6Mb present in all aggregating lines, but absent from solitary ones. The interval contained a single protein coding mutation in the *wrt-6* gene. The mutation changed a conserved threonine (T460I) which is essential for an auto cleavage processing that renders the protein functional. Thus, the *db102* is likely to be a null allele.

To confirm that *wrt-6* is the causal mutation for *db102* phenotype, we injected mutants with a wild type copy of the gene. Expressing wild type *wrt-6* rescued the *db102* O<sub>2</sub>-escape behaviour (Fig 3.9A), confirming that WRT-6 suppress O<sub>2</sub>-escape behaviour.

WRT-6 is part of large family of secreted proteins similar, in their domain structure, to ligands of the Hedgehog family. Like *fig-1* it is expressed in *C. elegans* glia cells. To test if mutating *wrt-6* had an effect on the O<sub>2</sub>-circuit, we first tested O<sub>2</sub>-evoked responses in URX. *wrt-6* mutants di not show a statistically significant difference in O<sub>2</sub>-perception compared to wild type (Fig 3.9B). Enhanced activity in RMG interneurons drives O<sub>2</sub>-escape behaviour to levels comparable to that of *wrt-6* mutants. We examined RMG activity upon oxygen stimulation and detected no difference between *wrt-6* and wild type (Fig 3.9C). Taking this data into account, we predict *wrt-6* affects the O<sub>2</sub>-circuit downstream of RMG interneurons.

### **3.11. The hyperactive mutant *db1220* is mapped to a small region on Chromosome V**

Aggregation is the result of avoidance of 21% O<sub>2</sub>. How other cues influence aggregation is less clear. In particular, very few mutants are known to confer aggregation without enhancing O<sub>2</sub>-responses. For this reason, we were intrigued by *db1219* and *db1220* mutants which showed aggregation and bordering but not O<sub>2</sub>-escape behaviour (Fig 3.3A,B).

# A

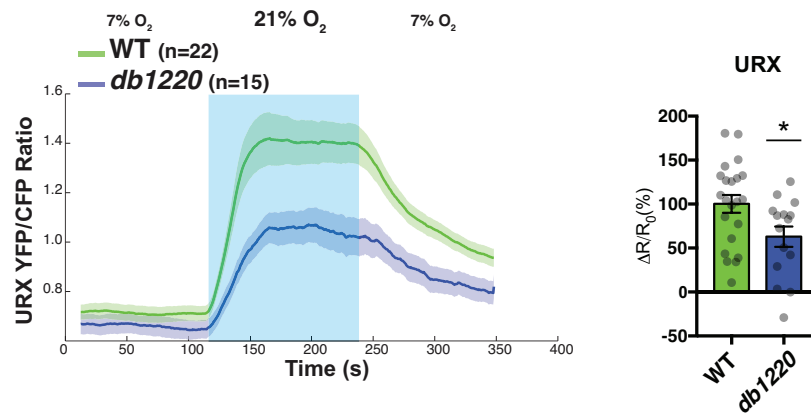


### Figure 3.10 *db1220* mutant impairs O<sub>2</sub>-perception in URX

(A) *db1220* shows impaired URX O<sub>2</sub>-evoked Ca<sup>2+</sup> activity. Plot shows average Ca<sup>2+</sup> response for URX upon 21% oxygen. Bar graph quantifies O<sub>2</sub>-evoked Ca<sup>2+</sup> responses. n=number of animals as reported in figure.  $\Delta R/R_0$  is calculated using an interval of 30s before and during stimulation (See methods). Statistical comparison between samples was performed using Mann-Whitney *U* test. If not differently specified each sample was tested against WT. \*=*p* value <0.05.

Firstly, we examined whole-genome sequencing data for *db1219* mutants. We identified a EMS-cluster on chromosome X (Fig 3.4E and Appendix 2.5). When we inspected *de novo* mutations inside the cluster, we realised many were shared with *db1221* mutants. Mutations on all other chromosomes were different, suggesting the two lines were not identical. Aware of the difficulties we encountered mapping *db1221*, we decided to leave *db1219* and to concentrate on the other mutant.

Analysis of *db1220* whole-genome sequencing data identified an EMS-cluster on Chromosome V (Fig 3.4-F). We screened mutations in the interval and did not find any good candidate. To further map the causal mutation, we employed 3-point mapping. We selected a *dpy-11(e224);unc-76(e911)* line which encompasses the 6.5Mb-15Mb interval. We screened recombinant lines linked to *dpy-11* and found 11 out of 16 aggregating recombinant lines. This placed *db1220* around 12.3 Mb. Next, we picked four unique mutations around 12.3Mb. Sequencing analysis highlighted a 1Mb interval between 13.2Mb and 14.2Mb that was present in all aggregating strains and absent from solitary (Appendix Table 15). Within the interval the best candidate was a missense mutation in the *nuaf-1* gene. However, several

rescue experiments injecting wild type copies of the genes failed (Data not shown). We concluded that the interval we mapped *db1220* was correct, but the causal mutation does not affect *nuaf-1*. There were no other protein-coding mutations within the 1Mb interval. We did not pursue the mapping of *db1220* further, instead we decided to focus our attention on the characterisation of genes we had already isolated.

*db1220* mutants show a characteristic high locomotory activity which does not change regardless of 21% O<sub>2</sub> stimulation (Fig 3.3A). To explain such behaviour, we propose that *db1220* has impaired O<sub>2</sub>-perception, but an overall higher RMG activity which drives the high locomotory activity. To test this hypothesis we tested O<sub>2</sub>-evoked activity in URX O<sub>2</sub>-sensing neurons. As expected mutants showed a marked decrease in their O<sub>2</sub>-evoked activity compared to wild type (Fig 3.10A). We next planned to test RMG O<sub>2</sub>-evoked activity, but a first trial resulted in too few neurons to do a significant comparison with wild type.

### 3.12. Summary

In this chapter we have described the successful isolation of a number of mutants conferring O<sub>2</sub>-escape behaviour on the non aggregating N2 reference strain. After an initial screen of two collections of aggregating strains, we selected 14 mutants which showed either aggregation or O<sub>2</sub>-escape behaviour. Among these mutants, 7 harboured loss of function mutations in *npr-1* and were therefore discarded from further characterisation. For the remaining 7 mutants, we performed whole-genome sequencing to isolate novel genes involved in O<sub>2</sub>-escape behaviour. We first identified *dgk-1* and successfully performed rescue experiments. DGK-1 is known to inhibit synaptic release, and therefore it is likely to regulate O<sub>2</sub>-escape behaviour by increasing synaptic output of URX and RMG neurons. Two other alleles we isolated might regulate O<sub>2</sub>-responses through a similar mechanism. In fact, *db107* and *db1221* both conferred enhanced O<sub>2</sub>-evoked activity on RMG. Unfortunately, multiple mapping attempts failed. While performing rescue experiments for *dgk-1*, we identified an additional allele which we named *db1239*. Mapping experiments led us to identify *fig-1*, a glial thrombospondin containing protein, as an inhibitor of O<sub>2</sub>-escape behaviour. We measured the effect of impairing *fig-1* on the O<sub>2</sub>-circuit and we concluded that the gene is likely to change the circuit downstream of RMG. We isolated a second glial gene, *wrt-6*, a secreted protein with domain similarities to the hedgehog protein family. Based on analysis of URX and RMG O<sub>2</sub>-evoked activity, we concluded that also *wrt-6* is likely to alter the O<sub>2</sub>-circuit downstream of RMG. Finally, we mapped *db1220* to a small 1Mb interval on Chromosome V, but

we failed to identify the causal mutation. This hyper active mutant does not respond to changes in oxygen concentration, which could be explained by defect in URX O<sub>2</sub>-evoked responses.

## **4. QUI-1, a NACHT/WD domains containing protein homologous to human NWD1, inhibits O<sub>2</sub>-escape behaviour and it is required for sensory perception**

### **4.1. Disrupting QUI-1 confers O<sub>2</sub>-escape behaviour**

EMS mutagenesis usually harbours a handful of high impact mutations. To search for mutations causing aggregation behaviour, we examined whole-genome sequencing data for all 8 mutants. A list of *de novo* high impact mutations in *db104* mutants highlighted a cytosine to thymine substitution that introduced a premature stop-codon (Q966Stop) within the *qui-1* gene (Fig 4.1A). To test if the *qui-1* mutation was responsible for the aggregation phenotype, we first examined multiple independent alleles of *qui-1*, including a deletion allele, *ok3571*, which deletes a large region of the protein. When assayed for O<sub>2</sub>-escape behaviour *db104* and *ok3571* showed indistinguishable responses (Fig 4.1B), confirming that loss of *qui-1* confers O<sub>2</sub>-escape behaviour and suggesting *db104* is a strong loss-of-function allele. To further validate *qui-1* effects on O<sub>2</sub>-escape behaviour, we injected a wild type copy of the gene and tested animals for O<sub>2</sub>-responses. Transgenic animals showed wild type-like responses (Fig 4.1C), confirming that *qui-1* inhibits O<sub>2</sub>-escape behaviour.

### **4.2. QUI-1 is a NACHT/WD40 domain containing protein, homologous to human NWD1**

Protein with similar sequences and domain structures tends to perform similar functions. The same is true for homologous proteins: proteins with sequence similarities in different species. To identify homologues, we compared QUI-1 sequence to protein databases. The presence of repeated WD domains in the QUI-1 protein sequence complicated the search for homology. To circumvent this confound, we devised a strategy where we used the QUI-1 N-terminus sequence as a query in our search, thus avoiding the repeated domains (1-900aa for isoform A and 1-642aa for isoform C). This approach identified NWD1 as the closest mammalian homologue (Fig 4.2B and Appendix 3). We also identified another *C. elegans* protein similar to QUI-1, T05C3.2. Phylogenetic analyses, led us to propose that T05C3.2 is a paralogue of QUI-1, since its mammalian homologue, NWD2, is a paralogue of mammalian NWD1 (Fig 4.2C).

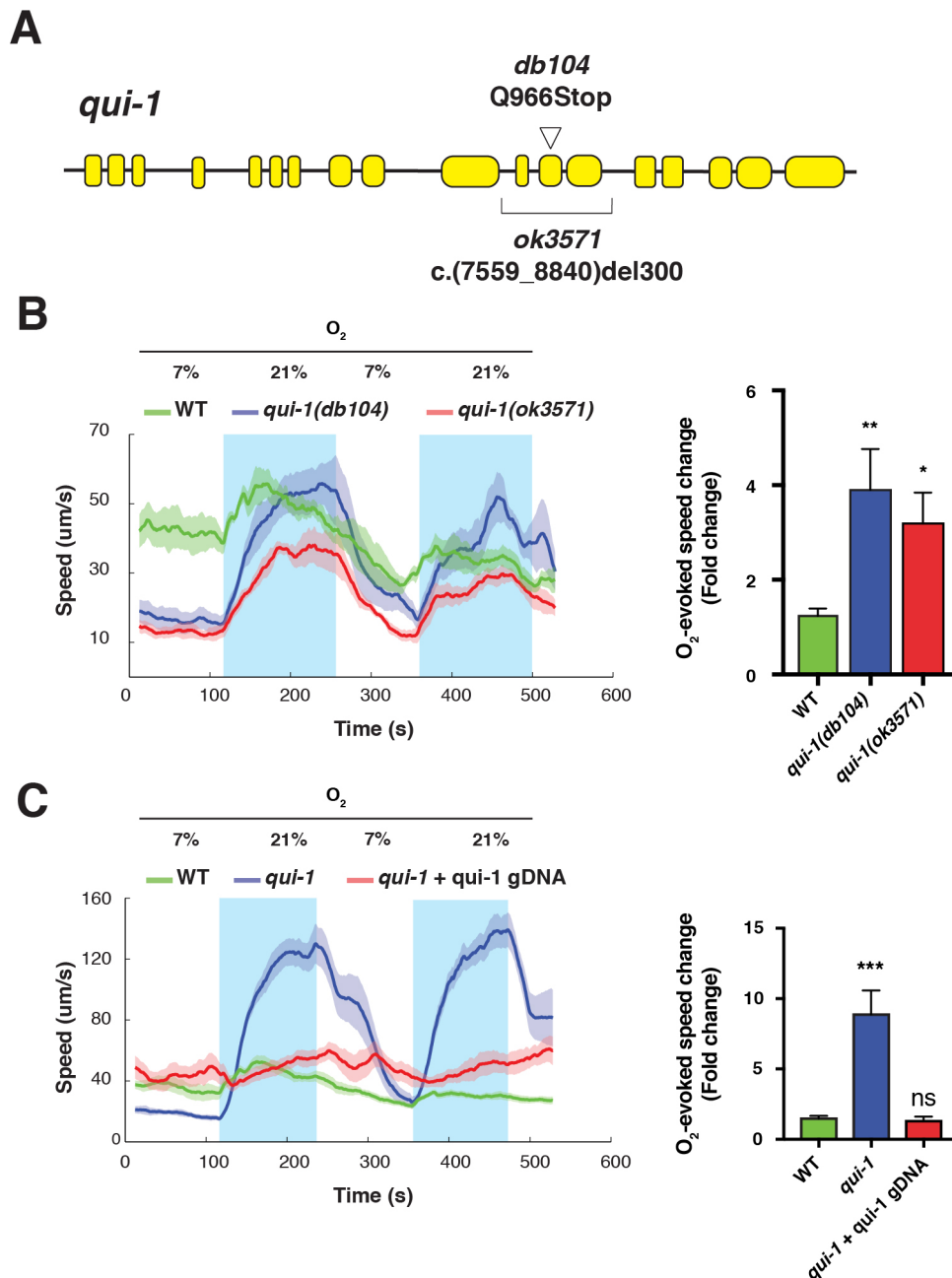


**Figure 4.1 *db104* is a loss of function allele of *qui-1*, a novel regulator of O<sub>2</sub>-escape behaviour**

**(A)** Schematic representation of *qui-1* locus. *db104* and *ok3571* alleles and their genetic lesions are shown. **(B)** *qui-1* and *ok3571* confer O<sub>2</sub>-escape behaviour with similar intensities. **(C)** A wild type copy of *qui-1* rescues the O<sub>2</sub>-escape behaviour of *qui-1* mutants. (B,C) Average speed of animal stimulated with 7% and 21% oxygen (blue rectangles). N= 6-9 assay. Bar graph shows quantification of O<sub>2</sub>-evoked speed change defined as the fold change between average speed at 21% oxygen and average speed at 7% oxygen (See Methods). Statistics: Statistical comparison between samples was performed using Mann-Whitney *U* test. If not differently specified each sample was tested against WT. \*=*p* value <0.05, \*\*=*p* value <0.01, \*\*\*=*p* value <0.001.

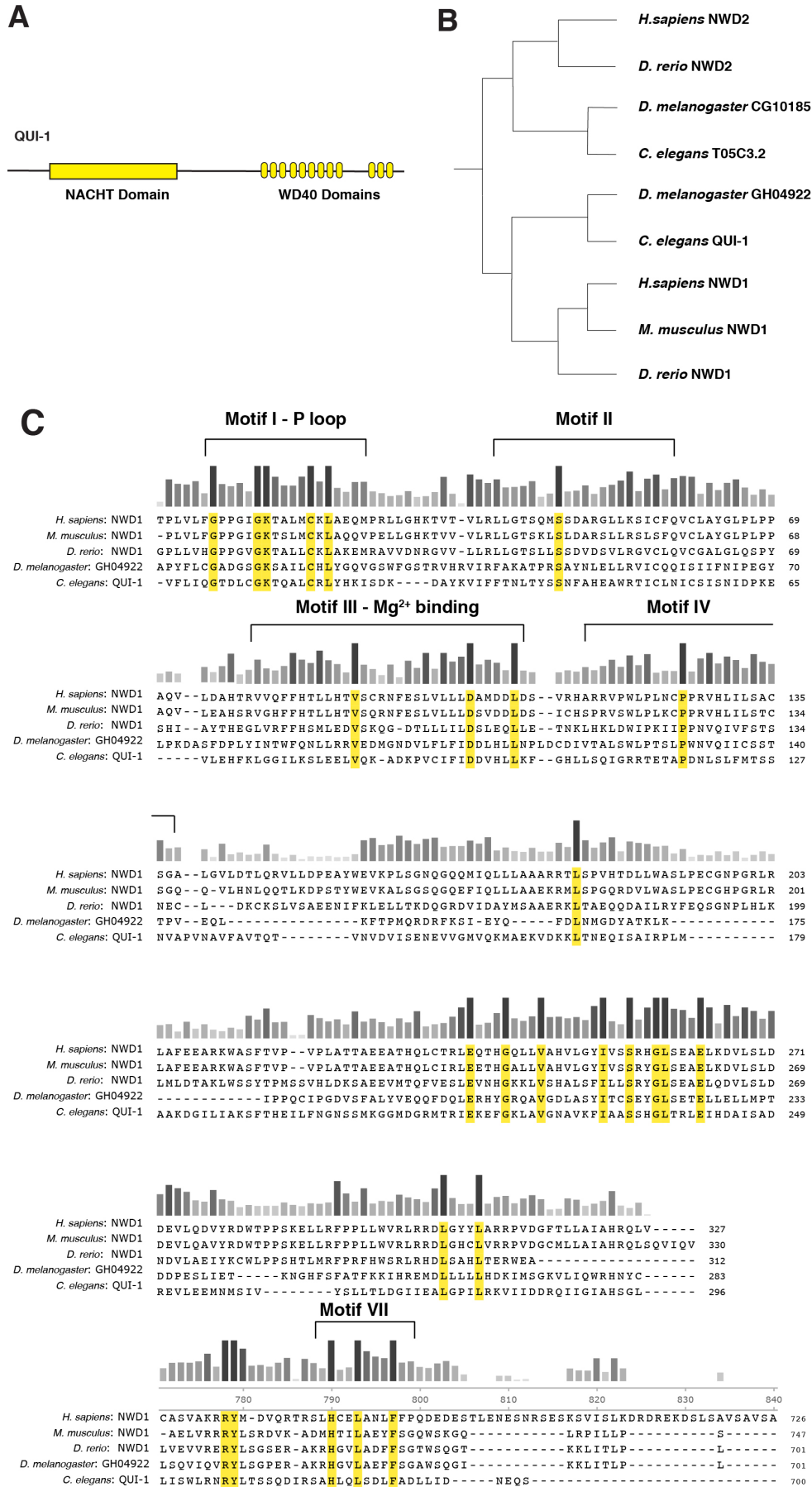


Figure legend in the next page.

**Figure 4.2 QUI-1 is the homologue of mammalian NACHT/WD40 containing protein NWD1**

(A) Schematic representation of QUI-1 protein structure. NACTH and WD40 domains are shown. (B) T05C3.2 is the *C. elegans* paralogue of QUI-1, and it is conserved with the mammalian paralogue of NWD1, NWD2. (C) Protein alignment of NACHT domain of QUI-1 and its homologues in model organisms. Essential components of the NACHT domain are shown. Yellow colour highlights conserved residues while bars show level of conservation.

NACHT domains are present in proteins involved in programmed cell death and transcription of the Major Histocompatibility Complex (MHC). NWD1 combines a NACHT domain with multiple WD40 domains. WD40 domains mediate protein-protein or protein-DNA interactions. We resolve to test if QUI-1 had similar domains, in the hope it could prompt prediction about its function. Based on our previous phylogenetic analysis, we compared the protein sequence of QUI-1 with its homologues in model organisms (Appendix 3). Sequence similarities highlighted a similar domain organisation as NWD1, with WD40 domains and a conserved NACHT domain (Appendix 3 and Fig 4.2C). NACHT domains have an NTPase domain that can mediate ATP/GTP hydrolysis. Most of the Walker A motif ( Motif 1 - P loop ) in this domain, which allows binding of ATP, is conserved between all homologues of QUI-1, suggesting the QUI-1 NACHT domain is likely to be functional.

Together, these data suggest QUI-1 is the *C. elegans* homologue of NWD1, a conserved protein of unknown function.

### **4.3. QUI-1 acts down-stream of neurons integrating O<sub>2</sub>-stimuli**

*qui-1* mutants were first reported in a screen for animals with defective quinine avoidance. Failure to avoid quinine could reflect specific impairment of quinine detection or a more general defect in sensory perception. To investigate if *qui-1* mutants show impaired O<sub>2</sub>-perception, we measured O<sub>2</sub>-evoked activity in URX sensory neurons. We did not detect any significant differences in URX O<sub>2</sub>-evoked activity when comparing *qui-1* mutants with wild type animals (Fig 4.3A). We conclude that *qui-1* does not affect O<sub>2</sub>-sensing per se.

Disrupting *qui-1* might increase escape from O<sub>2</sub> by abrogating sensory inputs that inhibit O<sub>2</sub>-escape behaviour. Escape from 21% O<sub>2</sub> requires the RMG interneurons, whose stimulation is sufficient to evoke high locomotory activity. Enhanced O<sub>2</sub>-evoked activity in RMG could explain how disrupting *qui-1* confers O<sub>2</sub>-escape behaviour at the circuit level. We measured RMG O<sub>2</sub>-evoked responses in *qui-1* mutants, but did not detect a significant difference compared to wild type (Fig

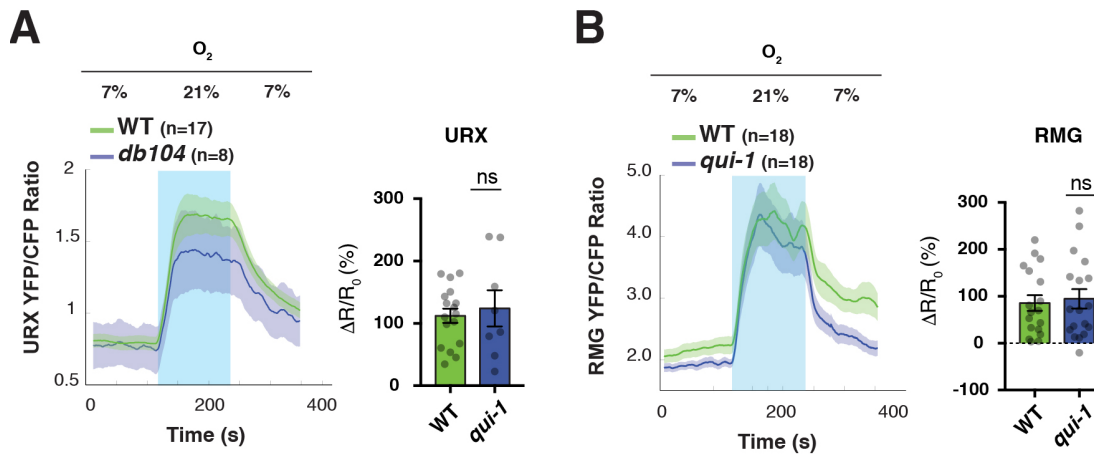


**Figure 4.3 QUI-1 does not affect the O<sub>2</sub>-circuit upstream of RMG interneurons**

**(A)** *qui-1* mutants perceive oxygen as well as wild types in URX. **(B)** *qui-1* mutants do not show defects in O<sub>2</sub>-evoked Ca<sup>2+</sup> activity. (B,C) Bar graphs quantify O<sub>2</sub>-evoked Ca<sup>2+</sup> responses. n=number of animals as reported in figure.  $\Delta R/R_0$  is calculated using an interval of 30s before and during stimulation (See methods). Statistical comparison between samples was performed using Mann-Whitney *U* test. If not differently specified each sample was tested against WT. ns = not significant.

4.3B). We conclude that *qui-1*, like other genes we isolated, likely exerts its effects on the O<sub>2</sub>-circuit downstream of RMG.

#### 4.4. QUI-1 is required in sensory neurons that sense avoidance cues and promote aggregation

Two additional sensory neurons, ASH and ADL, have previously been shown to promote escape from 21% O<sub>2</sub> without being themselves primary oxygen sensors. ASH and ADL are nociceptors that elicit avoidance from a variety of chemical and non-chemical stimuli, ranging from copper (ASH) to pheromones (ADL). Like URX, ASH and ADL are connected to RMG interneurons by gap junctions, and both neurons exhibit O<sub>2</sub>-evoked Ca<sup>2+</sup> responses. Moreover, their ablation disrupts aggregation. Previous work showed that *qui-1* is expressed in three sensory neurons, ASH ADL and PHB, and two interneurons, PVQ and RMD. We asked if *qui-1* acts in either ASH or ADL to inhibit O<sub>2</sub>-escape behaviour. Transgenic animals expressing *qui-1* exclusively in ASH neurons showed a reduced O<sub>2</sub>-response when compared to *qui-1* mutants (Fig 4.4A). The rescue was not complete as transgenic animals retained an O<sub>2</sub>-response significantly greater than wild type controls (Fig 4.4A). *qui-1* animals expressing *qui-1* in ADL alone also showed a marked reduction in O<sub>2</sub>-escape behaviour (Fig 4.4B). As for ASH rescue, rescued animals retained significantly higher locomotory activity at 21% O<sub>2</sub> than wild type animals (Fig 4.4B). We conclude that *qui-1* acts in ADL and ASH neurons to suppress O<sub>2</sub>-escape behaviour.

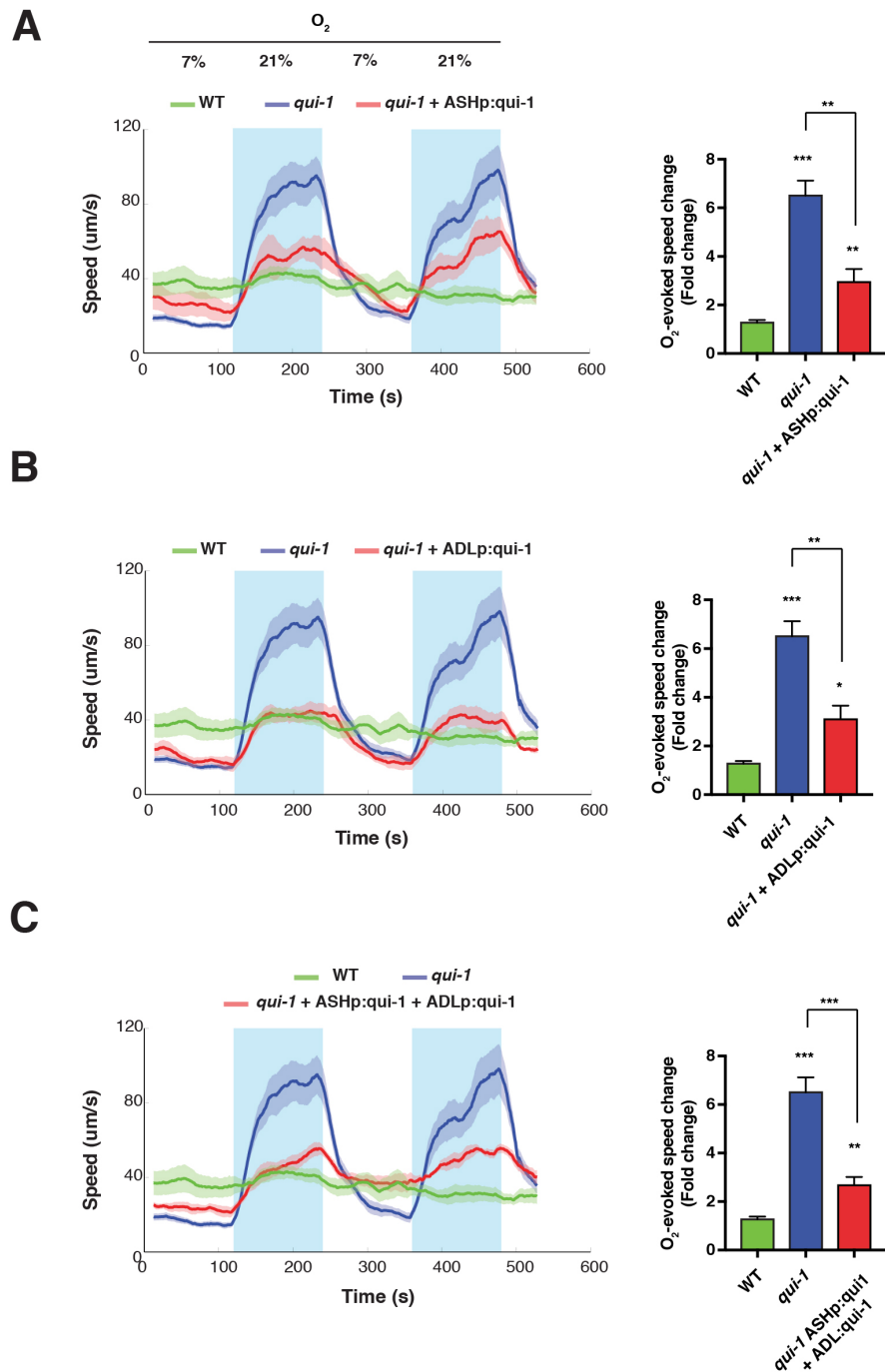


**Figure 4.4 QUI-1 is required in ASH and ADL sensory neurons to inhibit O<sub>2</sub>-escape behaviour**

**(A)** Expressing *qui-1* exclusively in ASH partially rescues the O<sub>2</sub>-escape behaviour of *qui-1* mutants. **(B)** Expressing *qui-1* exclusively in ADL partially rescues the O<sub>2</sub>-escape behaviour of *qui-1* mutants. **(C)** Expressing *qui-1* in combination in ASH and ADL is not sufficient to fully rescue O<sub>2</sub>-escape behaviour. (A-C) Average speed of animal stimulated with 7% and 21% oxygen (blue rectangles). N= 6-9 assay. Bar graph shows quantification of O<sub>2</sub>-evoked speed change defined as the fold change between average speed at 21% oxygen and average speed at 7% oxygen (See Methods). Statistics: Statistical comparison between samples was performed using Mann-Whitney *U* test. If not differently specified each sample was tested against WT. (A-C) Rescue lines expressing *qui-1* in ASH, ADL or ASH+ADL were tested against *qui-1* to show partial rescue. \* = p value < 0.05 \*\* = p value < 0.01, \*\*\*\* = p value < 0.0001.

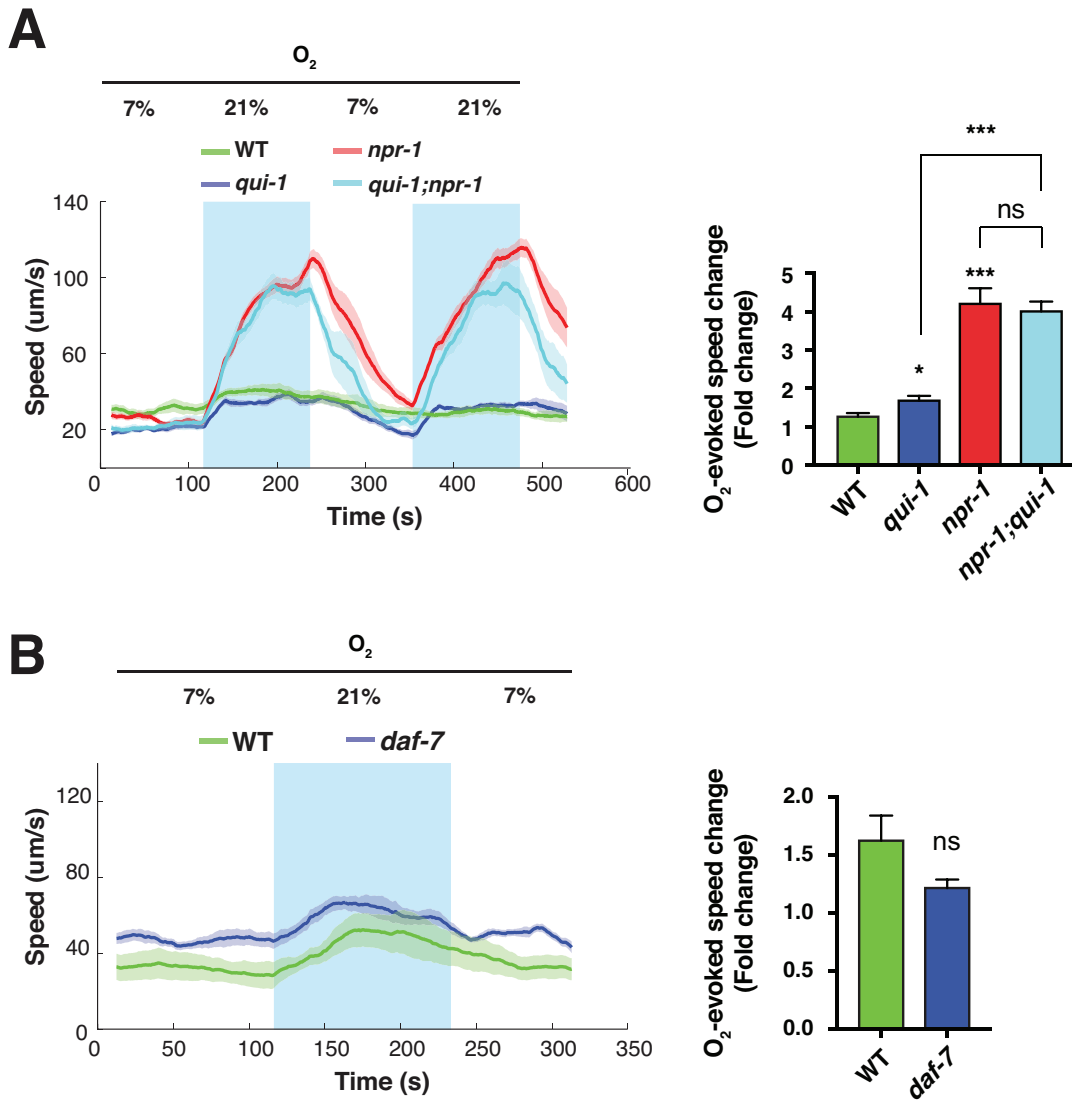


**Figure 4.5 *qui-1* is part of the *npr-1* genetic pathway**

**(A)** *qui-1;npr-1* double mutants resemble *npr-1* and not *qui-1* mutants. **(B)** *daf-7* mutants do not show O<sub>2</sub>-escape behaviour. (A,B) Average speed of animal stimulated with 7% and 21% oxygen (blue rectangles). N= 6-9 assay. Bar graph shows quantification of O<sub>2</sub>-evoked speed change defined as the fold change between average speed at 21% oxygen and average speed at 7% oxygen (See Methods). Statistics: Statistical comparison between samples was performed using Mann-Whitney U test. If not differently specified each sample was tested against WT. (A) *npr-1;qui-1* mutants were tested to against *qui-1* and *npr-1* to group *qui-1* into *npr-1* genetic pathway. \* = p value < 0.05, \*\*\* = p value < 0.0001, ns = not significant.

To test if QUI-1 needs to be expressed in both ASH and ADL neurons to completely suppress O<sub>2</sub>-escape behaviour in *qui-1* mutants, we selectively expressed *qui-1* in ASH and ADL, and assayed these animals for their O<sub>2</sub>-escape behaviour. The transgenic animals displayed a marked reduction in O<sub>2</sub>-evoked speed change compared to *qui-1* mutants (Fig 4.4C). Their O<sub>2</sub>-response was, however, still higher than wild type (Fig 4.4C). These data suggest that expressing *qui-1* in ASH and

ADL neurons is not sufficient to completely rescue the O<sub>2</sub>-escape behaviour of *qui-1* mutants. However, we cannot rule out that our heterologous promoters do not drive appropriate levels of *qui-1* expression.

#### **4.5. *qui-1* acts in the same genetic pathway as *npr-1***

Defects in a small number of genes confer on the N2 reference strain O<sub>2</sub>-escape behaviour and aggregation. These genes act in two distinct genetic pathways: the *npr-1* pathway and the *daf-7* pathway. Consistent with *npr-1* and *daf-7* regulating different genetic pathways, *npr-1;daf-7* double null mutants aggregate more strongly than either single null mutant. To test if *qui-1* acts in the *npr-1* pathway, we generated *qui-1;npr-1* double mutants and quantified their O<sub>2</sub>-escape behaviour. Unexpectedly, these animals tended to leave the bacterial lawn upon 21% oxygen stimulation, making analysis impossible. *qui-1* single mutants also left the bacterial lawn more frequently than N2 controls after 21% stimulation although less than the *qui-1;npr-1* double mutants. (Data not shown). To overcome this problem, we recorded O<sub>2</sub>-escape behaviour on a thicker bacterial lawn which suppressed *qui-1* and *qui-1;npr-1* food leaving. On a thicker bacterial lawn *qui-1* mutants showed a reduced but still significant O<sub>2</sub>-evoked speed change (Fig 4.5A). *qui-1;npr-1* double mutants showed a O<sub>2</sub>-response higher than *qui-1* mutants alone (Fig 4.5A), but undistinguishable from *npr-1* mutants (Fig 4.5A). This observation suggests *qui-1* acts in the same pathways as *npr-1* to inhibit O<sub>2</sub>-escape behaviour. In support of this result we find that disrupting *daf-7* did not significantly alter O<sub>2</sub>-escape behaviour (Fig 4.5B). We conclude that *qui-1* is likely to work in the same genetic pathway as *npr-1*.

#### **4.6. QUI-1 is required for pheromone sensing**

Although *qui-1* mutants show defective avoidance of quinine, QUI-1's role in chemo-sensation is not well understood. We examined if *qui-1* mutants fail to elicit a Ca<sup>2+</sup>-response upon chemical stimulation, which would implicate QUI-1 in sensory transduction. We tested this hypothesis by measuring pheromone sensing in the ADL sensory neurons as *qui-1* is expressed in ADL. In wild type animals ADL neurons respond to stimulation by the C9 ascaroside pheromone family with a transient influx of Ca<sup>2+</sup>, while, we observed a striking defect in *qui-1* mutants where stimulus-evoked Ca<sup>2+</sup> activity was completely abolished (Fig 4.6A). We concluded that QUI-1 is involved in sensory transduction and it mediates pheromones sensing by coupling stimulus detection to Ca<sup>2+</sup> intake. QUI-1 could achieve this coupling either directly or indirectly. To answer this question a more detailed characterisation of QUI-1 molecular function is needed.

# A

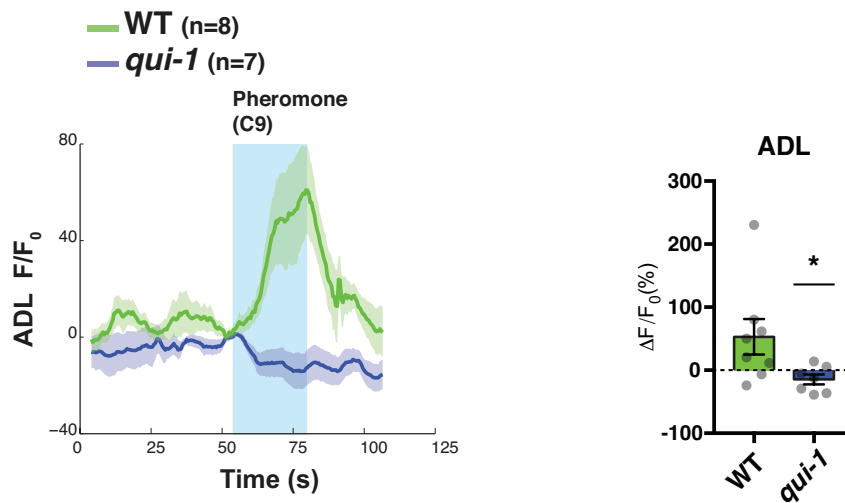


**Figure 4.6 QUI-1 is required for C9-sensing in ADL sensory neurons**

**(A)** Absence of *qui-1* abolishes C9-evoked Ca<sup>2+</sup> activity in ADL neurons. Bar graphs quantify O<sub>2</sub>-evoked Ca<sup>2+</sup> responses. n=number of animals as reported in figure. ΔF/F<sub>0</sub> is calculated using an interval of 30s before and during stimulation (See methods). Statistics: Statistical comparison between samples was performed using Mann-Whitney *U* test. If not differently specified each sample was tested against WT. \*=p value <0.05.

#### 4.7. *qui-1* mutant show enhanced dense core vesicles release from ADL neurons

Our data presented a conundrum. On one hand, ASH and ADL neurons promote aggregation behaviour and escape from 21% O<sub>2</sub>, since ablating these neurons disrupts both behaviours. On the other hand, mutations in *qui-1*, which disrupts sensory transduction in ADL and possibly ASH neurons, promote aggregation and escape from 21% O<sub>2</sub>. To resolve this issue we decided to investigate the effects of removing *qui-1* on their neurosecretion. We predict *qui-1* mutants might show enhanced neural secretion thus explaining their behavioural phenotypes. To address this question, we used a reporter transgenic line where an insulin-like peptide tagged with a fluorescent protein (DAF-28:mCherry) is expressed exclusively in ADL neurons. In *C. elegans* secreted proteins accumulate in scavengers cells, and measuring accumulation of fluorescence proteins in these cells provides a readout of neurosecretion. Our data showed a remarkable increase in ADL neural secretion in *qui-1* mutants compared to wild type (Fig 4.7A). We concluded that absence of *qui-1* enhances ADL neurosecretion.

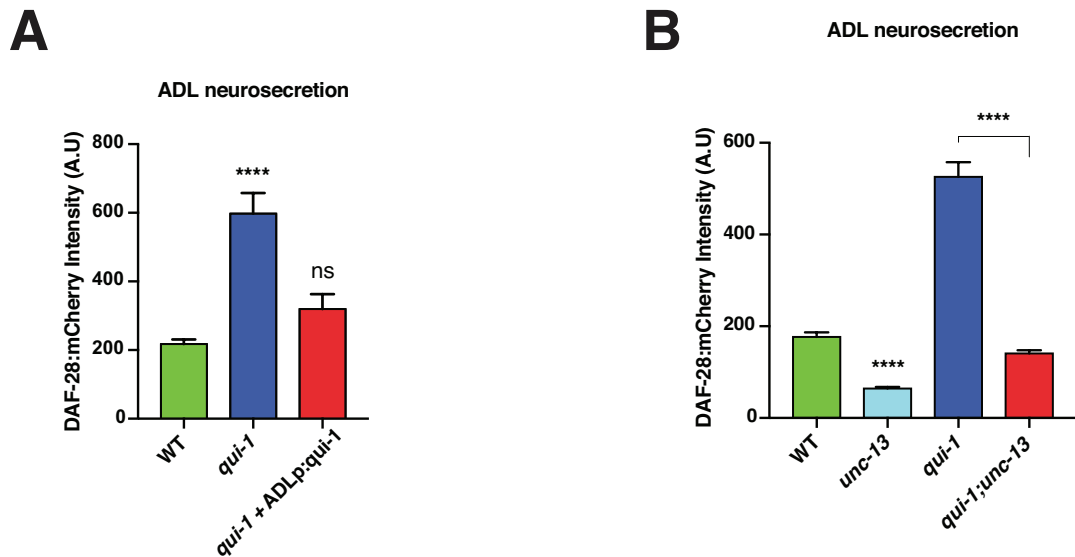


**Figure 4.7 Absence of *qui-1* enhances  $Ca^{2+}$ -triggered DCV release in ADL**

**(A)** *qui-1* shows enhanced DCV release from ADL which is rescued by expressing *qui-1* in ADL. **(B)** *qui-1* enhanced neurosecretion depends on components of the  $Ca^{2+}$ -mediated DCV release machinery (UNC-13). (A,B) Bar graphs show intensity of neurosecretion (See Methods). Statistics: Statistical comparison between samples was performed using Mann-Whitney *U* test. If not differently specified each sample was tested against WT (B) *qui-1* mutants were tested against *qui-1;unc-13* double mutants to show extent of suppression of neurosecretion by abolishing UNC-13-mediated release. \*\*\*\*=p value <0.0001.

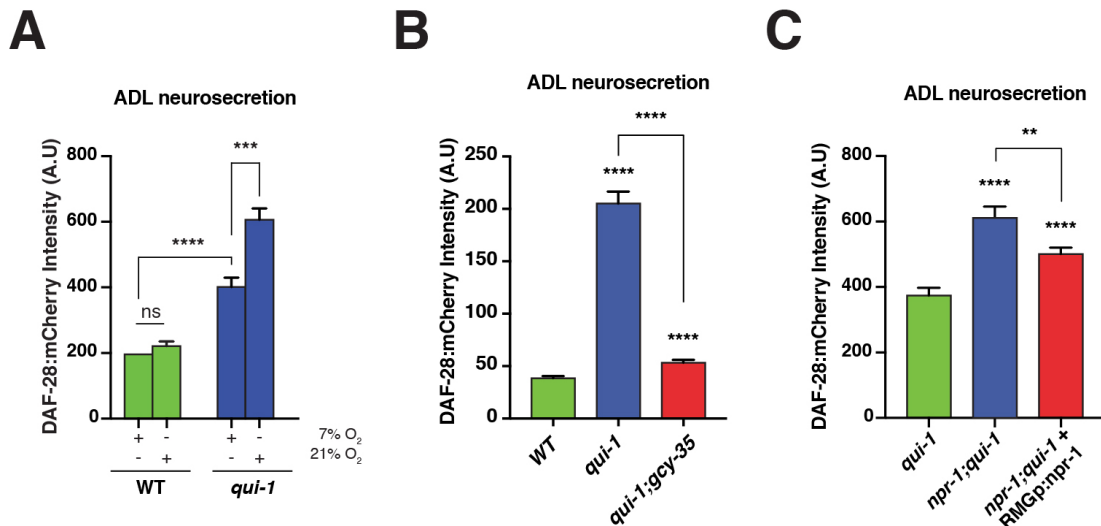
To test if QUI-1 acts in ADL to inhibit ADL neurosecretion we expressed *qui-1* exclusively in ADL, and looked for rescue of the enhanced neurosecretion phenotype of *qui-1* mutants. As expected, the *qui-1* phenotype was completely rescued (Fig 4.7A).

Insulin-like peptides are stored in dense-core vesicles (DCV) that are trafficked to the plasma membrane and often to synapses from where they are released upon  $Ca^{2+}$  entry.  $Ca^{2+}$ -triggered dense-core vesicles release is controlled in part by UNC-13, an active zone protein which mediate membrane fusion when  $Ca^{2+}$  concentration increases. To confirm that tagged DAF-28 was released through activity-triggered dense-core vesicles fusion, we measured ADL neural secretion in *unc-13* mutants. We observed a marked reduction of tagged DAF-28 accumulation in coelomocytes in *unc-13* mutants compared to wild type (Fig 4.7B). Similarly, when we compared *qui-1* mutants and *qui-1;unc-13* double mutants, we observed a drastic reduction in neural secretion (Fig 4.7B). These data show that DAF-28:mCherry is secreted in an  $Ca^{2+}$ -dependent manner using the DCV release machinery not only in wild type, but also in *qui-1* mutants (Fig 4.7B). We conclude that loss of *qui-1* enhances  $Ca^{2+}$ -dependent neural secretion from ADL.

#### 4.8. Removing *qui-1* recruits ADL in the O<sub>2</sub>-circuit

Why do *qui-1* mutants exhibit increased neurosecretion from ADL neurons? One hypothesis prompted by the increased O<sub>2</sub>-escape phenotype is that increased ADL neurosecretion reflects increased activation of ADL by pre-synaptic neurons, including O<sub>2</sub> sensors. To investigate this, we raised wild type and *qui-1* mutants at 7% and 21% oxygen and assayed ADL neural secretion. As expected, ADL neurosecretion in wild type animals was unaffected by the oxygen concentration they experienced (Fig 4.8A). By contrast, neurosecretion from ADL was significantly modulated by O<sub>2</sub> experience in *qui-1* mutants (Fig 4.8A). Mutants kept at low oxygen concentrations showed a marked reduction in ADL neurosecretion (Fig 4.8A). Dense-core vesicle release in *qui-1* mutants did not rely entirely on high oxygen levels. *qui-1* mutants exposed to low oxygen levels retained significantly higher neurosecretion than wild type controls (Fig 4.8A). Together, these data suggest that in *qui-1* mutants ADL neurons respond more strongly to input from pre-synaptic neurons, including O<sub>2</sub>-sensors, and that this leads to increased tonic neurosecretion from ADL.

*qui-1* mutants retained high levels of neurosecretion while experiencing low oxygen concentrations (Fig 4.8A). Is this activity coming from the O<sub>2</sub>-circuit or other pre-synaptic neurons to ADL? To address this question we crossed our *qui-1* reporter line into *gcy-35* mutants. GCY-35 is the main molecular oxygen sensor, it is expressed in O<sub>2</sub>-sensing neurons including AQR, PQR and URX, and *gcy-35* mutants fails to detect oxygen. Mutating *gcy-35* almost completely abolished *qui-1* induced ADL neurosecretion (Fig 4.8B), suggesting pre-synaptic inputs from the O<sub>2</sub>-circuit are responsible for ADL neurosecretion in *qui-1* mutants. To identify some of these pre-synaptic neurons, we tested if RMG, which is connected to ADL through electrical synapses, might alter ADL neurosecretion. This communication is inhibited by the gain of function NPR-1 215V isoform. To test this hypothesis, we assayed ADL neurosecretion in *qui-1* and *qui-1;npr-1* double mutants and as expected we observed an increase in ADL neurosecretion in *qui-1;npr-1* double mutants (Fig 4.8C). Although it has been proposed that NPR-1 function in RMG to inhibit RMG-ADL communication, this has not been properly tested yet. By expressing the gain of function NPR-1 215V isoform exclusively in RMG (Fig 4.8C), we showed NPR-1 acts, at least in part, in RMG neurons to suppress ADL neurosecretion. This suggest ADL O<sub>2</sub>-evoked neurosecretion is driven in part by pre-synaptic inputs from RMG.

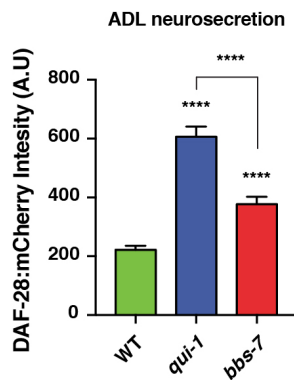
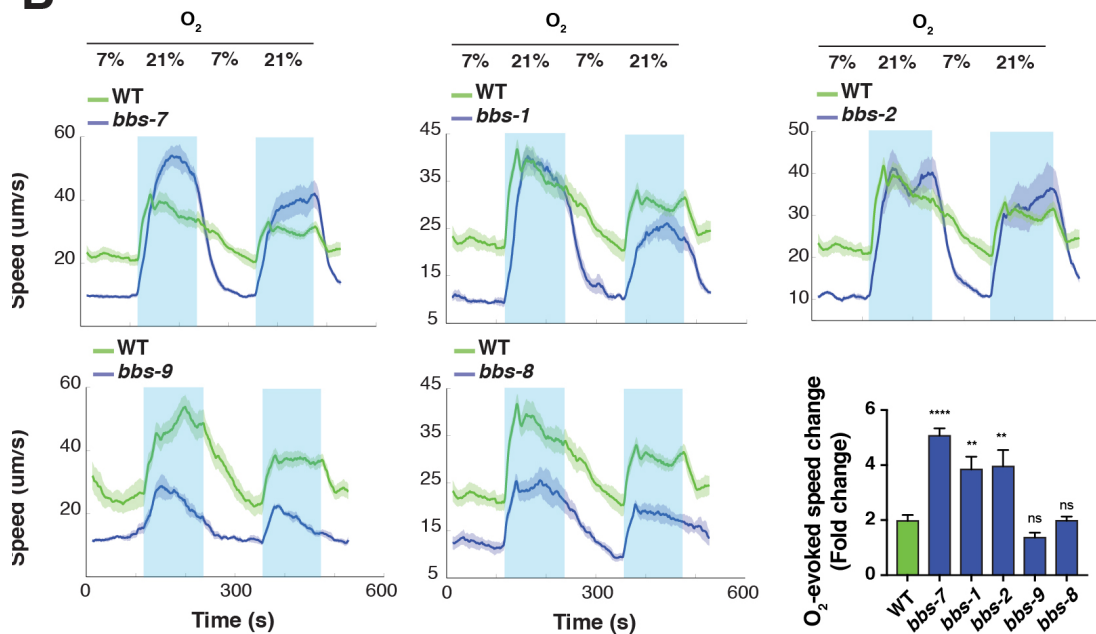


**Figure 4.8 Absence of *qui-1* confer O<sub>2</sub>-evoked neurosecretion on ADL which is modulated by the O<sub>2</sub>-circuit**

(A) Raising animals at high (21%) or low (7%) oxygen modulates ADL neurosecretion in *qui-1* mutants, but not in wild types. (B) ADL neurosecretion is dependent on oxygen detection. (C) ADL O<sub>2</sub>-evoked neurosecretion is modulated at least in part by activity of NPR-1 in RMG interneurons. (A-C) Bar graphs show intensity of neurosecretion (See Methods). Statistics: Statistical comparison between samples was performed using Mann-Whitney *U* test. If not differently specified each sample was tested against WT (A) *qui-1* mutants grown at 21% oxygen were tested against *qui-1* mutants grown at 7% to show O<sub>2</sub>-evoked neurosecretion in ADL. *qui-1* mutants grown at 7% oxygen were tested against wild types grown under same condition to show *qui-1* shows a still higher neurosecretion. Wild types were grown at 21% or 7% to show they do not modulated ADL neurosecretion. (B) *qui-1* mutants were tested against *qui-1;gcy-35* to show suppression of ADL neurosecretion by mutating GCY-35. (C) If not specified samples were tested against *qui-1* mutants. *npr-1;qui-1* were tested against *npr-1;qui-1 + RMGp:npr-1* to show NPR-1 acts partially in RMG. \*\*=*p* value <0.01, \*\*\*=*p* value <0.001, \*\*\*\*=*p* value <0.0001, ns= not significant.

#### 4.9. *bbs* mutants also exhibit increased O<sub>2</sub>-escape behaviour

Recently, a group of genes associated with Bardet-Biedl syndrome, called *bbs* genes in *C. elegans*, has been proposed to reduce, by unknown mechanism, neurosecretion. *bbs* genes encode components of a large protein complex, the BBsome, which binds cargo vesicles to motor proteins for their delivery to cilia. Several *bbs* mutants have been shown to confer on ADL neurons increased dense-core vesicle release. The phenotypic similarities between *bbs* and *qui-1* mutants, prompted us to compare these mutants further. We first compared ADL neurosecretion in *bbs-7* and *qui-1* mutants. As expected we observed a robust increase in ADL neurosecretion in *bbs-7* mutants compared to wild type (Fig 4.9A), although the *qui-1* phenotype was stronger. Moreover, when we measured O<sub>2</sub>-escape behaviour in five *bbs* mutants we found that three mutants, *bbs-7*, *bbs-1*, and *bbs-2* conferred O<sub>2</sub>-escape behaviour (Fig 4.9B). These data strengthen the link between increased ADL neurosecretion and increased escape from 21% O<sub>2</sub>.

**A****B**

#### Figure 4.9 *bbs-7*, *bbs-1* and *bbs-2* confer O<sub>2</sub>-escape behaviour

**(A)** *qui-1* mutants shows higher levels of neurosecretion from ADL compared to *bbs-7* mutants. Bar graphs show intensity of neurosecretion (See Methods). **(B)** Average speed of animal stimulated with 7% and 21% oxygen (blue rectangles). N= 6-9 assay. Bar graph shows quantification of O<sub>2</sub>-evoked speed change defined as the fold change between average speed at 21% oxygen and average speed at 7% oxygen (See Methods). Statistics: Statistical comparison between samples was performed using Mann-Whitney *U* test. If not differently specified each sample was tested against WT. (A) *qui-1* mutants were tested against *bbs-7* mutants to show higher levels of neurosecretion. \*\*=p value <0.01, \*\*\*\*=p value <0.0001, ns= not significant.

#### 4.10. High levels of neurosecretion are observed in several aggregating mutants

Does enhanced neurosecretion in *qui-1* and *bbs* mutants reflect a common defect? Is this common defect a deficit in sensory perception that result in a sensitisation of ADL to pre-synaptic inputs? To probe this hypothesis, we asked if other

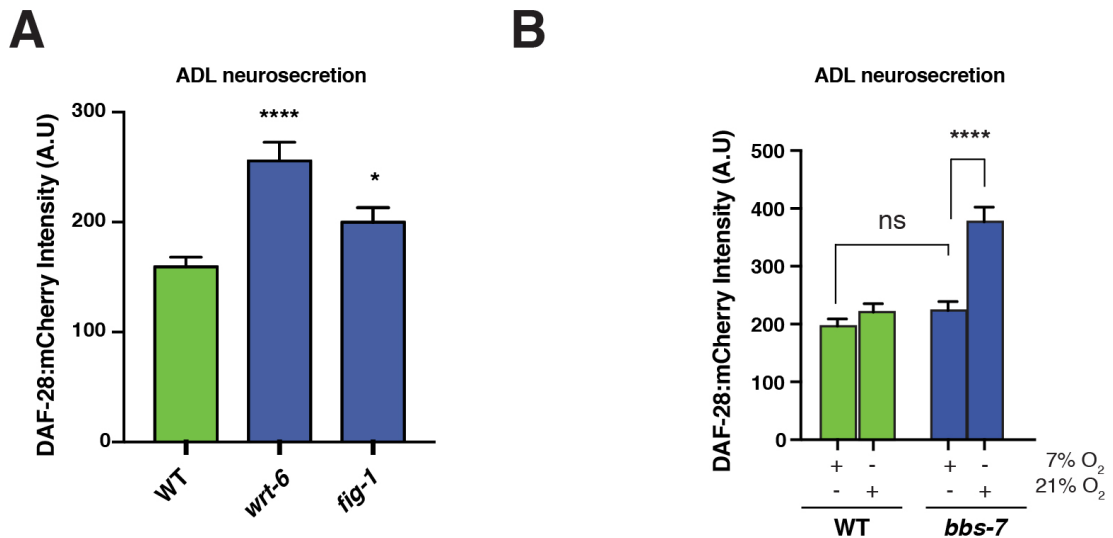


**Figure 4.10 Sensory defective mutants show O<sub>2</sub>-evoked neurosecretion in ADL**  
**(A)** Sensory defective mutants *wrt-6* and *fig-1* show enhanced ADL neurosecretion. **(B)** Rearing *bbs-7* mutants at high (21%) and low (7%) oxygen concentrations modulates their ADL neurosecretion. (A,B) Bar graphs show intensity of neurosecretion (See Methods). Statistics: Statistical comparison between samples was performed using Mann-Whitney *U* test. If not differently specified each sample was tested against WT. (B) *bbs-7* mutants reared at 7% oxygen were tested against *bbs-7* mutants reared at 21% oxygen and wild type reared at 7% oxygen to show *bbs-7* confers O<sub>2</sub>-evoked neurosecretion on ADL. \* = p value < 0.05, \*\*\*\* = p value < 0.0001, ns = not significant.

aggregation mutants in our collection showed defective sensory perception and increased ADL neural secretion. We focussed our search to mutants for which we had previously identified causal mutations (*dgk-1*, *wrt-6* and *fig-1*). DGK-1 modulates rather than sustains sensory perception, and *dgk-1* mutant do not show sensory defects. On the other hand, *wrt-6* and *fig-1* mutants have been reported to have sensory defects. Therefore, we measured ADL neurosecretion levels in these mutants, and observed a robust and significant increase compared to wild type (Fig 4.10A). We noted that *wrt-6* and *fig-1* are expressed in glia and not neurons, and are unlikely to regulate neural secretion directly. Instead, we hypothesise that losing *wrt-6* or *fig-1* impairs ADL sensory perception which sensitises ADL neurons to pre-synaptic inputs.

#### 4.11. Impairing sensory inputs confers O<sub>2</sub>-evoked neurosecretion on ADL sensory neurons

If depriving sensory neurons of their physiological responses through genetic deletion leads to sensitisation, then incoming neural activity should elicit a larger response. ADL does not detect oxygen on its own, but its O<sub>2</sub>-evoked responses are contingent to incoming activity from O<sub>2</sub>-circuit. We devised a strategy where we could measure ADL incoming activity by exposing animals to different oxygen

concentrations and measuring effect on ADL activity. To test this strategy, we raised sensory defective mutants, *bbs-7*, at 7% or 21% oxygen and measured ADL neurosecretion. *bbs-7* mutants grown at 7% oxygen completely lost they enhanced neurosecretion when compared to *bbs-7* mutants exposed to 21% oxygen (Fig 4.10B). Moreover, *bbs-7* mutants reverted to secretion levels indistinguishable from wild types when they were reared at 7% oxygen (Fig 4.10B). These data support our hypothesis and show that BBS-7 does not constitutively shape neurosecretion, but rather it sensitises neurons to incoming activity. In the case of ADL neurons, this results in O<sub>2</sub>-evoked neurosecretion.

#### 4.12. Summary

Following on the results of our genetic screen, we showed that *qui-1* inhibits O<sub>2</sub>-escape behaviour, by performing rescue experiments and comparing independent alleles of the same gene. Analysis of QUI-1 protein sequence, identified several homologues of QUI-1, suggesting a good level of conservation. Although removing *qui-1* strongly enhanced O<sub>2</sub>-escape behaviour, neither O<sub>2</sub>-perception nor O<sub>2</sub>-integration were changed in *qui-1* mutants. Thus, *qui-1* is likely to shape the O<sub>2</sub>-circuit downstream of RMG interneurons. In fact, *qui-1* is required in ASH and ADL sensory neurons to inhibit O<sub>2</sub>-responses. Neither re-introducing QUI-1 in ASH, ADL nor ASH and ADL in combination completely restored *qui-1* O<sub>2</sub>-responses to wild type levels, suggesting *qui-1* is active in these as well as other neurons.

By generating double mutants, we observed that *qui-1;npr-1* mutants showed O<sub>2</sub>-escape behaviour comparable to *npr-1* mutants. We concluded that *qui-1* acts in the same genetic pathway as *npr-1*. We further expanded the repertoire of molecules for which *qui-1* mutants are defective. We showed that *qui-1* mutants fails to detect the ascarosides pheromone C9. Impairing QUI-1 completely abolished ADL pheromone-evoked Ca<sup>2+</sup> responses when mutants were presented with C9.

Moreover, we showed that disrupting QUI-1 enhances ADL neurosecretion. We showed that this regulation is cell-autonomous and exogenously expressing *qui-1* exclusively in ADL completely restores secretion to wild type levels. Moreover, this effect is fully dependent on dense-core vesicles release machinery, as we showed that disrupting UNC-13 abruptly reduces *qui-1* enhanced dense-core vesicles release. Following on these results, we described how removing QUI-1 confers O<sub>2</sub>-evoked neurosecretion on ADL neurons. By comparing neurosecretion in wild types and *qui-1* mutants exposed to high and low oxygen levels, we showed that absence of *qui-1* confers O<sub>2</sub>-evoked neurosecretion on ADL. By mutating the

molecular oxygen sensor GCY-35 we showed ADL neurosecretion is dependent on pre-synaptic inputs from the O<sub>2</sub>-circuit. Among these pre-synaptic inputs we identified RMG, where NPR-1 acts to regulate O<sub>2</sub>-evoked neurosecretion in ADL. We identified several additional mutants similar to *qui-1*, where increase in ADL neurosecretion was linked to an enhanced O<sub>2</sub>-escape behaviour. Moreover, we found two sensory defective mutants in our collection of aggregating mutants, *wrt-6* and *fig-1*, that show increased ADL neurosecretion. These data suggested defects in sensory perception might enhance ADL neurosecretion. To test if this increase in ADL neurosecretion was dependent on pre-synaptic inputs as in *qui-1* mutants, we compared ADL neurosecretion of *bbs-7* mutants exposed to low or high levels of oxygen. We observed a sharp reduction in secretion levels in mutants reared at low oxygen, suggesting also absence of BBS-7 confers O<sub>2</sub>-evoked neurosecretion on ADL. These data led us to hypothesise that sensory defects promote sensitisation in ADL to incoming activity from the O<sub>2</sub>-circuit, thus increasing ADL neurosecretion and promoting O<sub>2</sub>-escape behaviour.

## 5. Oxygen-experience reprograms the expression profile of O<sub>2</sub>-sensing neurons

### 5.1. A transgenic reporter line combined with FACS allows to isolate and profile AQR, PQR and URX O<sub>2</sub>-sensing neurons

Neurons and neural circuits often respond to changes in their activity by altering their properties. In *C.elegans*, for example, recent oxygen experience can switch the valence of pheromones, such that pheromones that are attractive to animals acclimated to 21% oxygen are repulsive to animals acclimated to 7% oxygen. These changes likely occur through experience-dependent changes in gene expression. Although signalling cascades which mediate these changes have been identified for some forms of plasticity such as memory and learning, for others, such as homeostatic plasticity, they still remain elusive. Moreover, targets of these signalling pathways and the types of adjustments in neural properties they bring about are less understood.

To investigate the identity of genes which expression level is changed by oxygen experience, we decided to profile O<sub>2</sub>-sensing neurons AQR, PQR and URX after prolonged exposure to high (21%) or low (7%) oxygen. We performed all the experiments in an *npr-1* mutant background, hereafter referred to as wild type for simplicity. We chose this background as the N2 reference strain has acquired a gain-of-function mutation in *npr-1* during domestication that alters the properties of the oxygen circuit. To distinguish between expression changes mediated by O<sub>2</sub>-evoked activity and indirect effects of altered oxygen levels on metabolism, we profiled in parallel the same neurons from *npr-1;gcy-35;gcy-36* mutants, hereafter referred to as *gcy* for clarity. GCY-35 and GCY-36 are the molecular oxygen sensors in AQR, PQR and URX, and *gcy-35* or *gcy-36* mutants do not show O<sub>2</sub>-evoked activity in the O<sub>2</sub>-circuit. In addition, comparing wild types and *gcy* mutants would allow us to infer transcriptional changes due to an active or inactive O<sub>2</sub>-circuit.

To precisely isolate O<sub>2</sub>-sensing neurons, we used a reporter line (*gcy-37p:gfp*) where GFP labeled exclusively O<sub>2</sub>-sensing neurons AQR, PQR and URX (Data not shown). Briefly, the reporter line was crossed in our WT and *gcy* mutant backgrounds. To avoid differences associated with variation in developmental staging, we synchronised animals by bleaching (See Methods). After bleaching, eggs were seeded and allowed to hatch at 21% or 7% oxygen. Three days later

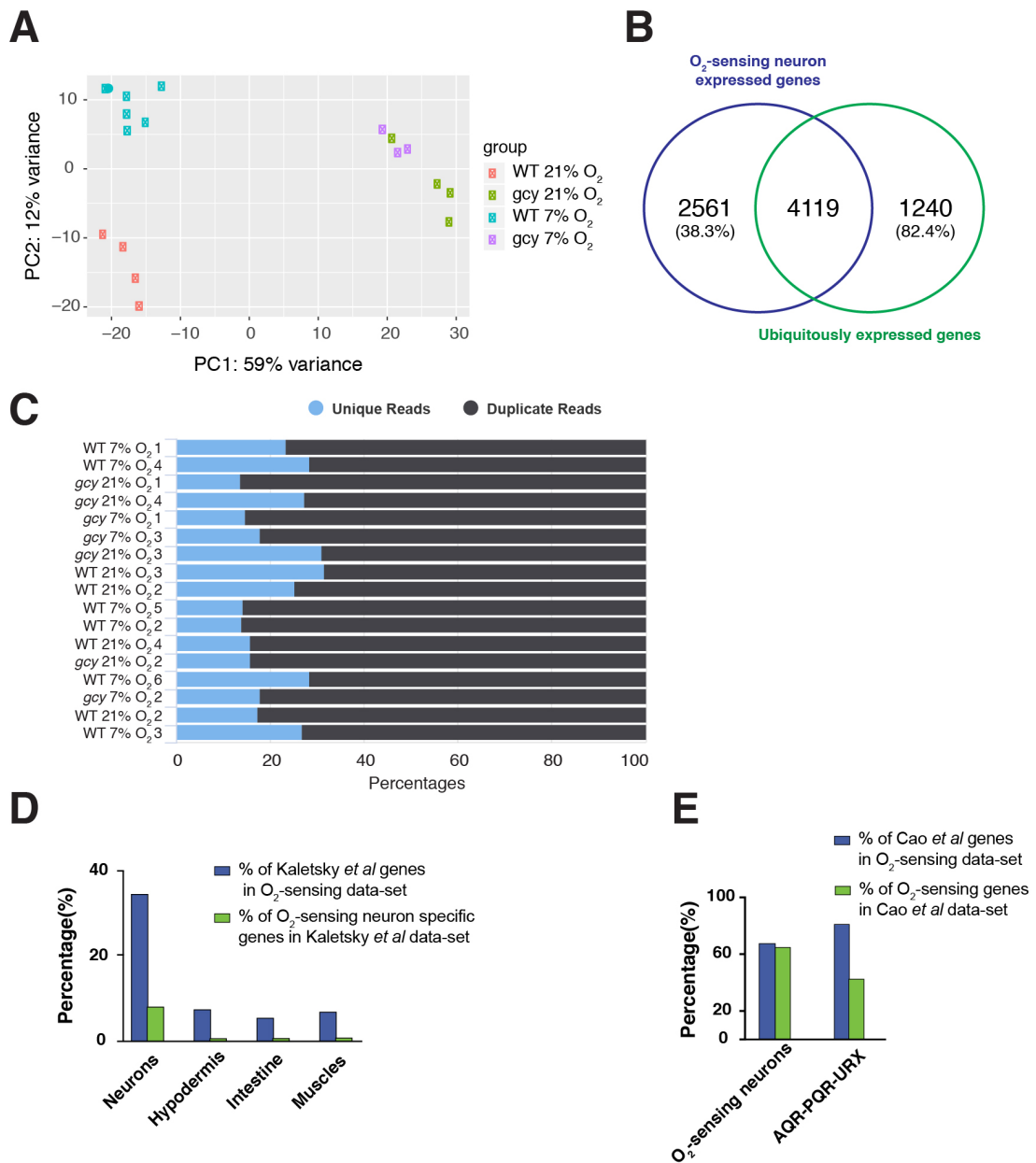


### FIGURE 5.1 RNA-SEQUENCING ANALYSIS OF GFP POSITIVE CELLS

(A) Data point cluster based on genotype and condition (high or low oxygen). Plot shows principal component analysis. (B) Venn diagram showing overlap between genes expressed in our data-set and Kaletsky *et al.* ubiquitously expressed genes. (C) Duplication plot showing the percentage of duplicated reads after ribosomal RNA removal. (D,E) Bar graph shows percentage of overlap between two data sets.

transgenic animals were collected and dissociated into single cells. Using FACS, we isolated GFP positive cells, from which we prepared cDNA libraries that were submitted for RNA-sequencing. To control for technical and experimental variation we collected between 3 and 6 biological replicates for each genotype and condition.

Principal component analysis of RNA-sequencing data showed that data points from independent biological replicates clustered according to genotype and oxygen experience (Fig 5.1A). This gave us confidence that our procedure was robust and suggested that we would be able to extract information on experience-dependent transcriptional changes. However, our sequencing reads contained high levels of duplication. This issue was partly resolved by removing reads aligning to ribosomal RNA genes which accounted, on average, for 79% of total reads. Residual reads still showed high levels of duplication (Fig 5.1C), but duplicated reads in the samples mainly aligned to highly expressed coding genes and therefore we did not remove them.

First, however, we wanted to confirm that FACS had enabled us to isolate our target cells, and to assess the extent of contamination from other tissues. To probe this we compared our data-set (Condition: WT 21% O<sub>2</sub>) to published profiles of each *C. elegans* tissue. Using data from Kaletsky *et al.*, we first compared our data-set to a list of genes expressed in all tissues. We observed that more than a third (38.2%) of our data-set comprised tissue specific genes (Fig 5.1B). Before performing further analysis, we generated a list of tissue specific genes by removing genes present in both our presumptive O<sub>2</sub>-sensing neurons genes AND Ubiquitously expressed genes. We compared our list of tissue specific genes to each tissue profile from Kaletsky *et al.* We observed the highest level of similarity between our data-set and the published neural tissue profile (Fig 5.1D). Moreover, contributions from other tissues was minimum (Fig 5.1D), suggesting that contamination in our preparation is likely to be small.

To test further if our data-set showed transcriptional features associated with O<sub>2</sub>-sensing neurons, we compared our data with a published report of single cell RNA-sequencing from *C. elegans* (Cao *et al.*). We extracted expression data for cells predicted by Cao *et al* to be O<sub>2</sub>-sensing neurons and data from our possible AQR, PQR and URX profiles. The two data-sets showed a high similarity (Fig 5.1E). Together, these data suggest we have obtained AQR-PQR-URX transcriptional profile with little contamination form other tissues.

In our previous analysis, we compared our data-set to predicted O<sub>2</sub>-sensing neurons. To take a more unbiased approach, we took advantage of a web-based tissue enrichment analysis tool (See Methods). When we searched for enriched cell types in our entire data-set, URX and PQR were first and second most enriched cell type (Fig 5.2A). If we performed the same search, but using instead our data-set after removing ubiquitous expressed genes, the most enriched cell types were

URX, PQR and AQR (Fig 5.2B). GO enrichment analysis of our data-set of AQR-PQR-URX specific genes revealed enriched terms related to neuropeptide signalling, ion channel activity and heme binding (Fig 5.2C). Together, these data give us confidence that we have successfully enriched AQR, PQR and URX O<sub>2</sub>-sensing neurons.

## 5.2. AQR, PQR and URX neurons are highly peptidergic

To further analyse the expression profile of AQR, PQR and URX, we ranked genes based on their expression. The most strongly expressed genes (Fig 5.2D) included neuropeptides (*flp-8*, *flp-14*, *flp-9*, *flp-19*, *nlp-50*, *nlp-21*, *flp-15*) and genes involved in neuropeptide maturation (*egl-21*, *sbt-1*, *pghm-1*, *pgal-1*, *cab-1*). Other highly expressed genes were involved in synaptic release or oxygen sensing, confirming the specific nature of AQR, PQR and URX as O<sub>2</sub>-sensing neurons (Fig 5.2D). It is worth noting that many highly expressed genes such as *flp-8*, *gcy-37* and *gcy-36* are known to be expressed and active in O<sub>2</sub>-sensing neurons, thus corroborating the specificity of our data-set.

URX neurons are known to be cholinergic, whereas AQR and PQR are thought to be glutamatergic. Consistent with this, we observed expression of genes involved with cholinergic transmission (*unc-17*; *cha-1*) as well as glutamatergic transmission (*eat-4*) (Fig 5.2E). We also observed some expression of the sole *C. elegans* glutamate decarboxylase, *unc-25*, and the vesicular GABA transporter *unc-47*, as well as *tdc-1* and *tbh-1* involved in the synthesis of tyramine and octopamine neuromodulators (Fig 5.2E). Whether these genes are genuinely expressed in one or more of AQR, PQR and URX, or reflect contamination by other neurons, is unclear.

To investigate synaptic inputs that might modulate O<sub>2</sub>-sensing neurons, we searched their profiles for known neurotransmitter receptors. We identified acetylcholine gated excitatory and inhibitory channels (*unc-38*, *acr-12*, *acc-3* and *acc-4*), and glutamate gated excitatory and inhibitory channels (*mgl-2*, *glc-4* and *avr-14*) (Fig 5.2F). We also observed expression of serotonin receptors, suggesting serotonin might modulate O<sub>2</sub>-evoked activity (Fig 5.2F). Other neuromodulator receptors expressed includes dopamine, tyramine and octopamine receptors (Fig 5.2F).

O<sub>2</sub>-sensing neurons express many neuropeptides. The most represented and highly expressed family of neuropeptides was FMRFamide-like peptides (*flp*) (Appendix 4), with *flp-8*, *flp-14* and *flp-9* among the highest expressed genes overall (Fig 5.2D). Other neuropeptides expressed at high levels were *nlp* (*nlp-50* and *nlp-21*) and a

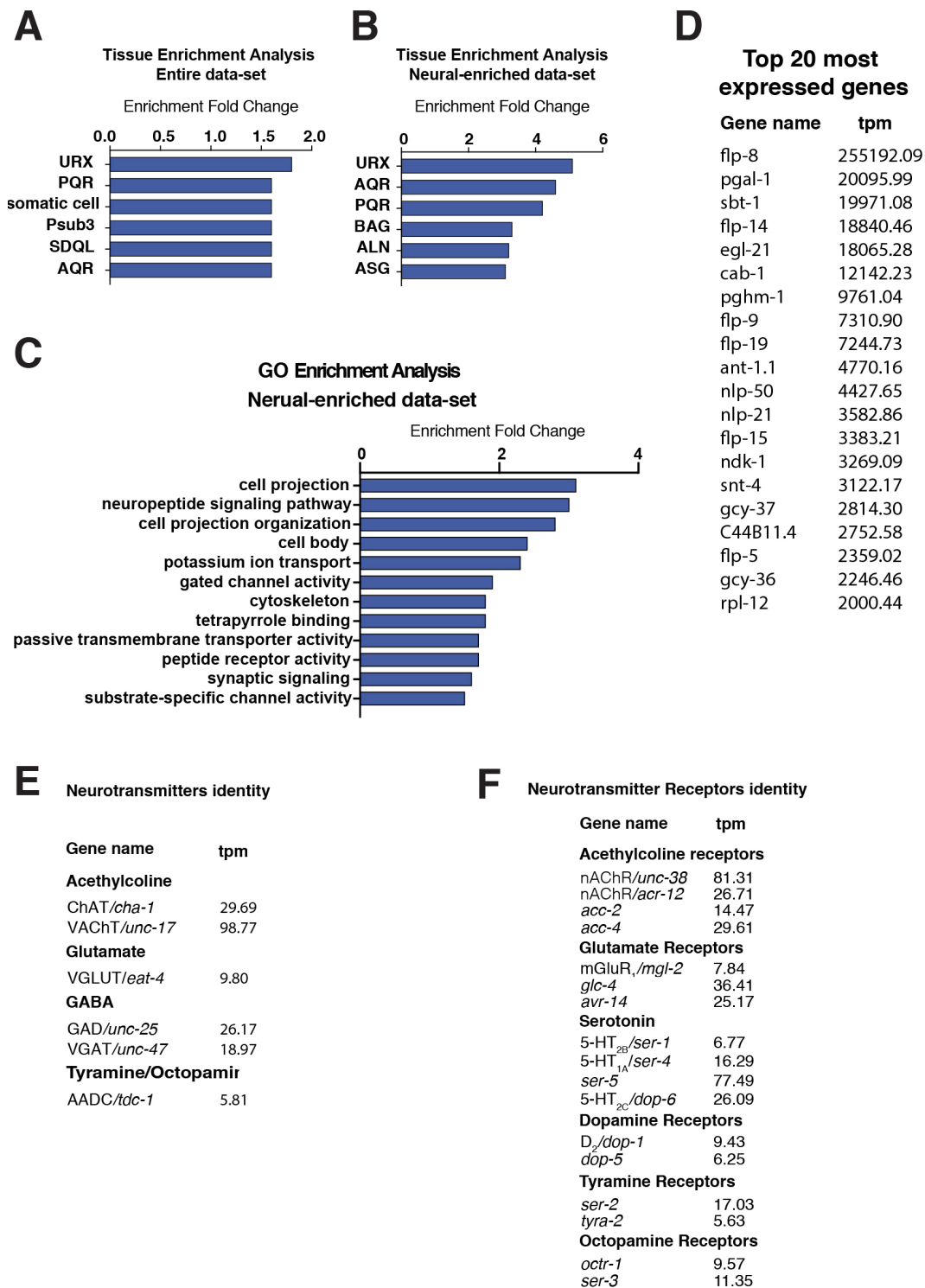


**Figure 5.2 Expression profile of AQR, PQR and URX O<sub>2</sub>-sensing neurons**

(A,B) GFP positive profile is most similar to expression profiles of URX, PQR and AQR. Bar graphs show enrichment fold change. (C) AQR, PQR, and URX expression profiles GO term enrichment analysis. (D) List of top 20 most highly expressed genes in AQR, PQR and URX. (E,F) List of genes expressed in AQR, PQR and URX that specify neural identity (e.g Neurotransmitters and Neurotransmitters receptors expressed).

few insulin-like peptides (Appendix 4). The importance of these peptides for O<sub>2</sub>-evoked changes in behaviour and physiology is, in most cases, unknown. In contrast with neuropeptides, O<sub>2</sub>-sensing neurons expressed a relatively small number of neuropeptide receptors (Appendix 5). The majority of neuropeptide receptors we identified were from “Neuropeptide Y(npr)/RFamide receptors group”, of which flp peptides are usually the cognate ligands. The most highly expressed receptors were related to somatostatin and galanin-like receptors (*npr-26* and *npr-16*).

### **5.3. O<sub>2</sub>-experience reprograms peptidergic properties of O<sub>2</sub>-sensing neurons**

Long term exposure to a stimulus can drive transcriptional changes that adjust neural properties. This form of experience-dependent plasticity underlines several important biological processes such as homeostatic plasticity, memory formation and learning. Cultivation in different oxygen environments is known to reprogram both the behaviour and physiology of *C. elegans*. To investigate if O<sub>2</sub>-sensing neurons showed experience-dependent plasticity in gene expression, we cultivated wild type animals at high (21%) and low (7%) oxygen concentrations, FAC-sorted the O<sub>2</sub>-sensing neurons, and looked for differentially expressed genes. We identified 455 differentially expressed genes (Fig 5.3A).

By clustering the fifty most up-regulated and down-regulated genes we show extensive differences in gene levels between wild type animals experiencing high or low oxygen concentrations (Fig 5.3B,C). We concluded that prolonged exposure to high or low oxygen causes transcriptional change in O<sub>2</sub>-sensing neurons.

To identify experience-dependent plastic changes due to O<sub>2</sub>-evoked activity, we compared AQR-PQR-URX profiles of wild type and *gcy* mutants. *gcy* mutants exposed to high and low oxygen showed a small number of differentially expressed genes (14) (Fig 5.4A). When we compared wild types and *gcy* mutants, only a small number of genes were differentially expressed in both conditions. The vast majority (99.5%) of transcriptional changes between wild types was lost in absence of GCY-35 and GCY36. In fact, when we compared the most up-regulated or down-regulated genes wild type animals at 21% oxygen, we observed that the expression of those same genes in *gcy* mutants resembled more wild types animals grown at 7% oxygen (Fig 5.3A,B), suggesting modulation of these genes requires O<sub>2</sub>-evoked activity. This data taken together demonstrate that almost all experience-dependent transcriptional changes in O<sub>2</sub>-sensing neurons are contingent on O<sub>2</sub>-evoked activity.

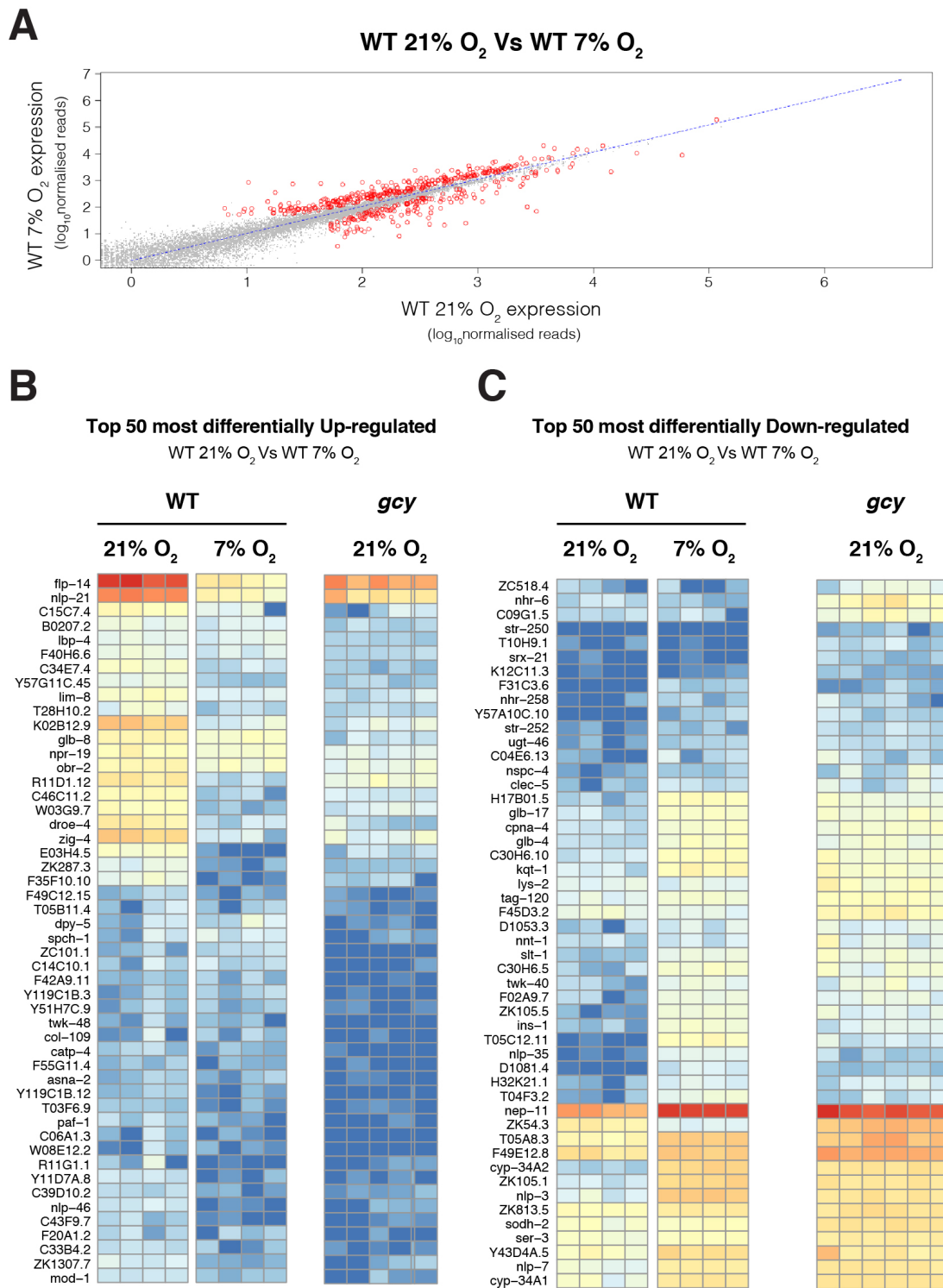


**Figure 5.3 Oxygen experience re-programs AQR, PQR and URX expression profiles**  
**(A)** Scatter plot shows genes differentially expressed between the conditions WT 21% O<sub>2</sub> and WT 7% O<sub>2</sub>. Red dots indicate genes which expression levels are significantly different. A cut-off removes all genes which levels are lower than 50 tpm in both conditions **(B,C)** Heat map of the 50 most highly **(A)** up-regulated and **(B)** down-regulated genes between wild type animals grown at high (21%) or low (7%) oxygen. *gcy* expression levels are shown as well. Colour intensity from Red to Blue is used to represent respectively High or Low expression

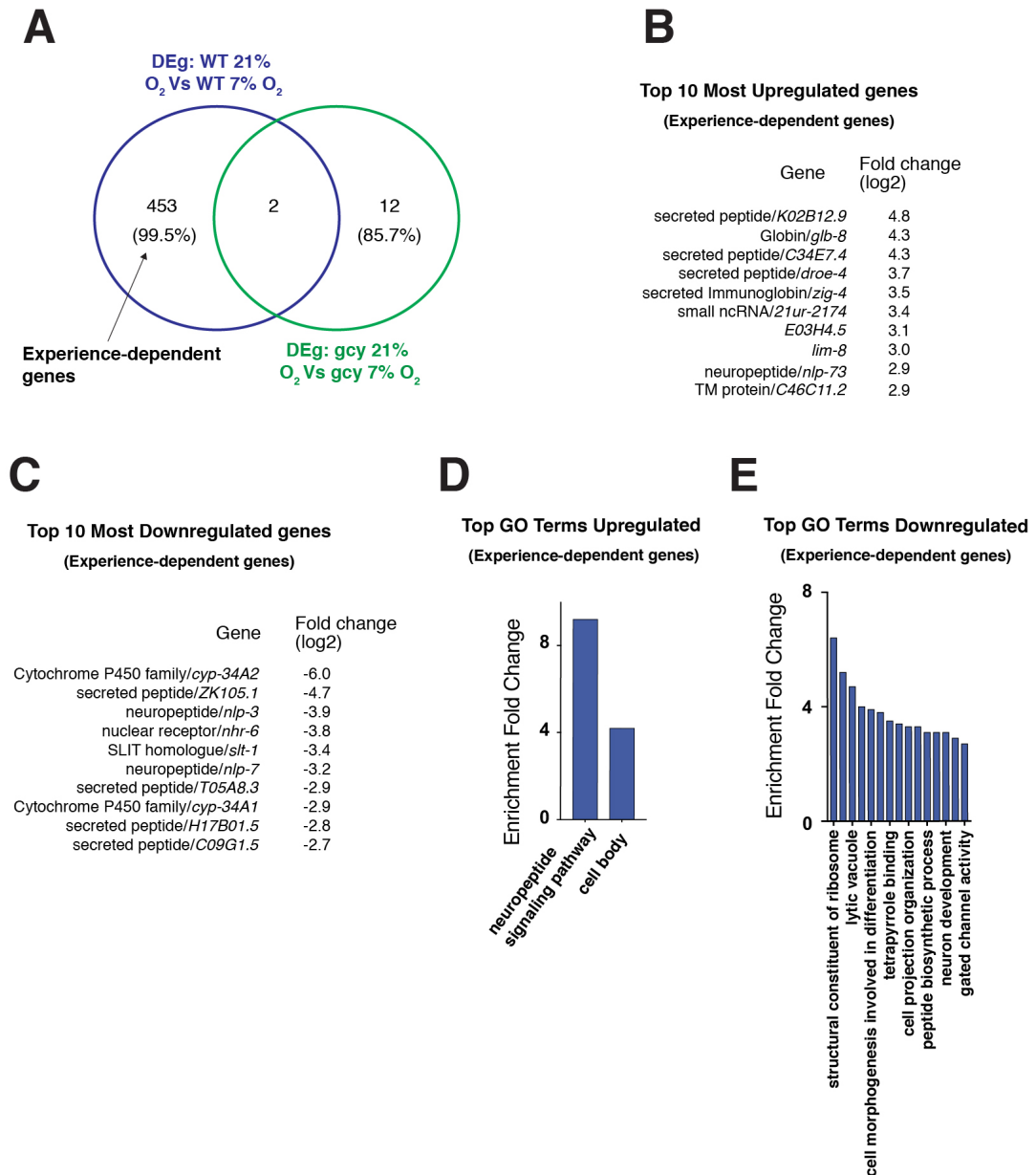


**Figure 5.4 Almost all experience-dependent transcriptional changes depend on O<sub>2</sub>-evoked activity**

(A) Venn diagram shows the overlap between genes differentially regulated between high and low oxygen in WT and *gcy* mutants. Values show the percentage over the total number of genes per condition. (B,C) List of top 10 most highly up-regulated or down-regulated genes between high and low oxygen in wild type animals. (D,E) Bar graphs show GO term enrichment analysis for all up-regulated or down-regulated genes in animals grown at high or low oxygen in wild types.

Experience-dependent plasticity refines neural properties and allows neurons to cope with a changing environment. To understand what kind of molecular remodelling O<sub>2</sub>-sensing neurons undergo, we examined in detail the genes that were up- or down- regulated in wild types acclimated to high or low oxygen. Several of the highest up-regulated genes (Fig 5.4B), encode unknown proteins that

share similar features: a signal peptide, followed by a short protein sequence suggesting they are likely to be secreted peptides. Similar proteins were also observed among down-regulated genes (Fig 5.4C). By comparing up and down-regulated genes, we observed a marked enrichment for neuropeptides and small secreted proteins (Fig 5.4B,C). To confirm our observation, we performed enrichment analysis for gene ontology terms on up and down-regulated genes. Up-regulated genes were greatly enriched for neuropeptides and neuropeptide receptors genes (Fig 5.4D). Consistently with a larger portion of experience-dependent genes being down-regulated, GO enrichment analysis revealed a larger number of enriched terms, including terms involved in oxygen binding (tetrapyrrole binding), peptide biosynthesis and channel activity (Fig 5.4E). Taking this data together, we conclude that experience-dependent plasticity is driven by O<sub>2</sub>-evoked activity and reprograms the expression of neuropeptides in O<sub>2</sub>-sensing neurons.

#### **5.4. O<sub>2</sub>-evoked activity regulates expression of distinct groups of genes at high and low oxygen**

Experience-dependent plasticity relies on activity-dependent regulation of gene expression levels. Rearing animals at high or low oxygen, alters O<sub>2</sub>-evoked Ca<sup>2+</sup> activity in the O<sub>2</sub>-sensing neurons over a certain range. It is possible that reducing Ca<sup>2+</sup> activity in these neurons even more might regulate the expression of some additional genes. To test this hypothesis we compiled a list of activity-dependent genes by using genes differentially regulated between wild types and *gcy* mutants both at high and low oxygen. Since *gcy* mutants abolish O<sub>2</sub>-evoked activity in AQR, PQR and URX, we expected genes that are differentially regulated between wild types and *gcy* mutants to be regulated by activity. We noticed a higher number of differentially regulated genes (1155 in WT 21% O<sub>2</sub> Vs *gcy* 21% O<sub>2</sub> and 908 in WT 7% O<sub>2</sub> Vs *gcy* 7% O<sub>2</sub>), confirming our hypothesis. Unexpectedly, we notice a high number of differentially expressed genes between wild types and *gcy* grown at low oxygen. In fact, comparing experience-dependent genes in wild type and *gcy* mutants suggested that *gcy* resemble more wild types animals exposed to low oxygen (5-3B,C). To investigate this further, we compared activity dependent changes (changes between wild types and *gcy* mutants) at high and low oxygen. We observed that the majority of activity-dependent changes occurred between wild types and *gcy* mutants at high oxygen (Fig 5.5A). This is consistent with a model where increase activity in the O<sub>2</sub>-circuit regulates transcription in O<sub>2</sub>-sensing neurons. However, we also observed a number of genes regulated between wild types and *gcy* mutants at low, but not high oxygen (Fig 5.5A), suggesting this group of genes is regulated by activity specifically at low oxygen.

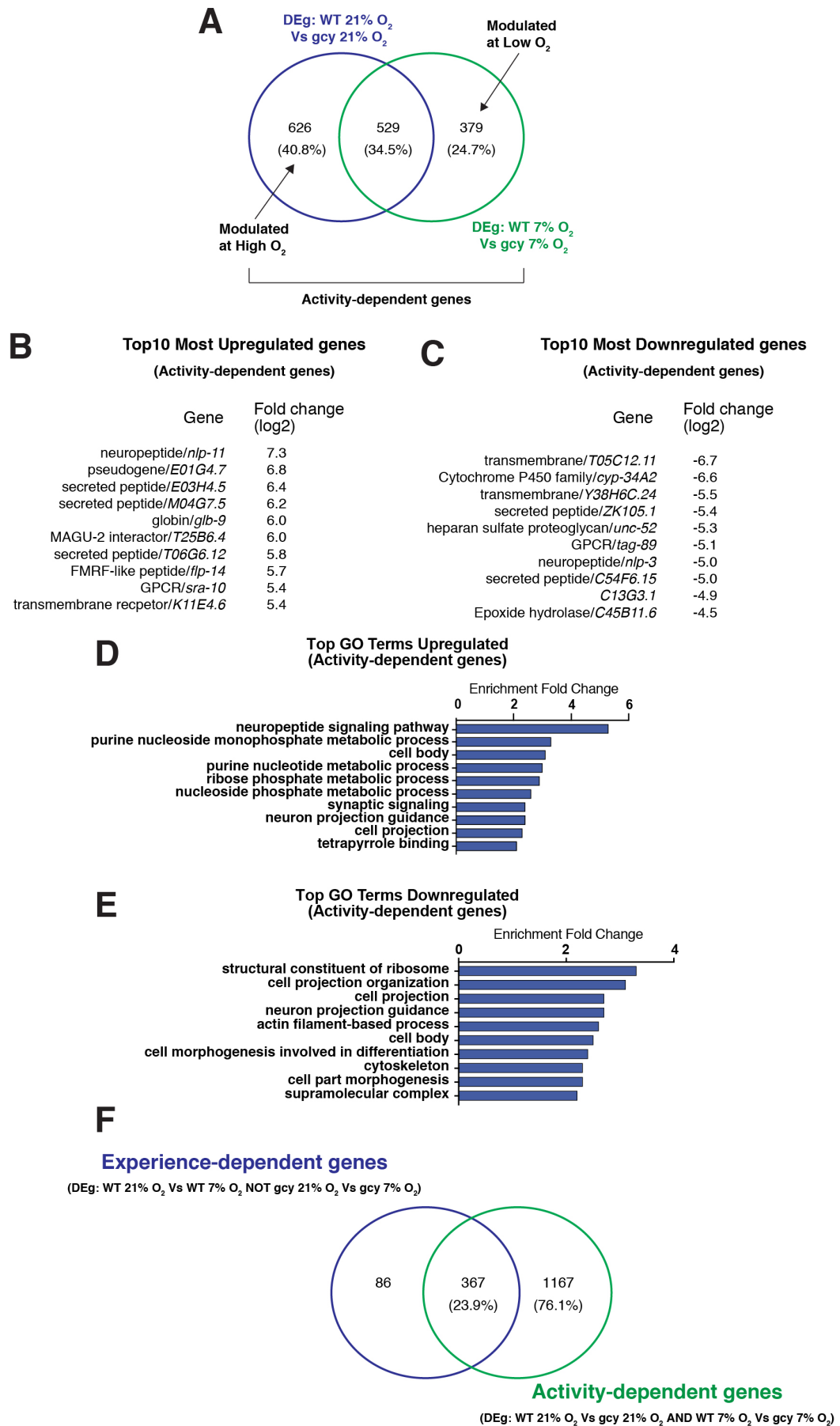


Figure legend in next page.

**Figure 5.5 Abolishing O<sub>2</sub>-evoked activity in O<sub>2</sub>-sensing neurons promotes larger changes than oxygen-experience**

(A) Venn diagram shows the overlap between activity-dependent genes at high and low oxygen. Comparison made to generate list of genes are written in figure. Values show the percentage over the total number of genes per condition. (B,C) List of top 10 most highly up-regulated and down-regulated activity-dependent genes. (D,E) Bar graphs show GO term enrichment analysis for all up-regulated or down-regulated activity-dependent genes.

To further characterise genes regulated by activity in O<sub>2</sub>-sensing neurons, we looked at the most differentially up-regulated and down-regulated genes between wild types and *gcy* mutants regardless of the condition they experienced. High activity up-regulated genes enriched for neuropeptides and small secreted proteins (Fig 5.5B). On the other hand, high activity strongly down-regulated a number of transmembrane proteins of unknown function (Fig 5.5C). We also performed GO enrichment analysis on activity-dependent up-regulated and down-regulated genes. Enrichment analysis confirmed a strong enrichment for neuropeptide signalling molecules in activity-dependent up-regulated genes, but also synaptic scaling and growth of neural projection (Fig 5.5D), suggesting high activity could promote structural rearrangement of AQR, PQR and URX. Also down-regulated genes showed enrichment for terms related to formation of neural processes, suggesting this process might be particularly sensitive to activity levels (Fig 5.5E).

To investigate the extent that abolishing O<sub>2</sub>-evoked activity has on AQR, PQR and URX profiling, we compared activity-dependent genes (wild types Vs *gcy* mutants) and genes regulated by oxygen experience (wild types at 21% O<sub>2</sub> Vs wild types at 7% O<sub>2</sub>). As expected the majority of experience-dependent genes were also regulated by activity (Fig 5.5F). On the contrary, the vast majority of activity-dependent genes was not regulated by O<sub>2</sub> experience. We noticed that 86 experience-dependent genes were not regulated by abolishing GCY-35 and CGY-36 signalling. These genes still require GCY-35 and GCY-36 signalling to be modulated by oxygen experience, yet they are not differentially expressed when comparing wild types and *gcy* mutants at high or low oxygen, suggesting their experience modulation must be modest. Taken together these data suggests that abolishing O<sub>2</sub>-evoked activity by removing GCY-35 and GCY-36, promotes a profound transcriptional reprogramming of O<sub>2</sub>-sensing neurons, more drastic than high or low oxygen experiences.

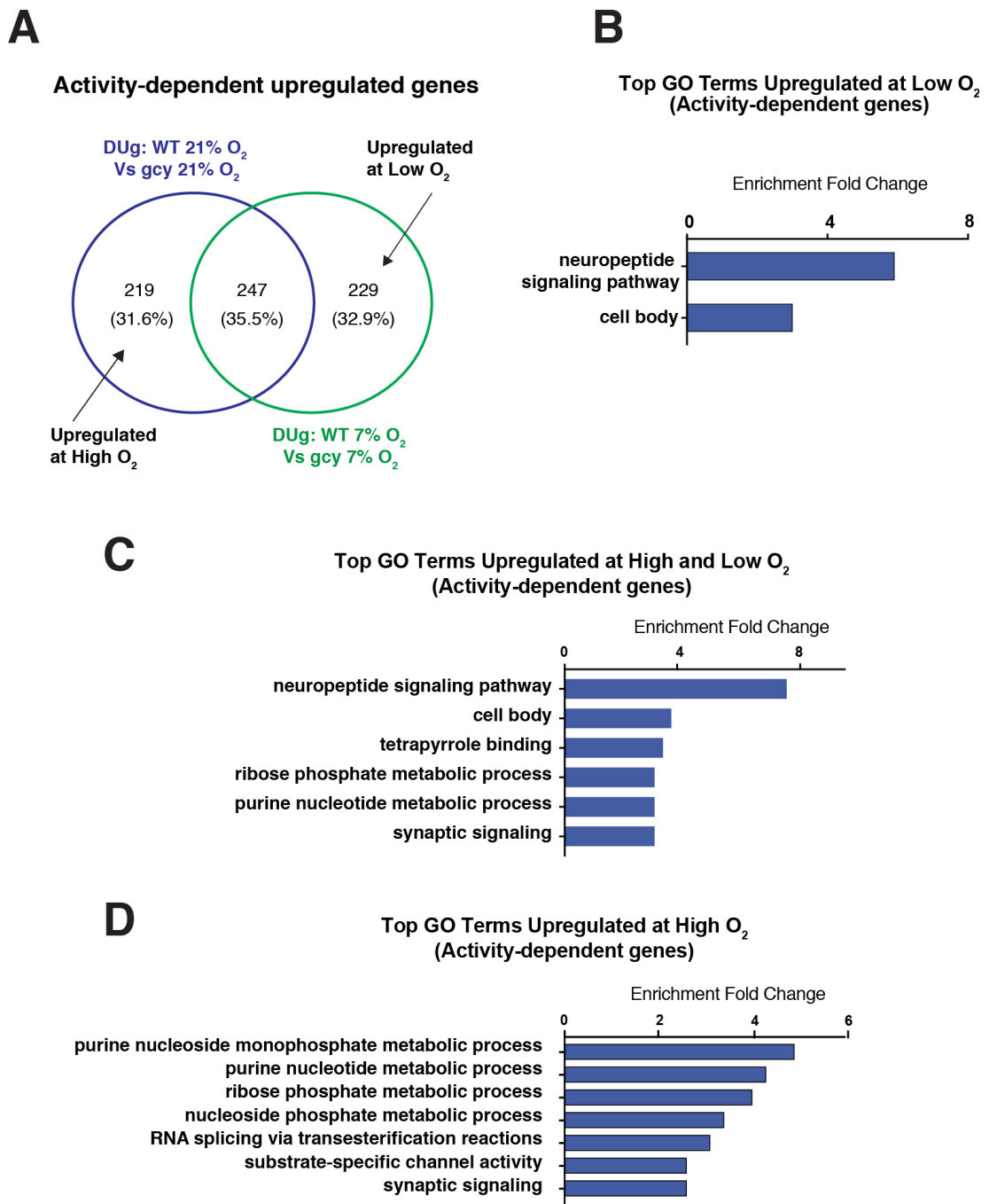


**Figure 5.6 O<sub>2</sub>-evoked activity regulates two distinct sets of neuropeptides**

**(A)** Venn diagram shows the overlap between activity-dependent up-regulated genes at high and low oxygen. Comparison made to generate list of genes are written in figure. Values show the percentage over the total number of genes per condition. **(B-D)** Bar graphs show GO term enrichment analysis for up-regulated activity-dependent genes.

### 5.5. O<sub>2</sub>-evoked activity drives expression of distinct sets of neuropeptides at high and low oxygen

We have shown that certain activity-dependent genes are regulated according to presence of high or low oxygen. To follow up on this interesting observation, we decided to test if among these genes were genes involved in neuropeptides

signalling. Since we have previously observed that neuropeptide signalling molecules are the most enriched GO terms for activity-dependent up-regulated genes, we decided to compare activity-dependent up-regulated genes according to high or low oxygen exposure (Fig 5.6A). Genes were divided equally among up-regulated at high or low oxygen or up-regulated in both conditions. However, when we performed enrichment analysis we observed neuropeptide signalling enrichment just in groups of genes exclusively up-regulated at low oxygen or up-regulated in both condition (Fig 5.6B,C,D). We concluded that O<sub>2</sub>-evoked activity drives expression of distinct sets of neuropeptide signalling molecules if animals are exposed to high or low oxygen.

## 5.6.Summary

*C. elegans* adapts a number of behaviours after prolonged exposure to high or low oxygen concentrations, thus showing experience dependent plasticity. To investigate this mechanism at the molecular level, we used a reporter line to isolate and profile AQR, PQR and URX O<sub>2</sub>-sensing neurons. We reared animals at high (21%) or low (7%) oxygen to study the experience-dependent transcriptional changes due to prolonged exposure to oxygen. Principal components analysis on RNA-seq data showed that biological replicates nicely clustered according to genotype and condition. Comparison of our data-set with published data and tissue enrichment analysis showed enrichment for neural genes, genes expressed in O<sub>2</sub>-sensing neurons and genes expressed in AQR,PQR and URX. We showed that O<sub>2</sub>-sensing neurons expressed genes involved in cholinergic, glutamatergic and gabaergic synaptic communication. Expression data also highlighted high levels and a larger variety of neuropeptides, especially of the FMRFamide family.

To study experience-dependent plasticity, we exposed animal to high and low oxygen and compared transcriptional profiles of O<sub>2</sub>-sensing neurons. We identified hundreds of experience-regulated genes. We showed that almost all (99.5%) of the experience-dependent genes are contingent on O<sub>2</sub>-evoked activity, since they are not changed in *gcy* mutants grown at high or low oxygen. Enrichment analyses showed experience-dependent up-regulated genes are enriched for neuropeptide signalling molecules. Moreover, among the top most highly regulated genes we identify several unknown genes sharing similar features which suggests they might be neuropeptides. We show that one set is up-regulated by high oxygen experience, while the other is up-regulated by low oxygen experience. This suggested to us that oxygen experience reprograms neuropeptide expression in AQR, PQR and URX. We also used wild types and activity silent mutants (*gcy*) to study the effect of O<sub>2</sub>-evoked activity on AQR, PQR and URX transcription. We showed that abolishing O<sub>2</sub>-evoked activity produced a more profound effect on gene expression levels that high and low oxygen experience. We performed GO

enrichment analysis on these genes which suggested growth of neural projection is a cellular mechanism particularly sensitive to O<sub>2</sub>-evoked activity. Moreover, by comparing activity-dependent genes regulated at high and low oxygen, we identified a group of genes specifically regulated at low oxygen. We further analysed these groups of genes and identified two discrete set of neuropeptide signalling molecules: one up-regulated by activity at low oxygen, and another up-regulated at both high and low oxygen.

## 6. Discussion and future directions

Innate behaviours offer useful paradigms to investigate how genes, neurons and neural circuits shape a behaviour. In this thesis, we use aggregation and O<sub>2</sub>-escape behaviour in *C. elegans* to discover novel conserved molecules involved in prominent functions of the nervous system. To genetically dissect these behaviours, we perform a forward genetic screen where we mutagenise non aggregating strains (N2 and *flp-21*) and use whole-genome sequencing to isolate 8 alleles conferring O<sub>2</sub>-escape behaviour. Of the 8 alleles we identify 4 genes which have not been previously implicated in O<sub>2</sub>-responses and, using calcium imaging, measure their effects on the O<sub>2</sub>-circuit. We proceed by analysing *qui-1* and showing it encodes a conserved NACHT/WD40 containing protein which is required in sensory neurons, and works in the same genetic pathway as *npr-1* to inhibit O<sub>2</sub>-escape responses. Abolishing QUI-1 functions results in increased Ca<sup>2+</sup>-dependent dense-core vesicle release from ADL, which we show is dependent on O<sub>2</sub>-evoked activity. We observe a similar increase in ADL neurosecretion in sensory defective mutants, *fig-1*, *wrt-6* and *bbs-7*, with the latter conferring O<sub>2</sub>-evoked neurosecretion. Taking together these results, we propose that impairing sensory perception sensitises sensory neurons to incoming neural activity.

In a separate effort to understand the molecular changes underlying experience-dependent modulation of behaviour, we isolate and profile O<sub>2</sub>-sensing neurons from *C. elegans* kept at high or low oxygen. We show that the majority of O<sub>2</sub>-dependent transcriptional changes are contingent on O<sub>2</sub>-evoked activity mediated by GCY-35 and GCY-36 oxygen sensors. We identify 455 experience-dependent genes and 1534 activity-dependent genes, which we further divide into distinct sub-set of genes regulated at high or low oxygen. Finally, we demonstrate O<sub>2</sub>-experience induces two distinct set of neuropeptide signalling molecules at high or low oxygen. We propose that neuropeptides differentially expressed at high or low oxygen concentration, might reconfigure the O<sub>2</sub>-circuit and other neural circuits according to previous oxygen experience.

### 6.1. Novel regulators of O<sub>2</sub>-escape behaviour

Although pathways promoting aggregation and O<sub>2</sub>-escape behaviour have been the subject of detailed molecular characterisation, little is known about genes inhibiting these behaviours. To address this question we screen a collection of aggregating *C.*

*elegans* mutants and identify novel genes involved in the suppression of both behaviours.

### **The genetic screen**

We isolate 14 aggregating mutants from two separate parental backgrounds (N2 and *flp-21*) by screening at least more than 5,000 genomes. While several of these mutants turned out to be *npr-1*, suggesting our screen reached saturation, we do not believe this is the case. More likely, the initial selective procedure is very efficient at isolating *npr-1* mutants. In fact, a few genes known to inhibit aggregation and O<sub>2</sub>-escape behaviour, such as *osm-3* and *daf-7*, were not isolated in our screen. Moreover, we show that many *bbs* mutants display O<sub>2</sub>-escape behaviour. While this behaviour was not previously reported, we did not isolate these mutants from our screen. The genetic screen was successful in characterising several new genes inhibiting aggregation, however an attempt at screening a larger number of genomes might identify more.

### ***dgk-1***

First, we find that mutating *dgk-1*, a diacylglycerol protein kinase homologous to mammalian DGK-1 $\theta$ , confers O<sub>2</sub>-escape behaviour on WT animals (Fig 3.5B). DGK-1 acts as an effector of inhibitory G<sub>o</sub> protein by converting diacylglycerol (DAG) to phosphatidic acid (PA), thus reducing UNC-13 mediated synaptic release (Nurrish et al., 1999). Since *dgk-1* and *npr-1* both show O<sub>2</sub>-escape behaviour (Fig 3.5B) and (Laurent et al., 2015)) and, the GPCR *npr-1* has been implicated in the activation of G<sub>o</sub> (Laurent et al., 2015), it is tempting to speculate that *dgk-1* is required for *npr-1* mediated control of neural outputs. Since *npr-1* is required to inhibit O<sub>2</sub>-escape behaviour in RMG, it will be interesting to test if *dgk-1* is required in the same neuron as well.

In accordance with *dgk-1* regulating synaptic release, although URX O<sub>2</sub>-evoked activity was greatly diminished in *dgk-1* mutants (Fig 3.6A), RMG O<sub>2</sub>-evoked responses were unchanged (Fig 3.6B). To rationalise this, we propose that, despite reduced activity, synaptic release from URX is increased in *dgk-1* mutants. If RMG activation is indistinguishable from WT, why do *dgk-1* mutants show enhanced behavioural responses? One possibility is that *dgk-1* acts in RMG as well. In this scenario, the absence of *dgk-1* would increase RMG outputs, thereby overcoming the effect of NPR-1 215V, to promote O<sub>2</sub>-escape behaviour. To test some of these models, it is paramount to assess if *dgk-1* is required in RMG, URX or both to

inhibit O<sub>2</sub>-escape behaviour. It will also be informative to build double mutants with *npr-1* to test if they act in the same genetic pathway.

### ***fig-1***

Another gene which has emerged from our screen is *fig-1*, a thrombospondin domain containing protein not previously implicated in the suppression of O<sub>2</sub>-escape behaviour. Although initial attempts at rescuing *fig-1* mutants failed, our observation that multiple independent alleles of *fig-1* confer O<sub>2</sub>-escape behaviour on the N2 reference strain indicate that mutations in this locus are associated with O<sub>2</sub>-escape behaviour (Fig 3.8D). Moreover, the behaviour of the *db1239* allele we isolated is indistinguishable from that of three *fig-1* null alleles (*gk640644*, *tm1270* and *tm2079*), indicating the allele we have isolated is likely to be a null. However, *tm10270* and *tm2079* should be extensively outcrossed and the experiment repeated before we can make definitive conclusion on the nature of *db1239* allele.

*fig-1* contains two TSP1 thrombospondin domains and eighteen C6 domains of unknown function, it is expressed exclusively in sheath glial cells, and, in its absence, mutants show defect in 1-octanol avoidance (Bacaj et al., 2008). Consistently with a sensory defective mutant, *fig-1* mutants do not take up the lipophilic dye Dil, which suggests their amphid neurons are not properly in contact with the external environment (Bacaj et al., 2008). However, these sensory defects do not affect URX and RMG O<sub>2</sub>-evoked activity (Fig 3.8E,F). Avoidance of 1-octanol in *C. elegans* is promoted in part by ADL (Troemel et al., 1995), indicating ADL activity may be defective in *fig-1* mutants. Surprisingly, we find that ADL neurosecretion is increased in *fig-1* mutants compared to WT (Fig 4.10A). This observation will be discussed at a later point in this chapter.

### ***wrt-6***

We isolate *wrt-6* as a further glial gene not previously known to inhibit O<sub>2</sub>-escape behaviour. Based on genetic sequence analysis, *wrt-6* is part of a class of *C. elegans* genes related to mammalian hedgehog signalling molecules (Bürglin, 1996). In addition to its similarity to hedgehog proteins, the presence of a signal peptide sequence in *wrt-6* suggests *wrt-6* is a secreted protein. Expression analysis show that *wrt-6* localises to socket glia cells (Aspöck et al., 1999), while abolishing its function produces severe defects in lipophilic dye uptake (Data not shown). Dye filling defects generally suggests a defect in sensory perception, however, *wrt-6* mutants do not show impairment in O<sub>2</sub>-evoked activity in URX or in RMG (Fig

3.9B,C). This indicates the defect might be restricted to amphid neurons. Despite a possible defect in sensory perception, *wrt-6* mutants show a marked increase in ADL neurosecretion (Fig 4.10A). Since *wrt-6* and *fig-1* share similar phenotypes and are both expressed in glia cells, it is tempting to hypothesize they might be regulators of similar mechanisms inhibiting O<sub>2</sub>-escape behaviour.

## **6.2. *qui-1* is a conserved protein homologous to NWD1**

Forward genetic screens are particularly helpful to discover conserved proteins of unknown function. Here we isolate *qui-1* a conserved NACHT/WD40 containing protein homologous to mammalian NWD1 (Fig 4.2B). According to genomic analysis, NWD1 is part of a peculiar class of NOD-like receptors, a group of signalling components that promote an immune response upon the detection of intracellular pathogens (Akira et al., 2006; Stein et al., 2007). These signalling proteins bind pathogens using their Leucine Rich Repeats (LRR) and oligomerise through their NACHT domain to initiate a signalling cascade. A peculiar feature of NWD1 is that the NACHT domain is followed by WD40 domains involved in protein-protein interaction, rather than LRR, suggesting it might not be involved in sensing pathogens. Consistent with this hypothesis, NWD1 expression has been reported in the brain (hippocampus, olfactory bulb, retina) as well as reproductive tissues (prostate and testis) (Correa et al., 2014; Yamada and Sakakibara, 2018). However, its function in intracellular signalling might have been preserved as it was reported that modulating NWD1 controls the steady-state levels of the androgen receptor (AR) in a model of prostate cancer, and that, after NWD1 depletion, prostate cells fail to induce AR-responsive genes upon androgens stimulation (Correa et al., 2014). These signalling function might be conserved in *C. elegans* as the NACHT domain in QUI-1 seem to be conserved and functional (Fig 4.2C). Additionally, we report that *qui-1* is required for neural activation in sensory neurons, since its absence completely abolishes C9-evoked Ca<sup>2+</sup> currents in ADL neurons (Fig 4.6A). Next, we want to perform cell-specific rescue experiments to exhaustively show that *qui-1* acts in ADL and thus demonstrating QUI-1 couples detection of C9 to Ca<sup>2+</sup> entry in ADL. Three observations support this prediction: (1) *qui-1* is expressed in ADL (Hilliard et al., 2004), (2) ADL senses C9 pheromone cell-autonomously (Jang et al., 2012) and (3) *qui-1* mutants fail to enter the dauer stage after C9 stimulation, a phenotype that can be rescued by overexpressing *qui-1* in ADL (Neal et al., 2016). Moreover, *qui-1* function in sensory perception does not appear to be restricted to pheromone-sensing, as *qui-1* mutants fails to detect a number of aqueous chemicals including quinine (Hilliard et al., 2004). Thus, we hypothesise that *qui-1* has a specific function in sensory perception. To characterise its molecular function in more detail we plan to perform

immunoprecipitation experiments to identify QUI-1 interactors in *C. elegans* neurons.

### **6.3. Absence of *qui-1* redirects the flow of information in the O<sub>2</sub>-circuit**

Although *C. elegans* elicits escape behaviour in response to activation of O<sub>2</sub>-sensing neurons, how other sensory modalities influence this behaviour is not clear. By performing cell specific rescue experiments, we show that *qui-1* is required at least in part in the polymodal sensory neurons ASH and ADL to inhibit O<sub>2</sub>-escape behaviour (Fig 4.4). Since the NPR-1 215V isoform inhibits O<sub>2</sub>-escape behaviour as well as RMG outputs in N2 animals, how does loss of *qui-1* overcome this suppression? Several experimental evidences, reviewed in more details in the Introduction, suggest ADL promotes aggregation downstream of RMG in the O<sub>2</sub>-circuit. Thus, a simple model to explain O<sub>2</sub>-escape behaviour in *qui-1* mutants would be that absence of *qui-1* increases ADL activity. Consistent with this model, we observe an enhanced secretion of dense-core vesicle from ADL in *qui-1* mutants (Fig 4.7A). This enhanced neural secretion is rescued by expressing a copy of *qui-1* exclusively in ADL (Fig 4.7A), indicating *qui-1* affects neurosecretion cell-autonomously. This effect was blocked by mutating the calcium binding protein UNC-13 (Fig 4.7B), suggesting the enhanced release is contingent on Ca<sup>2+</sup> entry. Moreover, *qui-1* mutants show normal O<sub>2</sub>-evoked responses in both URX and RMG neurons (Fig 4.3A,B), confirming the ability of *qui-1* to overcome NPR-1 215V suppression is not explained by increased RMG activity. Loss of *npr-1* generates a further increase in ADL neurosecretion in *qui-1* mutants, which is partially rescued by expressing NPR-1 215V isoform specifically in RMG (Fig 4.8C). This adds further support to our model and indicates activity from the O<sub>2</sub>-circuit propagates from RMG to ADL, and is modulated by NPR-1 activity in RMG as well as in other unidentified cells.

However, this model present some difficulties. In fact, previous studies showed that blocking ADL neurosecretion with Tetanous toxin did not affect O<sub>2</sub>-escape behaviour, and did not impaired O<sub>2</sub>-responses when RMG was activated using channelrhodopsin. One interpretation of these data would be that ADL acts upstream of RMG in the O<sub>2</sub>-circuit (Laurent et al., 2015). More experiments will be needed to address this issue.

How the enhanced release from ADL influence the rest of the downstream circuitry is less clear. Sustained stimulation with 21% O<sub>2</sub> activates neurons downstream of O<sub>2</sub>-circuit such as the motoneurons AVA, which promotes reversal, and the motoneurons AVB, which contributes to high speed and forward movement

(Laurent et al., 2015). ADL forms synapses with both motoneurons, suggesting in *qui-1* mutants ADL enhanced pre-synaptic activity could result in a stronger activation of AVA and AVB. While we do not have data supporting a functional role for these synaptic connections in O<sub>2</sub>-escape behaviour, ADL to AVA synapses have been implicated in pheromone avoidance where they promote reversal (Jang et al., 2012). The enhanced neural secretion from ADL is also likely to affect additional neural circuits in *qui-1* mutants. For example, changes in ADL activity have been associated with changes in intestinal fat storage, where increased activation of these sensory neurons leads to a depletion of fat (Hussey et al., 2017). ADL expresses also a large number of neuropeptides such as FMRFamide-like peptide (flp), neuropeptide-like protein (nlp) and insulin-like peptides (ilp) (Taylor et al., 2019). Many of these peptides have been showed to influence several aspects of *C. elegans* physiology unrelated to oxygen sensing, such as naive food preference (Yu et al., 2016) and learned food preference (Wu et al., 2019). Because neuropeptides acts extra-synaptically, it is likely that ADL increased neurosecretion largely re-shapes the physiology of *qui-1* mutants through the activation of downstream neurons that are part other several distinct neural circuits.

#### **6.4. Absence of sensory inputs sensitises *C. elegans* sensory neurons to incoming activity**

Experiments with *qui-1* mutants point to an apparent inconsistency in our results: deleting *qui-1* abolishes stimulus-evoked Ca<sup>2+</sup> activity in ADL, while at the same time increasing its neurosecretion. Work done on the visual cortex of mice shows that prolonged sensory deprivation promotes homeostatic plasticity (Desai et al., 2002). This plasticity renders neurons of the visual cortex more sensitive to electrical inputs thus enhancing their excitability compared to neurons of animals that have not been sensory deprived. Disrupting QUI-1 function in ADL results in a blunted response to pheromones and possibly several more sensory modalities. We hypothesise that these defects might resemble depriving ADL of sensory inputs. This deprivation would enhance ADL excitability through molecular mechanisms similar to those observed in the mouse visual cortex. Such mechanisms would be responsible for the enhanced neurosecretion of *qui-1* mutants. In accordance with our hypothesis, we show that stimulating ADL by increasing the activity of the O<sub>2</sub>-circuit elicits an increase in neurosecretion in *qui-1* mutants but not in wild types (Fig 4.8A). Furthermore, stimulating ADL in *qui-1* with low activity from the O<sub>2</sub>-circuit, still elicits a robust increase in neurosecretion much larger than that elicited in WT by either high and low O<sub>2</sub>-circuit activity (Fig 4.8A). This confirms that in *qui-1* mutants ADL is sensitised to subsequent activation from the O<sub>2</sub>-circuit.

If our prediction is correct, this model would also provides us with an explanation to how *qui-1* mutants overcome RMG suppression. In fact, ADL is connected to the O<sub>2</sub>-circuit at least in part through RMG, via coupling of electrical synapses, neuropeptides signalling or both. Based on our model, in animals expressing NPR-1 215V suppression of electrical synapses or neuropeptide signalling from RMG would not be complete and some activity would still pass through to ADL. This activity would be enhanced in the absence of *qui-1*, which would in turn increase ADL neurosecretion and promote O<sub>2</sub>-escape behaviour. By showing that NPR-1 regulates ADL neurosecretion at least in part by acting in RMG (Fig 4.8D), we provide further evidence in support of our model.

The molecular nature of this sensitisation however, it not clear. One hypothesis is that, impairing *qui-1* triggers molecular changes which remodels the properties of ADL to increase its activation. The first difficulty with this model however, is that homeostatic plasticity usually re-sets neural activity to homeostatic levels (Turrigiano, 2008), whereas in the case of *qui-1*, ADL activity is higher than in wild types (Fig 4.8A). This might be due to the fact that the N2 reference strain is not wild type and NPR-1 215V gain of function isoform might suppress ADL activity to levels that are lower than in natural wild type strains. Since homeostatic plasticity has not been described to directly regulate dense-core vesicle release, it is possible that the increase in release from ADL is a consequence of increased O<sub>2</sub>-evoked Ca<sup>2+</sup> activity in *qui-1* mutants. To test this hypothesis we plan to perform calcium imaging experiments in wild type and *qui-1* mutants to compare O<sub>2</sub>-evoked activity in ADL.

This, however, is not the only hypothesis capable of explaining the molecular nature of ADL sensitisation. *qui-1* might also regulate trafficking to the plasma membrane, in which case its absence could result in an accumulation of dense-core vesicles at ADL dendrites. In this scenario, incoming activity from the O<sub>2</sub>-circuit would result in the release of a larger number of dense-core vesicles, thus explaining ADL sensitisation and enhanced neurosecretion. To validate this model it will be essential to test if *qui-1* mutants show aberrant localisation of dense-core vesicles markers such as the protein IDA-1.

Is the effect of *qui-1* on ADL homeostatic plasticity direct or due to an impairment of sensory perception? Since we isolated additional mutants that share the general defect in sensory perception, and the characteristic increase in ADL neurosecretion (Fig 4.9A and 4.10A), we favour the latter hypothesis. Among these mutants, *bbs-7*, a conserved gene involved in trafficking of molecular cargos along the primary

cilium of neurons, displays defects in cilia formation and in sensory perception both in *C. elegans* and mammals (Tan et al., 2007). In support of our model, we show that absence of *bbs-7* also sensitises ADL neurosecretion to incoming activity from the O<sub>2</sub>-circuit, as shown by the fact that growing animals in high or low oxygen concentration changes ADL neurosecretion in *bbs-7* mutants, but not in wild types (Fig 4.10B). Nevertheless, *bbs-7* mutants do not seem to change ADL activity to the same extent as mutating *qui-1*, since low activity in the O<sub>2</sub>-circuit does not increase ADL neurosecretion to levels higher than wild types (Fig 4.10B). This might be due to the fact that *bbs-7* is likely to act in other neurons as well to affect ADL neurosecretion, as it has been demonstrated for other *bbs* mutants (Lee et al., 2011). Therefore, there are at least two possible mechanisms by which *bbs-7* could contribute to the regulation of ADL neurosecretion: it could either sensitise ADL to incoming activity from O<sub>2</sub>-circuit or facilitate the communication between the O<sub>2</sub>-circuit and ADL. We predict the first hypothesis is correct as *bbs* genes have well characterised functions in the trafficking of proteins to the sensory cilia, and have not been implicated in facilitation of neural communication. Finally, mutating the glial-expressed genes *fig-1* and *wrt-6* generates an increase in ADL neurosecretion as well as defects in sensory perception. Taking all these data together we propose that absence of sensory inputs initiate a homeostatic plasticity response which sensitises ADL neurosecretion to incoming activity from the O<sub>2</sub>-circuit and promotes O<sub>2</sub>-escape behaviour.

If this model is correct, our data would establish, to our knowledge, a first link between genetic deletions and homeostatic plasticity. So far, homeostatic plasticity has been studied by depriving wild type animals of sensory inputs using external means such as in the case of ocular deprivation, where a mouse's eyelids are surgically closed to block stimulation of the visual cortex. However, it is not clear if genetic mutations that affect sensory perception are also able to induce homeostatic plasticity. Our data provide a first evidence that this is the case. Further characterisation of our mutants will shed light on how mechanisms that induce homeostatic plasticity are similar in wild types and sensory mutants. This is particularly relevant since the loss of one or multiple sensory modalities is often the results of genetic disorders. How homeostatic plasticity mechanisms contribute to these diseases is not yet clear. In many of these conditions a defect in one sensory modality is often accompanied by the heightening sensitivity to a second modality. This phenomenon is referred to as cross-modal plasticity and it has been already described in *C. elegans* (Rabinowitch et al., 2016) where mechnosensory defective mutants show enhanced behavioural responses to odours. With our data we uncover an additional and novel mechanism of action for cross-modal plasticity. In

our model impairing sensory perception in ADL triggers homeostatic plasticity which in turn recruits the ADL sensory neurons into the O<sub>2</sub>-circuit, thus heightening the O<sub>2</sub>-escape responses of sensory defective mutants. This is an addition to the previously described mechanism where genetical disrupting mechanosensation in sensory neurons enhanced the output of a distinct neural class of chemosensory neurons by reducing the release of an inhibitory neuropeptide (Rabinowitch et al., 2016).

We realise, however, that the correlation we have observed between defective sensory perception, increased ADL neurosecretion and O<sub>2</sub>-escape behaviour, in multiple mutants does not itself validate our hypothesis. Therefore, we plan a series of experiment to manipulate this system and prove the causality between these phenotypes. First, we plan to exclusively impair sensory perception in ADL neurons to test if this results in an increase in neurosecretion. To do so, we intend to measure ADL neurosecretion after specifically knocking-down the regulatory factor X transcription factor *daf-19*, which is necessary for cilia formation, in ADL (Swoboda et al., 2000). Next, we plan to assess if increased ADL neurosecretion in *qui-1* mutants is sufficient to promote O<sub>2</sub>-escape behaviour. To do so, we intend to disrupt dense-core vesicles release from ADL in *qui-1* mutants and measure its effect on O<sub>2</sub>-escape behaviour. Finally, to understand the molecular changes that ADL undergoes in response to absence of *qui-1*, we plan to compare the ADL expression profiles of wild type and *qui-1* mutants and search for differentially expressed genes that might constitute a signature of homeostatic plasticity.

## **6.5. Oxygen experience reprograms neuropeptide expression in AQR, PQR and URX**

Neurons and neural circuits alter their gene expression levels in response to prolonged sensory experiences, thus allowing animals to thrive in a changing environment. Likewise, *C. elegans* adapts its behaviour and neural physiology to prolonged exposure to different oxygen concentrations. To investigate the transcriptional changes promoted by oxygen exposure, we isolate the main oxygen sensing neurons AQR, PQR and URX from animals grown at high (21%) and low (7%) oxygen concentrations and perform RNA-sequencing. The quality of our data-set shows our approach is robust, as biologically independent replicates cluster together in a principal component analysis and the most differently expressed genes also show consistent expression across biological replicates ( Fig 5.1A and Fig 5.3B,C). Our preparation is also likely to be reasonably pure. In fact, comparing our data-set with published profiles of *C. elegans* tissues and neural types (Cao et al., 2017; Kaletsky et al., 2018) shows our data-set is most enriched in neural genes

and most similar to the neural cell types URX, AQR and PQR. Based on these results we are confident our experimental procedure successfully generates a robust transcription profile of the main oxygen sensing neurons AQR, PQR and URX.

Rearing *C. elegans* at different oxygen concentrations reprograms some of its avoidance behaviours, and the neural properties of URX (Cheung et al., 2005; Fenk and de Bono, 2017). To investigate if oxygen experience modulates gene expression in the main O<sub>2</sub>-sensing neurons, we reared *npr-1* mutant animals (hereafter referred to WT for simplicity) at high (21%) and low (7%) oxygen concentrations and compared their transcriptional profiles. To refine our analysis and exclude changes in transcription due to the effects of oxygen on cell metabolism, we included in our experimental set up a *npr-1;gcy-35;gcy-36* triple mutant line (hereafter referred to *gcy* for simplicity). GCY-35 and GCY-36 function as the main molecular oxygen receptors and they are necessary for O<sub>2</sub>-evoked Ca<sup>2+</sup> activity in AQR, PQR and URX. They serve as a control to identify transcriptional changes dependent on O<sub>2</sub>-evoked activity since these changes should be abolished in *gcy* mutants.

By isolating genes differentially expressed in wild types at high and low oxygen, but not in *gcy* mutants grown in the same conditions, we isolate 455 experience-dependent genes (Fig 5.3A and 5.4A). Remarkably, among this group we find a large number of uncharacterised genes, many of which are short and encode a signal peptide. This suggests they might be unknown neuropeptides (Fig 5.4B,C). Moreover, using a more unbiased analysis we show that genes up-regulated by exposure to high oxygen are highly enriched for neuropeptides and neuropeptide receptors (Fig 5.4D). Interestingly, our analysis also points to oxygen being able to re-program neuropeptide expression in O<sub>2</sub>-sensing neurons; one group of neuropeptides are more highly expressed at high oxygen levels and another more highly expressed at low oxygen (Fig 5.4B,C). These neuropeptides may signal prolonged alteration in oxygen concentration to the O<sub>2</sub>-circuit and other neural circuits of the animal. It will be interesting to examine the expression pattern of known cognate receptors for these neuropeptides to identify possible target neurons.

Sensory neurons in *C. elegans* adapts their neural properties to experience not just of oxygen, but also of different sensory stimuli, including temperature. AFD, the main temperature-sensitive neuron, adapts its temperature-evoked Ca<sup>2+</sup> activity depending on previous temperature experiences, and regulates thermotaxis

behaviour accordingly (Hawk et al., 2018; Kobayashi et al., 2016). It has been shown that in AFD expression of *gcy-8*, *gcy-18* and *gcy-23*, which are thought to be the main temperature detectors (Goodman and Sengupta, 2018), are modulated after prolonged exposure to temperature warmer than the cultivation temperature. Therefore sensory guanylyl cyclases might be a substrate for experience-dependent changes (Yu et al., 2014). Consistent with this idea, AQR, PQR and URX sense oxygen through soluble guanylyl cyclase (GCY-35 and GCY-36) and URX adapts its O<sub>2</sub>-evoked Ca<sup>2+</sup> responses to prolonged exposure to low oxygen. However, levels of *gcy-35*, *gcy-36* or other guanylyl cyclases are not influenced by oxygen exposure (Data not shown). This difference could reflect the need for AFD and O<sub>2</sub>-sensing neurons to remodel different physiological properties in order to adapt to experiences. In fact, while AFD are phasic neurons activated by thermal fluctuations higher than the cultivation temperature, while AQR, PQR and URX are tonic neurons activated by increases in oxygen concentrations (Busch et al., 2012). It is possible that the different biophysical demands of phasic and tonic neurons underlies their different transcriptional signatures during adaptation.

High levels of neural activity in the nervous system promotes transcriptional changes. Although the molecular pathways inducing these changes are well known, which types of genes are regulated by activity and what effect they have on neural physiology is less clear. By comparing wild type with *gcy* mutants, we isolate genes whose transcription is modulated by O<sub>2</sub>-evoked activity (Fig 5.5A). We show that genes induced by neural activity in O<sub>2</sub>-sensing neurons are particularly enriched for neuropeptide and neuropeptide receptors. This observation is consistent with work done in mice where exogenously activating the dentate gyrus promotes activity-dependent changes in the accessibility of the promoters of neuropeptide and neuropeptide receptor genes. These changes are sustained for 24h suggesting their expression is induced over long time scales (Su et al., 2017).

We also compare wild types and *gcy* mutants exposed to low oxygen. In this case, our prediction is that in wild type animals at low oxygen the O<sub>2</sub>-sensing neurons are silent, and should therefore resemble *gcy* mutants. Remarkably, this is not the case and we observe a large number of genes, especially neuropeptides and neuropeptides receptors, that are induced in wild types exposed to low oxygen compared to *gcy* mutants exposed to the same condition (Fig 5.6A,B). This suggests that GCY-35 and GCY-36 are still active at low oxygen and necessary to induce gene expression. However, a simple model where GCY-35 and GCY-36 would drive the expression of this group of genes is incorrect as at high oxygen, where the guanylyl cyclases are more active, these genes are not induced.

Therefore, either the precise levels of GCY-35 and GCY-36 activation regulate the expression of these genes, or their induction is contingent on a second signal present exclusively at low oxygen.

Studying the expression profiles of O<sub>2</sub>-sensing neurons exposed to high or low oxygen provides us with a rich dataset with which to make predictions about the function of experience-dependent genes. Since the O<sub>2</sub>-circuit can reprogram other sensory modalities according to previous exposure to oxygen, we are keen to test if some of the neuropeptides we have identified as differentially expressed at high or low oxygen are involved in this reprogramming. Furthermore, not much is known about what regulates experience-dependent changes in gene expression at the circuit level. One possibility is that each neuron of the circuit adapts to changes in Ca<sup>2+</sup> activity independently. Alternatively, a subset of neurons might be devoted to the detection of changes in Ca<sup>2+</sup> activity and signal these changes to the rest of the circuit. By studying the effect that these neuropeptide have on the ability of other O<sub>2</sub>-circuit neurons to adapt to oxygen experience, we hope to be able to address this issue. We are also planning to isolate additional neurons of the O<sub>2</sub>-circuit using the same experimental procedure used for AQR, PQR and URX.

This will allow us to classify and study genes that are regulated similarly in multiple neural types, and genes whose regulation is restricted to one cell type. Furthermore, it will also be possible to test if some of the neuropeptides we have identified are required to induce experience dependent changes in transcription in other O<sub>2</sub>-circuit neurons.

## **6.6. Concluding remarks**

Despite the fact that O<sub>2</sub>-escape behaviour has been study in depth, we identify additional and novel genetic regulators, suggesting there is more to learn about its genetics. By characterising these mutants we uncover an unexpected plasticity in ADL neural properties. Defects in sensory perception sensitises ADL to pre-synaptic activity coming from the O<sub>2</sub>-circuit. Molecular characterisation of this sensitisation might shed light on conserved molecular mechanisms regulating cross-talk plasticity between sensory modalities.

Prolonged oxygen exposure remodels *C. elegans* behavioural strategies and physiology. We show that O<sub>2</sub>-sensing neurons AQR, PQR and URX reprograms their neuropeptide expression based on oxygen experience. Many of these are possibly new and unidentified neuropeptides. We propose reprogramming of neuropeptides expression might signal oxygen experience to the O<sub>2</sub>-circuit as well as other neural circuits. This will coordinate oxygen-dependent changes in *C. elegans* behaviour and physiology.



## Bibliography

- Adams, M.D., Celniker, S.E., Holt, R.A., Evans, C.A., Gocayne, J.D., Amanatides, P.G., Scherer, S.E., Li, P.W., Hoskins, R.A., Galle, R.F., *et al.* (2000). The genome sequence of *Drosophila melanogaster*. *Science* 287, 2185-2195.
- Akira, S., Uematsu, S., and Takeuchi, O. (2006). Pathogen recognition and innate immunity. *Cell* 124, 783-801.
- Allada, R., White, N.E., So, W.V., Hall, J.C., and Rosbash, M. (1998). A mutant *Drosophila* homolog of mammalian Clock disrupts circadian rhythms and transcription of period and timeless. *Cell* 93, 791-804.
- Angeles-Albores, D., RY, N.L., Chan, J., and Sternberg, P.W. (2016). Tissue enrichment analysis for *C. elegans* genomics. *BMC Bioinformatics* 17, 366.
- Arellano-Carbajal, F., Briseño-Roa, L., Couto, A., Cheung, B.H.H., Labouesse, M., and de Bono, M. (2011). Macoilin, a Conserved Nervous System-Specific ER Membrane Protein That Regulates Neuronal Excitability. *PLOS Genetics* 7, e1001341.
- Aspöck, G., Kagoshima, H., Niklaus, G., and Bürglin, T.R. (1999). *Caenorhabditis elegans* has scores of hedgehog-related genes: sequence and expression analysis. *Genome research* 9, 909-923.
- Bacaj, T., Tevlin, M., Lu, Y., and Shaham, S. (2008). Glia Are Essential for Sensory Organ Function in *C. elegans*. *Science* 322, 744-747.
- Bargmann, C.I. (1998). Neurobiology of the *Caenorhabditis elegans* Genome. *Science* 282, 2028-2033.
- Bargmann, C.I. (2006). Chemosensation in *C. elegans*. *WormBook*, 1-29.
- Bargmann, C.I. (2012). Beyond the connectome: How neuromodulators shape neural circuits. *BioEssays* 34, 458-465.
- Ben-Shahar, Y., Robichon, A., Sokolowski, M.B., and Robinson, G.E. (2002). Influence of gene action across different time scales on behavior. *Science* 296, 741-744.
- Bendesky, A., and Bargmann, C.I. (2011). Genetic contributions to behavioural diversity at the gene-environment interface. *Nat Rev Genet* 12, 809-820.
- Benzer, S. (1971). From the Gene to Behavior. *JAMA* 218, 1015-1022.
- Brenner, S. (1973). The genetics of behaviour. *British Medical Bulletin* 29, 269-271.
- Brenner, S. (1974). The Genetics of *Caenorhabditis elegans*. *Genetics* 77, 71-94.
- Bürglin, T.R. (1996). Warthog and Groundhog, novel families related to Hedgehog. *Current Biology* 6, 1047-1050.

Busch, K.E., Laurent, P., Soltesz, Z., Murphy, R.J., Faivre, O., Hedwig, B., Thomas, M., Smith, H.L., and de Bono, M. (2012). Tonic signaling from O<sub>2</sub> sensors sets neural circuit activity and behavioral state. *Nature Neuroscience* 15, 581-591.

Cao, J., Packer, J.S., Ramani, V., Cusanovich, D.A., Huynh, C., Daza, R., Qiu, X., Lee, C., Furlan, S.N., Steemers, F.J., *et al.* (2017). Comprehensive single-cell transcriptional profiling of a multicellular organism. *Science* 357, 661-667.

Carlezon, W.A., Duman, R.S., and Nestler, E.J. (2005). The many faces of CREB. *Trends in Neurosciences* 28, 436-445.

Carrillo, M.A., Guillermin, M.L., Rengarajan, S., Okubo, R.P., and Hallem, E.A. (2013). O<sub>2</sub>-sensing neurons control CO<sub>2</sub> response in *C. elegans*. *The Journal of Neuroscience* 33, 9675-9683.

Chang, A.J., Chronis, N., Karow, D.S., Marletta, M.A., and Bargmann, C.I. (2006). A distributed chemosensory circuit for oxygen preference in *C. elegans*. *PLOS Biol* 4, e274.

Cheadle, L., Tzeng, C.P., Kalish, B.T., Harmin, D.A., Rivera, S., Ling, E., Nagy, M.A., Hrvatin, S., Hu, L., Stroud, H., *et al.* (2018). Visual Experience-Dependent Expression of Fn14 Is Required for Retinogeniculate Refinement. *Neuron* 99, 525-539.e510.

Chen, C., Itakura, E., Nelson, G.M., Sheng, M., Laurent, P., Fenk, L.A., Butcher, R.A., Hegde, R.S., and de Bono, M. (2017). IL-17 is a neuromodulator of *Caenorhabditis elegans* sensory responses. *Nature*.

Chen, C., Itakura, E., Weber, K.P., Hegde, R.S., and de Bono, M. (2014). An ER complex of ODR-4 and ODR-8/Ufm1 specific protease 2 promotes GPCR maturation by a Ufm1-independent mechanism. *PLOS Genetics* 10, e1004082.

Cheung, B.H.H., Arellano-Carbajal, F., Rybicki, I., and de Bono, M. (2004). Soluble Guanylate Cyclases Act in Neurons Exposed to the Body Fluid to Promote *C. elegans* Aggregation Behavior. *Current Biology* 14, 1105-1111.

Cheung, B.H.H., Cohen, M., Rogers, C., Albayram, O., and de Bono, M. (2005). Experience-Dependent Modulation of *C. elegans* Behavior by Ambient Oxygen. *Current Biology* 15, 905-917.

Chronis, N., Zimmer, M., and Bargmann, C.I. (2007). Microfluidics for in vivo imaging of neuronal and behavioral activity in *Caenorhabditis elegans*. *Nature Methods* 4, 727-731.

Consortium, C.e.S. (1998). Genome sequence of the nematode *C. elegans*: A platform for investigating biology. *Science* 282, 2012-2018.

Cook, S.J., Jarrell, T.A., Brittin, C.A., Wang, Y., Bloniarz, A.E., Yakovlev, M.A., Nguyen, K.C.Q., Tang, L.T., Bayer, E.A., Duerr, J.S., *et al.* (2019). Whole-animal connectomes of both *Caenorhabditis elegans* sexes. *Nature* 571, 63-71.

Correa, R.G., Krajewska, M., Ware, C.F., Gerlic, M., and Reed, J.C. (2014). The NLR-related protein NWD1 is associated with prostate cancer and modulates androgen receptor signaling. *Oncotarget* 5, 1666-1682.

Coulson, A., Sulston, J., Brenner, S., and Karn, J. (1986). Toward a Physical Map of the Genome of the Nematode *Caenorhabditis-Elegans*. *Proceedings of the National Academy of Sciences of the United States of America* 83, 7821-7825.

DasGupta, S., Ferreira, C.H., and Miesenbock, G. (2014). FoxP influences the speed and accuracy of a perceptual decision in *Drosophila*. *Science* 344, 901-904.

de Bono, M., and Bargmann, C.I. (1998). Natural variation in a neuropeptide Y receptor homolog modifies social behavior and food response in *C. elegans*. *Cell* 94, 679-689.

de Bono, M., Tobin, D.M., Davis, M.W., Avery, L., and Bargmann, C.I. (2002). Social feeding in *Caenorhabditis elegans* is induced by neurons that detect aversive stimuli. *Nature* 419, 899-903.

Debelle, J.S., and Sokolowski, M.B. (1987). Heredity of Rover Sitter - Alternative Foraging Strategies of *Drosophila-Melanogaster* Larvae. *Heredity* 59, 73-83.

Deisseroth, K., Bitto, H., and Tsien, R.W. (1996). Signaling from synapse to nucleus: postsynaptic CREB phosphorylation during multiple forms of hippocampal synaptic plasticity. *Neuron* 16, 89-101.

Desai, N.S., Cudmore, R.H., Nelson, S.B., and Turrigiano, G.G. (2002). Critical periods for experience-dependent synaptic scaling in visual cortex. *Nat Neurosci* 5, 783-789.

Dill, L.M., and Ydenberg, R.C. (1987). The Group-Size - Flight Distance Relationship in Water Striders (*Gerris-Remigis*). *Canadian Journal of Zoology-Revue Canadienne De Zoologie* 65, 223-226.

Dudai, Y., Jan, Y.N., Byers, D., Quinn, W.G., and Benzer, S. (1976). *dunce*, a mutant of *Drosophila* deficient in learning. *Proc Natl Acad Sci U S A* 73, 1684-1688.

Dusenbery, D.B. (1980). Appetitive Response of the Nematode *Caenorhabditis-Elegans* to Oxygen. *J Comp Physiol* 136, 333-336.

Dwyer, N.D., Troemel, E.R., Sengupta, P., and Bargmann, C.I. (1998). Odorant Receptor Localization to Olfactory Cilia Is Mediated by ODR-4, a Novel Membrane-Associated Protein. *Cell* 93, 455-466.

Ebert, D.H., and Greenberg, M.E. (2013). Activity-dependent neuronal signalling and autism spectrum disorder. *Nature* 493, 327-337.

Evans, D.A., Stempel, A.V., Vale, R., and Branco, T. (2019). Cognitive Control of Escape Behaviour. *Trends Cogn Sci* 23, 334-348.

Fenk, L.A., and de Bono, M. (2015). Environmental CO<sub>2</sub> inhibits *Caenorhabditis elegans* egg-laying by modulating olfactory neurons and evokes widespread

changes in neural activity. *Proceedings of the National Academy of Sciences*, 201423808.

Fenk, L.A., and de Bono, M. (2017). Memory of recent oxygen experience switches pheromone valence in *Caenorhabditis elegans*. *Proceedings of the National Academy of Sciences* 114, 4195-4200.

Flavell, S.W., and Greenberg, M.E. (2008). Signaling Mechanisms Linking Neuronal Activity to Gene Expression and Plasticity of the Nervous System. *Annual review of neuroscience* 31, 563-590.

Frooninckx, L., Van Rompay, L., Temmerman, L., Van Sinay, E., Beets, I., Janssen, T., Husson, S.J., and Schoofs, L. (2012). Neuropeptide GPCRs in *C. elegans*. *Frontiers in Endocrinology* 3.

Goodman, M.B., and Sengupta, P. (2018). The extraordinary AFD thermosensor of *C. elegans*. *Pflugers Arch* 470, 839-849.

Graf, S.A., and Sokolowski, M.B.J.J.o.I.B. (1989). Rover/sitter *Drosophila melanogaster* larval foraging polymorphism as a function of larval development, food-patch quality, and starvation. 2, 301-313.

Gray, J.M., Karow, D.S., Lu, H., Chang, A.J., Chang, J.S., Ellis, R.E., Marletta, M.A., and Bargmann, C.I. (2004). Oxygen sensation and social feeding mediated by a *C. elegans* guanylate cyclase homologue. *Nature* 430, 317-322.

Greenwald, I. (2012). Notch and the Awesome Power of Genetics. *Genetics* 191, 655-669.

Groschner, L.N., Hak, L.C.W., Bogacz, R., DasGupta, S., and Miesenböck, G. (2018). Dendritic Integration of Sensory Evidence in Perceptual Decision-Making. *Cell* 173, 894-905.e813.

Gumienny, T.L., and Savage-Dunn, C. (2013). TGF-beta signaling in *C. elegans*. *WormBook*, 1-34.

Hawk, J.D., Calvo, A.C., Liu, P., Almoril-Porras, A., Aljobeh, A., Torruella-Suárez, M.L., Ren, I., Cook, N., Greenwood, J., Luo, L., *et al.* (2018). Integration of Plasticity Mechanisms within a Single Sensory Neuron of *C. elegans* Actuates a Memory. *Neuron* 97, 356-367.e354.

Hilliard, M.A., Bergamasco, C., Arbucci, S., Plasterk, R.H., and Bazzicalupo, P. (2004). Worms taste bitter: ASH neurons, QUI-1, GPA-3 and ODR-3 mediate quinine avoidance in *Caenorhabditis elegans*. *The EMBO Journal* 23, 1101-1111.

Hobert, O. (2013). The neuronal genome of *Caenorhabditis elegans*. *WormBook*, 1-106.

Hodgkin, J. (1989). Early Worms. *Genetics* 121, 1-3.

Hodgkin, J.A., and Brenner, S. (1977). Mutations causing transformation of sexual phenotype in the nematode *Caenorhabditis elegans*. *Genetics* 86, 275-287.

Hong, E.J., McCord, A.E., and Greenberg, M.E. (2008a). A Biological Function for the Neuronal Activity-Dependent Component of Bdnf Transcription in the Development of Cortical Inhibition. *Neuron* 60, 610-624.

Hong, R.L., Witte, H., and Sommer, R.J. (2008b). Natural variation in *Pristionchus pacificus* insect pheromone attraction involves the protein kinase EGL-4. *Proc Natl Acad Sci U S A* 105, 7779-7784.

Horvitz, H.R., and Sulston, J.E. (1980). Isolation and genetic characterization of cell-lineage mutants of the nematode *Caenorhabditis elegans*. *Genetics* 96, 435-454.

Hussey, R., Stieglitz, J., Mesgarzadeh, J., Locke, T.T., Zhang, Y.K., Schroeder, F.C., and Srinivasan, S. (2017). Pheromone-sensing neurons regulate peripheral lipid metabolism in *Caenorhabditis elegans*. *PLoS Genet* 13, e1006806.

Ibata, K., Sun, Q., and Turrigiano, G.G. (2008). Rapid synaptic scaling induced by changes in postsynaptic firing. *Neuron* 57, 819-826.

Inglis, P.N., Ou, G., Leroux, M.R., and Scholey, J.M. (2007). The sensory cilia of *Caenorhabditis elegans*. *WormBook*, 1-22.

Ingram, K.K., Oefner, P., and Gordon, D.M. (2005). Task-specific expression of the foraging gene in harvester ants. *Mol Ecol* 14, 813-818.

Insel, T.R., Wang, Z.X., and Ferris, C.F. (1994). Patterns of brain vasopressin receptor distribution associated with social organization in microtine rodents. *J Neurosci* 14, 5381-5392.

Jang, H., Kim, K., Neal, S.J., Macosko, E., Kim, D., Butcher, R.A., Zeiger, D.M., Bargmann, C.I., and Sengupta, P. (2012). Neuromodulatory State and Sex Specify Alternative Behaviors through Antagonistic Synaptic Pathways in *C. elegans*. *Neuron* 75, 585-592.

Jang, H., Levy, S., Flavell, S.W., Mende, F., Latham, R., Zimmer, M., and Bargmann, C.I. (2017). Dissection of neuronal gap junction circuits that regulate social behavior in *Caenorhabditis elegans*. *Proceedings of the National Academy of Sciences* 114, E1263-E1272.

Jarrell, T.A., Wang, Y., Bloniarz, A.E., Brittin, C.A., Xu, M., Thomson, J.N., Albertson, D.G., Hall, D.H., and Emmons, S.W. (2012). The Connectome of a Decision-Making Neural Network. *Science* 337, 437-444.

Kaletsky, R., Yao, V., Williams, A., Runnels, A.M., Tadych, A., Zhou, S., Troyanskaya, O.G., and Murphy, C.T. (2018). Transcriptome analysis of adult *Caenorhabditis elegans* cells reveals tissue-specific gene and isoform expression. *PLOS Genetics* 14, e1007559-1007529.

Kandel, E.R. (2012). The molecular biology of memory: cAMP, PKA, CRE, CREB-1, CREB-2, and CPEB. *Molecular Brain* 5.

Kandel, E.R., Dudai, Y., and Mayford, M.R. (2014). The Molecular and Systems Biology of Memory. *Cell* 157, 163-186.

Kim, S.M., Su, C.Y., and Wang, J.W. (2017). Neuromodulation of Innate Behaviors in *Drosophila*. *Annu Rev Neurosci* 40, 327-348.

King, D.P., Zhao, Y., Sangoram, A.M., Wilsbacher, L.D., Tanaka, M., Antoch, M.P., Steeves, T.D., Vitaterna, M.H., Kornhauser, J.M., Lowrey, P.L., *et al.* (1997). Positional cloning of the mouse circadian clock gene. *Cell* 89, 641-653.

Knappek, S., Kahsai, L., Winther, A.M., Tanimoto, H., and Nassel, D.R. (2013). Short neuropeptide F acts as a functional neuromodulator for olfactory memory in Kenyon cells of *Drosophila* mushroom bodies. *J Neurosci* 33, 5340-5345.

Ko, K.I., Root, C.M., Lindsay, S.A., Zaninovich, O.A., Shepherd, A.K., Wasserman, S.A., Kim, S.M., and Wang, J.W. (2015). Starvation promotes concerted modulation of appetitive olfactory behavior via parallel neuromodulatory circuits. *Elife* 4.

Kobayashi, K., Nakano, S., Amano, M., Tsuboi, D., Nishioka, T., Ikeda, S., Yokoyama, G., Kaibuchi, K., and Mori, I. (2016). Single-Cell Memory Regulates a Neural Circuit for Sensory Behavior. *Cell Reports* 14, 11-21.

Konopka, R.J., and Benzer, S. (1971). Clock mutants of *Drosophila melanogaster*. *Proc Natl Acad Sci U S A* 68, 2112-2116.

Lakhina, V., Arey, R.N., Kaletsky, R., Kauffman, A., Stein, G., Keyes, W., Xu, D., and Murphy, C.T. (2015). Genome-wide functional analysis of CREB/long-term memory-dependent transcription reveals distinct basal and memory gene expression programs. *Neuron* 85, 330-345.

Lander, E.S., Consortium, I.H.G.S., Linton, L.M., Birren, B., Nusbaum, C., Zody, M.C., Baldwin, J., Devon, K., Dewar, K., Doyle, M., *et al.* (2001). Initial sequencing and analysis of the human genome. *Nature* 409, 860-921.

Laurent, P., Soltesz, Z., Nelson, G.M., Chen, C., Arellano-Carbajal, F., Levy, E., and de Bono, M. (2015). Decoding a neural circuit controlling global animal state in *C. elegans*. *Elife* 4.

Lee, B.H., Liu, J., Wong, D., Srinivasan, S., and Ashrafi, K. (2011). Hyperactive Neuroendocrine Secretion Causes Size, Feeding, and Metabolic Defects of *C. elegans* Bardet-Biedl Syndrome Mutants. *PLOS Biol* 9, e1001219.

Lim, M.M., Wang, Z., Olazabal, D.E., Ren, X., Terwilliger, E.F., and Young, L.J. (2004). Enhanced partner preference in a promiscuous species by manipulating the expression of a single gene. *Nature* 429, 754-757.

Lima, S.L., and Dill, L.M. (1990). Behavioral Decisions Made under the Risk of Predation - a Review and Prospectus. *Can J Zool* 68, 619-640.

Ludewig, A.H., and Schroeder, F.C. (2012). Ascaroside signaling in *C. elegans*. In ([wormbook.org](http://wormbook.org)), pp. 585-592.

Macosko, E.Z., Pokala, N., Feinberg, E.H., Chalasani, S.H., Butcher, R.A., Clardy, J., and Bargmann, C.I. (2009). A hub-and-spoke circuit drives pheromone attraction and social behaviour in *C. elegans*. *Nature* 458, 1171-1175.

Maffei, A., and Turrigiano, G.G. (2008). Multiple modes of network homeostasis in visual cortical layer 2/3. *J Neurosci* 28, 4377-4384.

Mardinly, A.R., Spiegel, I., Patrizi, A., Centofante, E., Bazinet, J.E., Tzeng, C.P., Mandel-Brehm, C., Harmin, D.A., Adesnik, H., Fagiolini, M., *et al.* (2016). Sensory experience regulates cortical inhibition by inducing IGF1 in VIP neurons. *Nature* 531, 371-375.

Miller, K.G., Emerson, M.D., and Rand, J.B. (1999). Gqalpha and diacylglycerol kinase negatively regulate the Gqalpha pathway in *C. elegans*. *Neuron* 24, 323-333.

Mukherjee, D., Ignatowska-Jankowska, B.M., Itskovits, E., Gonzales, B.J., Turm, H., IZakson, L., Haritan, D., Bleistein, N., Cohen, C., Amit, I., *et al.* (2018). Salient experiences are represented by unique transcriptional signatures in the mouse brain. *eLife* 7, e31220.

Neal, S.J., Park, J., DiTirro, D., Yoon, J., Shibuya, M., Choi, W., Schroeder, F.C., Butcher, R.A., Kim, K., and Sengupta, P. (2016). A Forward Genetic Screen for Molecules Involved in Pheromone-Induced Dauer Formation in *Caenorhabditis elegans*. *G3 (Bethesda)* 6, 1475-1487.

Nicoll, R.A. (2017). A Brief History of Long-Term Potentiation. *Neuron* 93, 281-290.

Nurrish, S., Segalat, L., and Kaplan, J.M. (1999). Serotonin inhibition of synaptic transmission: Galpha(0) decreases the abundance of UNC-13 at release sites. *Neuron* 24, 231-242.

Nusbaum, M.P., Blitz, D.M., and Marder, E. (2017). Functional consequences of neuropeptide and small-molecule co-transmission. *Nat Rev Neurosci* 18, 389-403.

O'Leary, T., Williams, A.H., Caplan, J.S., and Marder, E. (2013). Correlations in ion channel expression emerge from homeostatic tuning rules. *Proc Natl Acad Sci U S A* 110, E2645-2654.

Oikonomou, G., Perens, E.A., Lu, Y., Watanabe, S., Jorgensen, E.M., and Shaham, S. (2011). Opposing activities of LIT-1/NLK and DAF-6/patched-related direct sensory compartment morphogenesis in *C. elegans*. *PLoS Biol* 9, e1001121.

Oikonomou, G., and Shaham, S. (2011). The Glia of *Caenorhabditis elegans*. *Glia* 59, 1253-1263.

Osborne, K.A., Robichon, A., Burgess, E., Butland, S., Shaw, R.A., Coulthard, A., Pereira, H.S., Greenspan, R.J., and Sokolowski, M.B. (1997). Natural behavior polymorphism due to a cGMP-dependent protein kinase of *Drosophila*. *Science* 277, 834-836.

Panda, S., Hogenesch, J.B., and Kay, S.A. (2002). Circadian rhythms from flies to human. *Nature* 417, 329-335.

Perens, E.A., and Shaham, S. (2005). *C. elegans* daf-6 encodes a patched-related protein required for lumen formation. *Dev Cell* 8, 893-906.

Perkins, L.A., Hedgecock, E.M., Thomson, J.N., and Culotti, J.G. (1986). Mutant Sensory Cilia in the Nematode *Caenorhabditis-Elegans*. *Developmental Biology* 117, 456-487.

Persson, A., Gross, E., Laurent, P., Busch, K.E., Bretes, H., and de Bono, M. (2009). Natural variation in a neural globin tunes oxygen sensing in wild *Caenorhabditis elegans*. *Nature* 458, 1030-1033.

Picelli, S., Faridani, O.R., Björklund, A.K., Winberg, G., Sagasser, S., and Sandberg, R. (2014). Full-length RNA-seq from single cells using Smart-seq2. *Nature Protocols* 9, 171-181.

Pinsker, H., Kupfermann, I., Castellucci, V., and Kandel, E. (1970). Habituation and Dishabituation of Gill-Withdrawal Reflex in *Aplysia*. *Science* 167, 1740-+.

Pinsker, H.M., Hening, W.A., Carew, T.J., and Kandel, E.R. (1973). Long-Term Sensitization of a Defensive Withdrawal Reflex in *Aplysia*. *Science* 182, 1039-1042.

Rabinowitch, I., Laurent, P., Zhao, B., Walker, D., Beets, I., Schoofs, L., Bai, J., Schafer, W.R., and Treinin, M. (2016). Neuropeptide-Driven Cross-Modal Plasticity following Sensory Loss in *Caenorhabditis elegans*. *PLoS Biol* 14, e1002348.

Rogers, C., Persson, A., Cheung, B., and de Bono, M. (2006). Behavioral Motifs and Neural Pathways Coordinating O<sub>2</sub> Responses and Aggregation in *C. elegans*. *Current Biology* 16, 649-659.

Rogers, C., Reale, V., Kim, K., Chatwin, H., Li, C., Evans, P., and de Bono, M. (2003). Inhibition of *Caenorhabditis elegans* social feeding by FMRFamide-related peptide activation of NPR-1. *Nature Neuroscience* 6, 1178-1185.

Root, C.M., Ko, K.I., Jafari, A., and Wang, J.W. (2011). Presynaptic facilitation by neuropeptide signaling mediates odor-driven food search. *Cell* 145, 133-144.

Rutherford, L.C., DeWan, A., Lauer, H.M., and Turrigiano, G.G. (1997). Brain-derived neurotrophic factor mediates the activity-dependent regulation of inhibition in neocortical cultures. *J Neurosci* 17, 4527-4535.

Rutila, J.E., Suri, V., Le, M., So, W.V., Rosbash, M., and Hall, J.C. (1998). CYCLE is a second bHLH-PAS clock protein essential for circadian rhythmicity and transcription of *Drosophila* period and timeless. *Cell* 93, 805-814.

Schulenburg, H., and Felix, M.A. (2017). The Natural Biotic Environment of *Caenorhabditis elegans*. *Genetics* 206, 55-86.

Sehgal, A., Price, J.L., Man, B., and Young, M.W. (1994). Loss of circadian behavioral rhythms and per RNA oscillations in the *Drosophila* mutant timeless. *Science* 263, 1603-1606.

Sengupta, P., Chou, J.H., and Bargmann, C.I. (1996). odr-10 encodes a seven transmembrane domain olfactory receptor required for responses to the odorant diacetyl. *Cell* 84, 899-909.

Sidenkiamos, I., Saunders, R.D.C., Spanos, L., Majerus, T., Treanear, J., Savakis, C., Louis, C., Glover, D.M., Ashburner, M., and Kafatos, F.C. (1990). Towards a Physical Map of the *Drosophila-Melanogaster* Genome - Mapping of Cosmid Clones within Defined Genomic Divisions. *Nucleic Acids Research* 18, 6261-6270.

Sokolowski, M.B. (2001). *Drosophila*: genetics meets behaviour. *Nat Rev Genet* 2, 879-890.

Spiegel, I., Mardinly, A.R., Gabel, H.W., Bazinet, J.E., Couch, C.H., Tzeng, C.P., Harmin, D.A., and Greenberg, M.E. (2014). Npas4 regulates excitatory-inhibitory balance within neural circuits through cell-type-specific gene programs. *Cell* 157, 1216-1229.

Stein, C., Caccamo, M., Laird, G., and Leptin, M. (2007). Conservation and divergence of gene families encoding components of innate immune response systems in zebrafish. *Genome Biology* 8, R251.

Stellwagen, D., and Malenka, R.C. (2006). Synaptic scaling mediated by glial TNF- $\alpha$ . *Nature* 440, 1054-1059.

Su, Y., Shin, J., Zhong, C., Wang, S., Roychowdhury, P., Lim, J., Kim, D., Ming, G.-I., and Song, H. (2017). Neuronal activity modifies the chromatin accessibility landscape in the adult brain. *Nature Neuroscience* 20, 476-483.

Sudhof, T.C. (2017). Molecular Neuroscience in the 21st Century: A Personal Perspective. *Neuron* 96, 536-541.

Swoboda, P., Adler, H.T., and Thomas, J.H. (2000). The RFX-type transcription factor DAF-19 regulates sensory neuron cilium formation in *C. elegans*. *Mol Cell* 5, 411-421.

Taghert, P.H., and Nitabach, M.N. (2012). Peptide Neuromodulation in Invertebrate Model Systems. *Neuron* 76, 82-97.

Tan, P.L., Barr, T., Inglis, P.N., Mitsuma, N., Huang, S.M., Garcia-Gonzalez, M.A., Bradley, B.A., Coforio, S., Albrecht, P.J., Watnick, T., *et al.* (2007). Loss of Bardet Biedl syndrome proteins causes defects in peripheral sensory innervation and function. *Proceedings of the National Academy of Sciences of the United States of America* 104, 17524-17529.

Taylor, S.R., Santpere, G., Reilly, M., Glenwinkel, L., Poff, A., McWhirter, R., Xu, C., Weinreb, A., Basavaraju, M., Cook, S.J., *et al.* (2019). Expression profiling of the mature *C. elegans* nervous system by single-cell RNA-Sequencing. *bioRxiv*, 737577.

Troemel, E.R., Chou, J.H., Dwyer, N.D., Colbert, H.A., and Bargmann, C.I. (1995). Divergent seven transmembrane receptors are candidate chemosensory receptors in *C. elegans*. *Cell* 83, 207-218.

Turrigiano, G., Abbott, L.F., and Marder, E. (1994). Activity-dependent changes in the intrinsic properties of cultured neurons. *Science* 264, 974-977.

Turrigiano, G.G. (2008). The Self-Tuning Neuron: Synaptic Scaling of Excitatory Synapses. *Cell* 135, 422-435.

Turrigiano, G.G., Leslie, K.R., Desai, N.S., Rutherford, L.C., and Nelson, S.B. (1998). Activity-dependent scaling of quantal amplitude in neocortical neurons. *Nature* 391, 892-896.

Venter, J.C., Adams, M.D., Myers, E.W., Li, P.W., Mural, R.J., Sutton, G.G., Smith, H.O., Yandell, M., Evans, C.A., Holt, R.A., *et al.* (2001). The sequence of the human genome. *Science* 291, 1304-+.

Waggoner, L.E., Hardaker, L.A., Golik, S., and Schafer, W.R. (2000). Effect of a neuropeptide gene on behavioral states in *Caenorhabditis elegans* egg-laying. *Genetics* 154, 1181-1192.

Waterston, R.H., Lindblad-Toh, K., Birney, E., Rogers, J., Abril, J.F., Agarwal, P., Agarwala, R., Ainscough, R., Alexandersson, M., An, P., *et al.* (2002). Initial sequencing and comparative analysis of the mouse genome. *Nature* 420, 520-562.

Wellborn, G.A., and Robinson, J.V. (1987). Microhabitat Selection as an Antipredator Strategy in the Aquatic Insect *Pachydiplax-Longipennis* Burmeister (Odonata, Libellulidae). *Oecologia* 71, 185-189.

West, A.E., Chen, W.G., Dalva, M.B., Dolmetsch, R.E., Kornhauser, J.M., Shaywitz, A.J., Takasu, M.A., Tao, X., and Greenberg, M.E. (2001). Calcium regulation of neuronal gene expression. *Proc Natl Acad Sci U S A* 98, 11024-11031.

White, J.G., Southgate, E., Thomson, J.N., and Brenner, S. (1986). The Structure of the Nervous System of the Nematode *Caenorhabditis elegans*. *Philosophical Transactions of the Royal Society of London B: Biological Sciences* 314, 1-340.

Wu, T., Duan, F., Yang, W., Liu, H., Caballero, A., Fernandes de Abreu, D.A., Dar, A.R., Alcedo, J., Ch'ng, Q., Butcher, R.A., *et al.* (2019). Pheromones Modulate Learning by Regulating the Balanced Signals of Two Insulin-like Peptides. *Neuron* 104, 1095-1109 e1095.

Yamada, S., and Sakakibara, S.i. (2018). Expression profile of the STAND protein *Nwd1* in the developing and mature mouse central nervous system. *Journal of Comparative Neurology* 8, 141.

Yap, E.-L., and Greenberg, M.E. (2018). Activity-Regulated Transcription: Bridging the Gap between Neural Activity and Behavior. *Neuron* 100, 330-348.

- Young, L.J., Nilsen, R., Waymire, K.G., MacGregor, G.R., and Insel, T.R. (1999). Increased affiliative response to vasopressin in mice expressing the V1a receptor from a monogamous vole. *Nature* 400, 766-768.
- Yu, Y.L., Zhi, L.T., Guan, X.M., Wang, D.Y., and Wang, D.Y. (2016). FLP-4 neuropeptide and its receptor in a neuronal circuit regulate preference choice through functions of ASH-2 trithorax complex in *Caenorhabditis elegans*. *Scientific Reports* 6.
- Yu, Y.X.V., Bell, H.W., Glauser, D.A., Van Hooser, S.D., Goodman, M.B., and Sengupta, P. (2014). CaMKI-Dependent Regulation of Sensory Gene Expression Mediates Experience-Dependent Plasticity in the Operating Range of a Thermosensory Neuron. *Neuron* 84, 919-926.
- Zigmond, R.E., and Ben-Ari, Y. (1977). Electrical stimulation of preganglionic nerve increases tyrosine hydroxylase activity in sympathetic ganglia. *Proc Natl Acad Sci U S A* 74, 3078-3080.
- Zimmer, M., Gray, J.M., Pokala, N., Chang, A.J., Karow, D.S., Marletta, M.A., Hudson, M.L., Morton, D.B., Chronis, N., and Bargmann, C.I. (2009). Neurons Detect Increases and Decreases in Oxygen Levels Using Distinct Guanylate Cyclases. *Neuron* 61, 865-879.
- Zuchero, J.B., and Barres, B.A. (2015). Glia in mammalian development and disease. *Development* 142, 3805-3809.
- Zucker, R.S., and Regehr, W.G. (2002). Short-term synaptic plasticity. *Annu Rev Physiol* 64, 355-405.
- Zuryn, S., Le Gras, S., Jamet, K., and Jarriault, S. (2010). A Strategy for Direct Mapping and Identification of Mutations by Whole-Genome Sequencing. *Genetics* 186, 427-430.





Table 2: SNPs-mapping of db1221 allele on Chr X Mav non Dpy

	9Mb	9.5Mb	10.5Mb	11.5Mb	12Mb	12.5Mb	13.5Mb	Phenotype
	<b>T25B6.1</b>	<b>F49E2.2_9</b>	<b>frm-9</b>	<b>sdc-2</b>	<b>C23H4.8</b>	<b>lips-1</b>	<b>C40C9.7</b>	
10.1	WT_A	WT_C	WT_G	WT_C	WT_C	WT_C	WT_C	WT
10.3	WT_A	WT_C	WT_G	WT_C	WT_C	/	WT_C	WT
7.3	Mut_T	WT_C	WT_G	WT_C	WT_C	WT_C	WT_C	WT
17.1	Mut_T	Mut_T	Mut_A/ WT_G	WT_C	WT_C	WT_C	WT_C	C
1.1	Mut_T	Mut_T	Mut_A	WT_C	WT_C	WT_C	WT_C	WT
12.2	Mut_T	Mut_T	Mut_A	WT_C	Mut_T/ WT_C	WT_C	WT_C	C++
12.4	Mut_T	Mut_T	Mut_A	WT_C	Mut_T/ WT_C	WT_C	WT_C	C++
14.2	Mut_T	Mut_T	Mut_A	WT_C	WT_C	WT_C	WT_C	C
18.5	Mut_T	Mut_T	Mut_A	WT_C/ Mut_T	Mut_T/ WT_C	WT_C/ Mut_T	WT_C/ Mut_T	C
2.1	Mut_T	Mut_T	/	Mut_T	Mut_T/ WT_C	WT_C/ Mut_T	/	WT
5.3	Mut_T	Mut_T	Mut_A	Mut_T	Mut_T	WT_T	WT_C	C
6.3	Mut_T	Mut_T	Mut_A	Mut_T	Mut_T	Mut_T	WT_C	C++
4.2	/	Mut_T	Mut_A	Mut_T	/	Mut_T	Mut_T	C
8.2	Mut_T	Mut_T	Mut_A	Mut_T	/	Mut_T	Mut_T	WT
11.3	Mut_T	Mut_T	Mut_A	Mut_T	Mut_T	Mut_T	/	C
12.7	Mut_T	Mut_T	Mut_A	Mut_T	Mut_T	Mut_T	Mut_T	C
18.3	/	/	Mut_A	Mut_T	Mut_T	Mut_T	Mut_T	C
18.6	Mut_T	Mut_T	Mut_A	Mut_T	Mut_T	Mut_T	Mut_T	WT
20.3	Mut_T	Mut_T	Mut_A	Mut_T	/	Mut_T	Mut_T	WT
3.2	Mut_T	Mut_T	Mut_A	Mut_T	Mut_T/ WT_C	Mut_T	Mut_T	WT

Table 3: Mapping db1221 to Chromosome II Independent line 1

Isolate number	1		Fluorescence marker	n Clumpers	%Clumpers
<b>Clumpers</b>	28		+/+	5	18
<b>Total plates</b>	50		+/-	5	18
			-/-	18	64
<b>% Clumpers</b>	56				

Table 4: Mapping db1221 to Chromosome II Independent line 2

Isolate number	2		Fluorescence marker	n Clumpers	%Clumpers
<b>Clumpers</b>	35		+/+	3	9
<b>Tot</b>	50		+/-	9	26
			-/-	23	66
<b>% Clumpers</b>	70				

Table 5: Mapping db1221 to Chromosome II Independent line 3

Isolate number	3		Fluorescence marker	n Clumpers	%Clumpers
<b>Clumpers</b>	30		+/+	2	7
<b>Tot</b>	50		+/-	8	27
			-/-	19	63
<b>% Clumpers</b>	60				

Table 6: Mapping db1221 to Chromosome IV Independent line 1

Isolate number	1		Fluorescence marker	n Clumpers	%Clumpers
<b>Clumpers</b>	24		+/+	8	33
<b>Tot</b>	50		+/-	13	54
			-/-	7	29
<b>% Clumpers</b>	48				

Table 7: Mapping db1221 to Chromosome V Independent line 1

Isolate number	1		Fluorescence marker	n Clumpers	%Clumpers
<b>Clumpers</b>	31		+/+	5	16
<b>Tot</b>	50		+/-	17	55
			-/-	9	29
<b>% Clumpers</b>	62				

Table 8: 3-point Mapping of db1221 allele Mav non Roller

Recombinant line	Phenotype
db1221 Mav non Rol Rec 1	C+ and WT
db1221 Mav non Rol Rec 2	WT
db1221 Mav non Rol Rec 3	WT
db1221 Mav non Rol Rec 4	WT
db1221 Mav non Rol Rec 5	WT
db1221 Mav non Rol Rec 6	WT
db1221 Mav non Rol Rec 7	WT
db1221 Mav non Rol Rec 8	WT
db1221 Mav non Rol Rec 9	C+
db1221 Mav non Rol Rec 10	WT
db1221 Mav non Rol Rec 11	WT
db1221 Mav non Rol Rec 12	C+

Table 9: 3-point Mapping of db1221 allele Mav non Unc

Recombinant line	Phenotype
db1221 Mav non Unc Rec 1	WT
db1221 Mav non Unc Rec 2	WT
db1221 Mav non Unc Rec 3	C
db1221 Mav non Unc Rec 4	WT
db1221 Mav non Unc Rec 5	C+ and WT
db1221 Mav non Unc Rec 6	WT
db1221 Mav non Unc Rec 7	WT
db1221 Mav non Unc Rec 8	?
db1221 Mav non Unc Rec 9	WT
db1221 Mav non Unc Rec 10	C+ and WT
db1221 Mav non Unc Rec 11	WT
db1221 Mav non Unc Rec 12	WT

Table 10: 3-point Mapping of db1221 allele Roller non

Recombinant line	Phenotype
db1221 Rol non Unc Rec 1	WT
db1221 Rol non Unc Rec 2	WT
db1221 Rol non Unc Rec 3	C
db1221 Rol non Unc Rec 4	WT
db1221 Rol non Unc Rec 5	WT
db1221 Rol non Unc Rec 6	WT
db1221 Rol non Unc Rec 7	WT
db1221 Rol non Unc Rec 8	WT/C+
db1221 Rol non Unc Rec 9	WT/C+
db1221 Rol non Unc Rec 10	WT

Table 11: SNPs-mapping of db1239 allele on Chr V Dpy non Unc

	9.0 Mb	10.2 Mb	11.2 Mb	11.8 Mb	13.2 Mb	Phenotype
	srx-3	tftc-3	clec-223	sulp-4	uig-1	
Dpy 1	Mut_T	Mut_A	Mut_T	Mut_T	Mut_A	C
Dpy 3	Mut_T	Mut_A	Mut_T	Mut_T	Mut_A	C
Dpy 5	Mut_T	Mut_A	Mut_T	Mut_T	Mut_A	C
Dpy 8	Mut_T	Mut_A	Mut_T	Mut_T	Mut_A	C
Dpy 9	Mut_T	Mut_A	Mut_T	Mut_T	Mut_A	C
Dpy 12	Mut_T	Mut_A	Mut_T	Mut_T	Mut_A	C
Dpy 2	WT_C	Mut_A	Mut_T	Mut_T	Mut_A	C
Dpy 11	WT_C	WT_G	Mut_T	Mut_T	Mut_A	C
Dpy 6	WT_C	WT_G	Mut_T	Mut_T	Mut_A	WT
Dpy 4	WT_C	WT_G	WT_C	WT_C	Mut_A	WT
Dpy 7	WT_C	WT_G	WT_C	WT_C	WT_G	WT
Dpy 10	WT_C	WT_G	WT_C	WT_C	WT_G	WT
Dpy 13	WT_C	WT_G	WT_C	WT_C	WT_G	WT

Table 12: SNPs-mapping of db1239 allele on Chr V Dpy non Unc

	9.0 Mb	10.2 Mb	10.4 Mb	10.9 Mb	11.2 Mb	11.8 Mb	13.2 Mb	Pheno type
	srx-3	tftc-3	snf-10	fig-1	clec-223	sulp-4	uig-1	
db1239_33	Het_T/C	Mut_A			Mut_T	Mut_T	Mut_A	C
db1239_2	WT_C	Het_A/G			Het_T/C	Het_T/C	Het_A/G	C
db1239_7	WT_C	Het_A/G			Het_T/C	Het_T/C	Het_A/G	C
db1239_23	WT_C	Het_A/G			Het_T/C	Het_T/C	Het_A/G	C
db1239_64	WT_C	Het_A/G			Het_T/C	Het_T/C	Het_A/G	C
db1239_77	WT_C	Het_A/G			Het_T/C	Het_T/C	Het_A/G	C
db1239_85	WT_C	Het_A/G			Het_T/C	Het_T/C	Het_A/G	C
db1239_87	WT_C	Het_A/G			Het_T/C	Het_T/C	Het_A/G	C
db1239_91	WT_C	Het_A/G			Het_T/C	Het_T/C	Het_A/G	C
db1239_38	WT_C	Het_A/G			Het_T/C	Het_T/C	Het_A/G	C
db1239_50	WT_C	Het_A/G			Het_T/C	Het_T/C	Het_A/G	C
db1239_15	WT_C	WT_G	WT_G	Het_A/G	Het_T/C	Het_T/C	Het_A/G	C
db1239_57	WT_C	WT_G	WT_G	Het_A/G	Het_T/C	Het_T/C	Het_A/G	C
db1239_63	WT_C	WT_G	WT_G	Het_A/G	Het_T/C	Het_T/C	Het_A/G	C
db1239_46	WT_C	WT_G	WT_G	WT_G	Het_T/C	Het_T/C	Het_A/G	WT
db1239_3	WT_C	WT_G			WT_C	Het_T/C	Het_A/G	WT
db1239_5	WT_C	WT_G			WT_C	Het_T/C	Het_A/G	WT
db1239_9	WT_C	WT_G			WT_C	Het_T/C	Het_A/G	WT
db1239_19	WT_C	WT_G			WT_C	Het_T/C	Het_A/G	WT
db1239_30	WT_C	WT_G			WT_C	Het_T/C	Het_A/G	WT
db1239_41	WT_C	WT_G			WT_C	Het_T/C	Het_A/G	WT
db1239_48	WT_C	WT_G			WT_C	Het_T/C	Het_A/G	WT
db1239_52	WT_C	WT_G			WT_C	Het_T/C	Het_A/G	WT
db1239_66	WT_C	WT_G			WT_C	Het_T/C	Het_A/G	WT
db1239_69	WT_C	/			WT_C	Het_T/C	Het_A/G	WT
db1239_89	WT_C	WT_G			/	Het_T/C	Het_A/G	WT
db1239_18	WT_C	WT_G			WT_C	WT_C	Het_A/G	C
db1239_14	WT_C	WT_G			WT_C	WT_C	Het_A/G	WT
db1239_20	WT_C	WT_G			WT_C	WT_C	Het_A/G	WT
db1239_22	WT_C	WT_G			WT_C	WT_C	Het_A/G	WT

db1239_36	WT_C	WT_G			WT_C	WT_C	Het_A/G	WT
db1239_42	WT_C	WT_G			WT_C	WT_C	Het_A/G	WT
db1239_49	WT_C	WT_G			WT_C	WT_C	Het_A/G	WT
db1239_54	WT_C	WT_G			WT_C	WT_C	Het_A/G	WT
db1239_72	WT_C	WT_G			WT_C	WT_C	Het_A/G	WT
db1239_78	WT_C	WT_G			WT_C	WT_C	Het_A/G	WT
db1239_84	WT_C	WT_G			WT_C	WT_C	Het_A/G	WT
db1239_96	WT_C	WT_G			WT_C	WT_C	Het_A/G	WT
db1239_1	Het_T/C						Het_A/G	
db1239_4	Het_T/C						Het_A/G	
db1239_8	Het_T/C						Het_A/G	
db1239_13	Het_T/C						Het_A/G	
db1239_16	Het_T/C						Het_A/G	
db1239_17	Het_T/C						Het_A/G	
db1239_24	Het_T/C						Het_A/G	
db1239_37	Het_T/C						Het_A/G	
db1239_43	Het_T/C						Het_A/G	
db1239_44	Het_T/C						Het_A/G	
db1239_55	Het_T/C						Het_A/G	
db1239_56	Het_T/C						Het_A/G	
db1239_59	Het_T/C						Het_A/G	
db1239_60	Het_T/C						Het_A/G	
db1239_61	Het_T/C						Het_A/G	
db1239_65	Het_T/C						Het_A/G	
db1239_67	Het_T/C						Het_A/G	
db1239_71	Het_T/C						Het_A/G	
db1239_73	Het_T/C						Het_A/G	
db1239_74	Het_T/C						Het_A/G	
db1239_75	Het_T/C						Het_A/G	
db1239_79	Het_T/C						Het_A/G	
db1239_82	Het_T/C						Het_A/G	
db1239_86	Het_T/C						Het_A/G	
db1239_88	Het_T/C						Het_A/G	

db1239_90	Het_T/C						Het_A/G	
db1239_6	WT_C						WT_G	
db1239_11	WT_C						WT_G	
db1239_12	WT_C						WT_G	
db1239_21	WT_C						WT_G	
db1239_25	WT_C						WT_G	
db1239_26	WT_C						WT_G	
db1239_27	WT_C						WT_G	
db1239_28	WT_C						WT_G	
db1239_29	WT_C						WT_G	
db1239_31	WT_C						WT_G	
db1239_32	WT_C						WT_G	
db1239_34	WT_C						WT_G	
db1239_35	WT_C						WT_G	
db1239_39	WT_C						WT_G	
db1239_40	WT_C						WT_G	
db1239_45	WT_C						WT_G	
db1239_47	WT_C						WT_G	
db1239_51	WT_C						WT_G	
db1239_53	WT_C						WT_G	
db1239_58	WT_C						WT_G	
db1239_62	WT_C						WT_G	
db1239_68	WT_C						WT_G	
db1239_70	WT_C						WT_G	
db1239_76	WT_C						WT_G	
db1239_80	WT_C						WT_G	
db1239_81	WT_C						WT_G	
db1239_83	WT_C						WT_G	
db1239_92	WT_C						WT_G	
db1239_93	WT_C						WT_G	
db1239_94	WT_C						WT_G	
db1239_95	WT_C						WT_G	

Table 13: SNPs-mapping of db102 allele on Chr X Lon non Unc

	3.2 Mb	3.4 Mb	3.6 Mb	3.7 Mb	3.8 Mb	Phenotype
	pqn-37	wrt-6	del-9	C01C4.2	erp-1	
lon 2	WT_G	WT_C	WT_G	WT_C	WT_G	WT
lon 6	WT_G	WT_C	WT_G	WT_C	WT_G	WT
lon 10B	WT_G	WT_C	WT_G	WT_C	WT_G	WT
lon 12	WT_G	WT_C	WT_G	WT_C	WT_G	WT
lon 14	WT_G	WT_C	WT_G	WT_C	WT_G	WT
lon 13	Mut_A	WT_C	WT_G	WT_C	WT_G	WT
lon 3	Mut_A	Mut_T	Mut_A	Mut_T	Mut_A	C
lon 4	Mut_A	Mut_T	Mut_A	Mut_T	Mut_A	C
lon 7	Mut_A	Mut_T	Mut_A	Mut_T	Mut_A	C
lon 10A	Mut_A	Mut_T	Mut_A	Mut_T	Mut_A	C

Table 14: SNPs-mapping of db102 allele on Chr X Lon non Unc

	3.2 Mb	3.4 Mb	3.6 Mb	3.7 Mb	3.8 Mb	Phenotype
	pqn-37	wrt-6	del-9	C01C4.2	erp-1	
lon_25	WT_G	WT_C	WT_G	WT_C	WT_G	WT
lon_33	WT_G	WT_C	WT_G	WT_C	WT_G	WT
lon_2	Mut_A_Het	WT_C	WT_G	WT_C	WT_G	WT
lon_3	Mut_A_Het	WT_C	WT_G	WT_C	WT_G	WT
lon_8	Mut_A_Het	WT_C	WT_G	WT_C	WT_G	WT
lon_14	Mut_A_Het	WT_C	WT_G	WT_C	WT_G	WT
lon_16	Mut_A_Het	WT_C	WT_G	WT_C	WT_G	WT
lon_24	Mut_A_Het	WT_C	WT_G	WT_C	WT_G	WT

lon_29	Mut_A_Het	WT_C	WT_G	WT_C	WT_G	WT
lon_26	Mut_A_Het	Mut_T_Het	WT_G	WT_C	WT_G	C+
lon_38	/	Mut_T_Het	WT_G	WT_C	WT_G	C+
lon_40	/	Mut_T_Het	WT_G	WT_C	WT_G	C+
lon_36	/	Mut_T_Het	Mut_A_Het	WT_C	WT_G	C+
lon_6	Mut_A_Het	Mut_T_Het	Mut_A_Het	WT_C	WT_G	C+
lon_35	Mut_A_Het	Mut_T_Het	Mut_A_Het	WT_C	WT_G	C+
lon_9	Mut_A_Het	Mut_T_Het	Mut_A_Het	Mut_T_Het	WT_G	C+
lon_1	Mut_A_Het	Mut_T_Het	Mut_A_Het	Mut_T_Het	Mut_A_Het	C+
lon_5	Mut_A_Het	Mut_T_Het	Mut_A_Het	Mut_T_Het	Mut_A_Het	C+

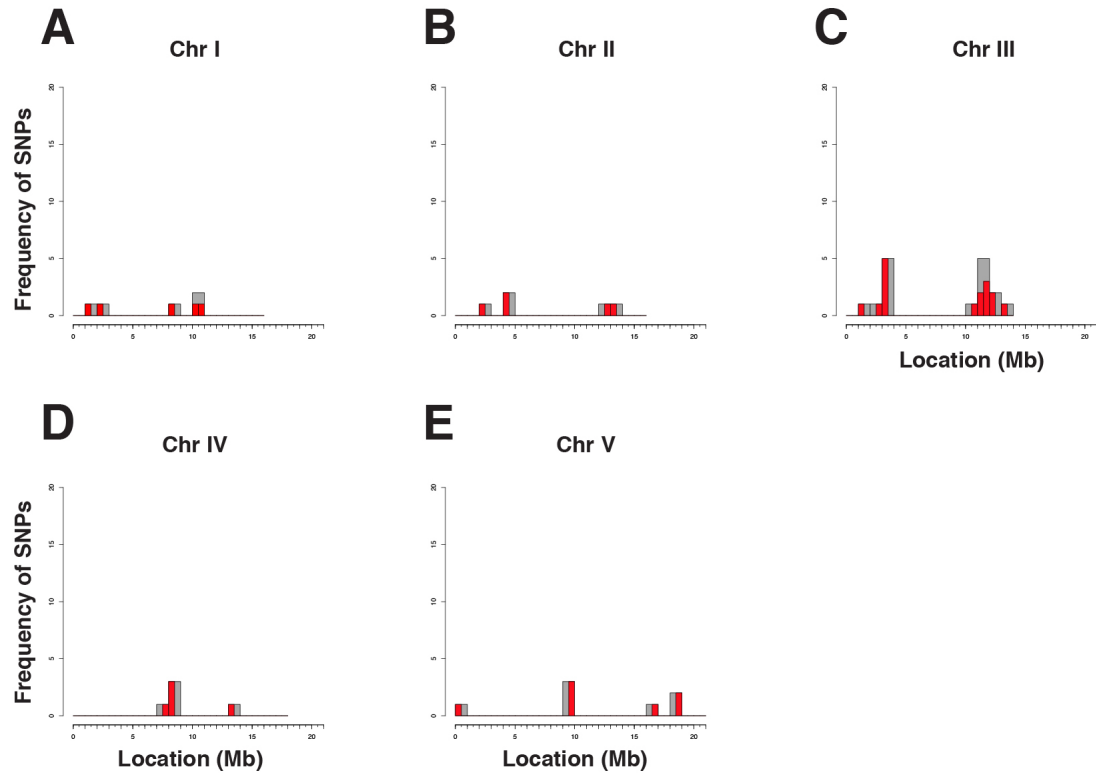
Table 15: SNPs-mapping of db1220 allele on Chr V

	8Mb	9.5Mb	11.8Mb	13.2Mb	14.2M	14.3M	Phenot ype
	<b>asp-5</b>	<b>rgef-1</b>	<b>D2023.4</b>	<b>C34D14.4</b>	<b>F14D7.1</b>	<b>vha-13</b>	
				Left limit	Right limit		
9.1	Mut_T	Mut_A	Mut_A	Mut_T			C
11.1	Mut_T	Mut_A	Mut_A	Mut_T			C+
15.1	Mut_T	Mut_A	Mut_A	Mut_T			C+
23.1	Mut_T	Mut_A	Mut_A	Mut_T			C+
1.2	WT_C	Mut_A	Mut_A	Mut_T			C+
2.3	WT_C	Mut_A	Mut_A	Mut_T			C+
3.2	WT_C	Mut_A	Mut_A	Mut_A	Mut_A		C+
5.3	WT_C	WT_G	Mut_A	Mut_T			C+
16.1	WT_C	WT_G	Mut_A	Mut_T			C+

21.1	Het Mut_T/ WT_C	Het Mut_T/ WT_C	Mut_A	Mut_T			C
10.1	WT_C	WT_G	WT_G	Mut_T			C+
6.3	WT_C	Mut_A	Mut_A	Het Mut_T/ WT_C	Het Mut_A/ WT_G	Het Mut_A/ WT_G	WT
7.1	WT_C	WT_G	WT_G	WT_C	Mut_A	Mut_A	WT
14.2	WT_C	WT_G	WT_G	WT_C	Mut_A	Mut_A	WT
24.2	WT_C	WT_G	WT_G	WT_C	Mut_A	Mut_A	WT
8.2	WT_C	WT_G	WT_G	WT_C	WT_G	WT_G	WT

## Appendix 2 - EMS induced SNPs

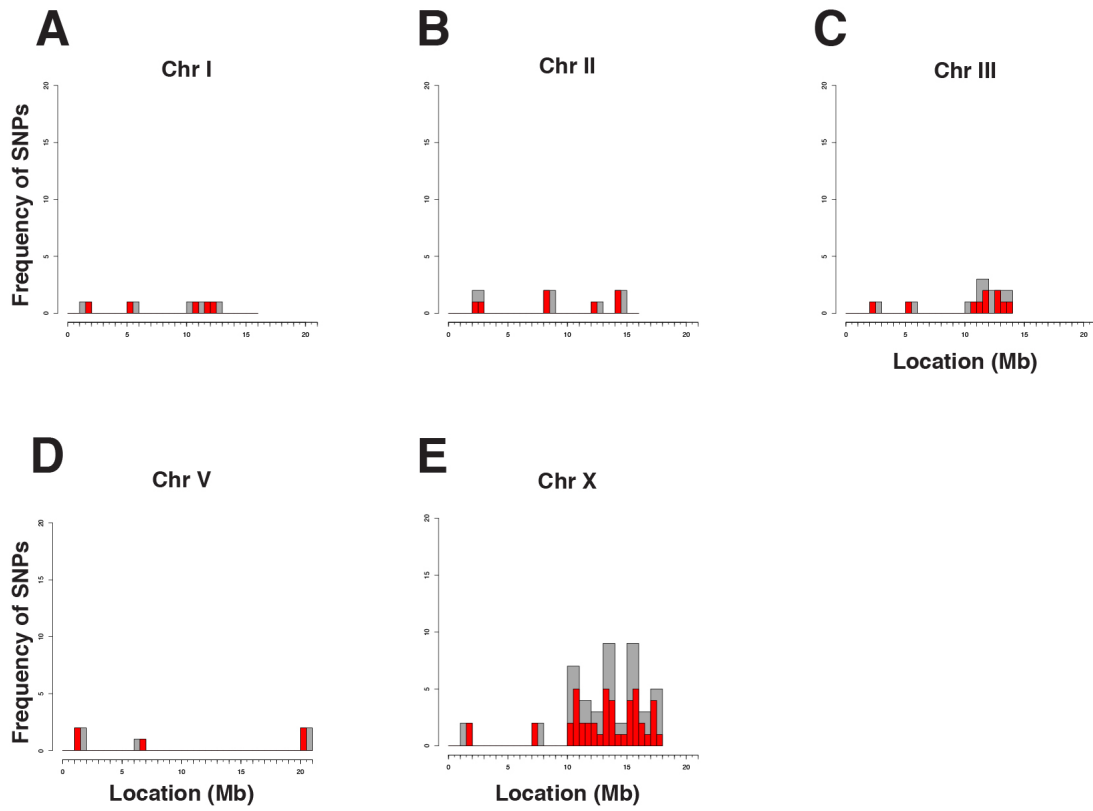
*db102*



### Appendix 2.1 EMS-induced SNPs plots for chromosomes unlinked to *db102*

(A-E) Plots show the frequency of SNPs generated by EMS mutagenesis over the length of chromosomes. Chromosomes with no clear cluster are shown.

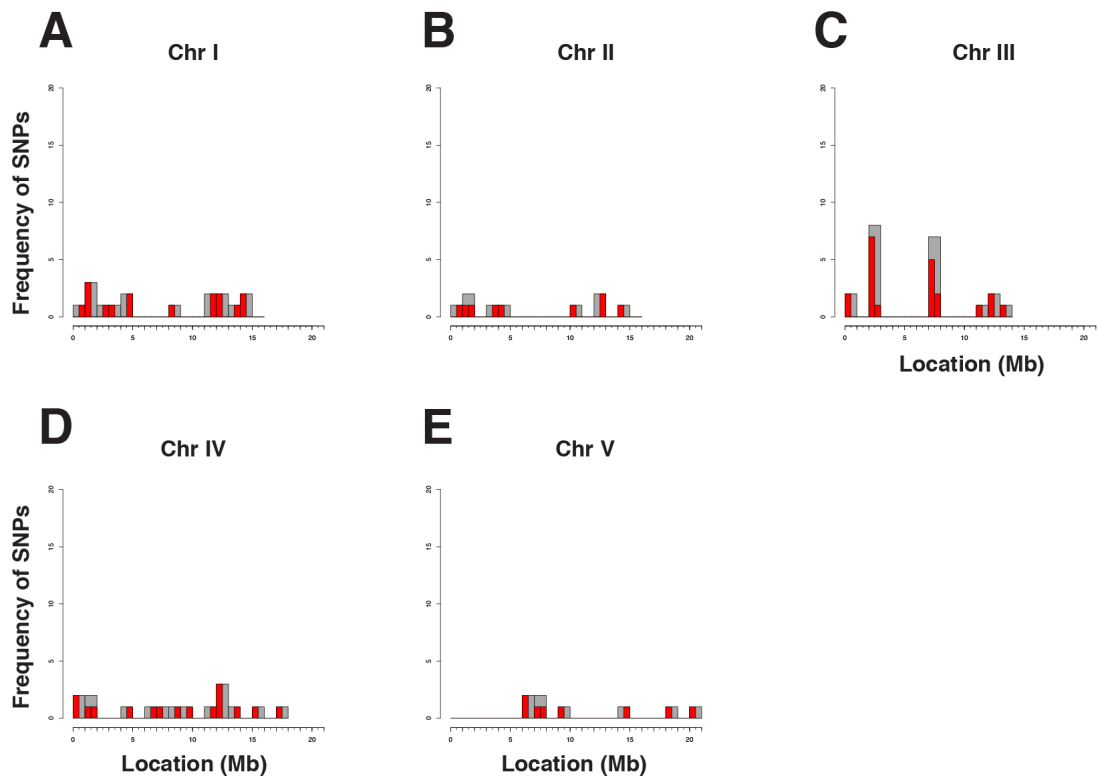
*db104*



**Appendix 2.2 EMS-induced SNPs plots for chromosomes unlinked to *db104***

(A-E) Plots show the frequency of SNPs generated by EMS mutagenesis over the length of chromosomes. Chromosomes with no clear cluster are shown.

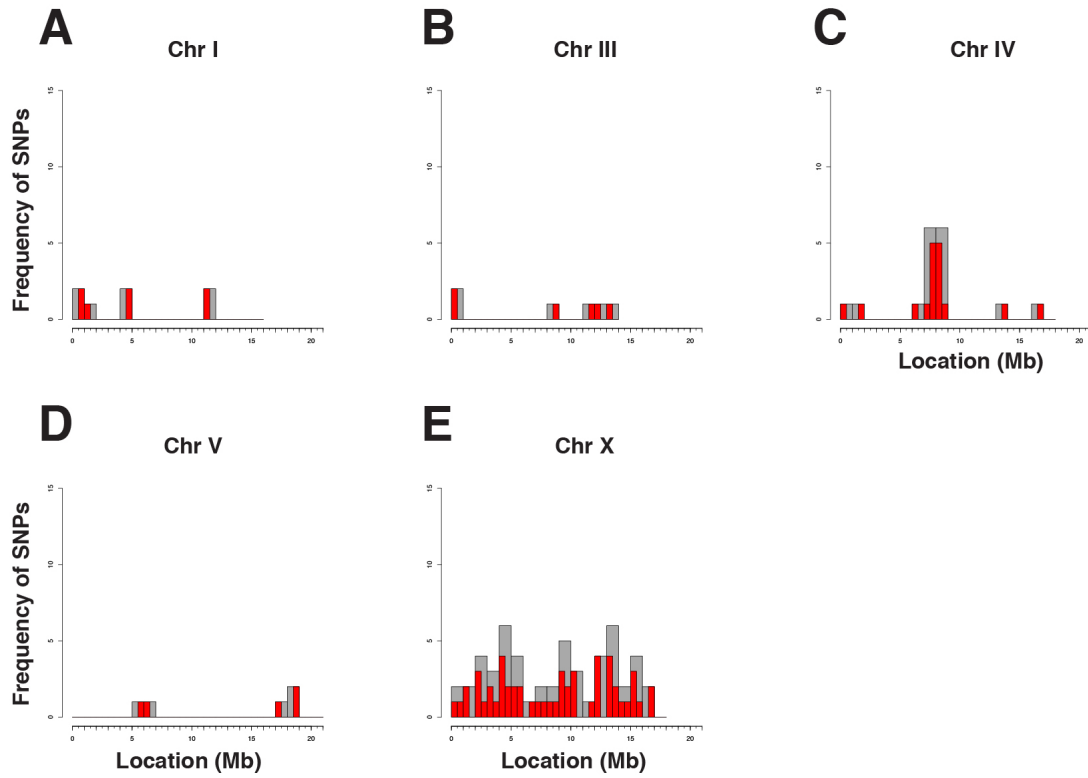
*db106*



**Appendix 2.3 EMS-induced SNPs plots for chromosomes unlinked to *db106***

(A-E) Plots show the frequency of SNPs generated by EMS mutagenesis over the length of chromosomes. Chromosomes with no clear cluster are shown.

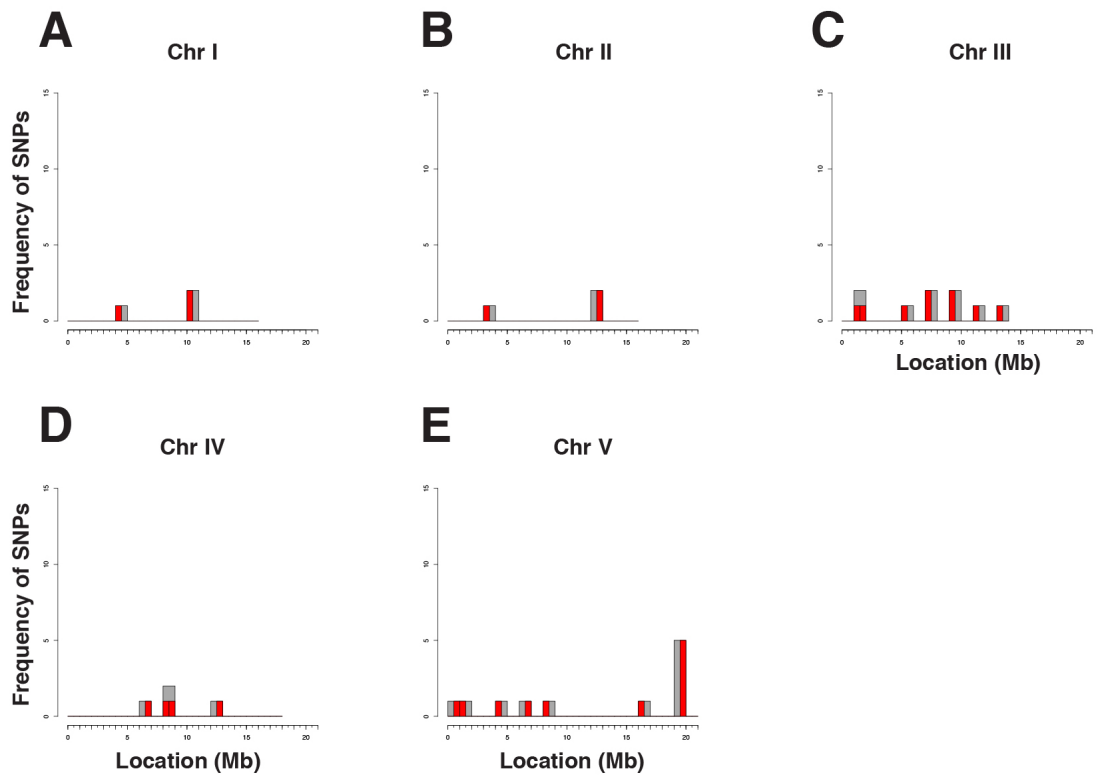
*db107*



**Appendix 2.4 EMS-induced SNPs plots for chromosomes unlinked to *db107***

**(A-E)** Plots show the frequency of SNPs generated by EMS mutagenesis over the length of chromosomes. Chromosomes with no clear cluster are shown.

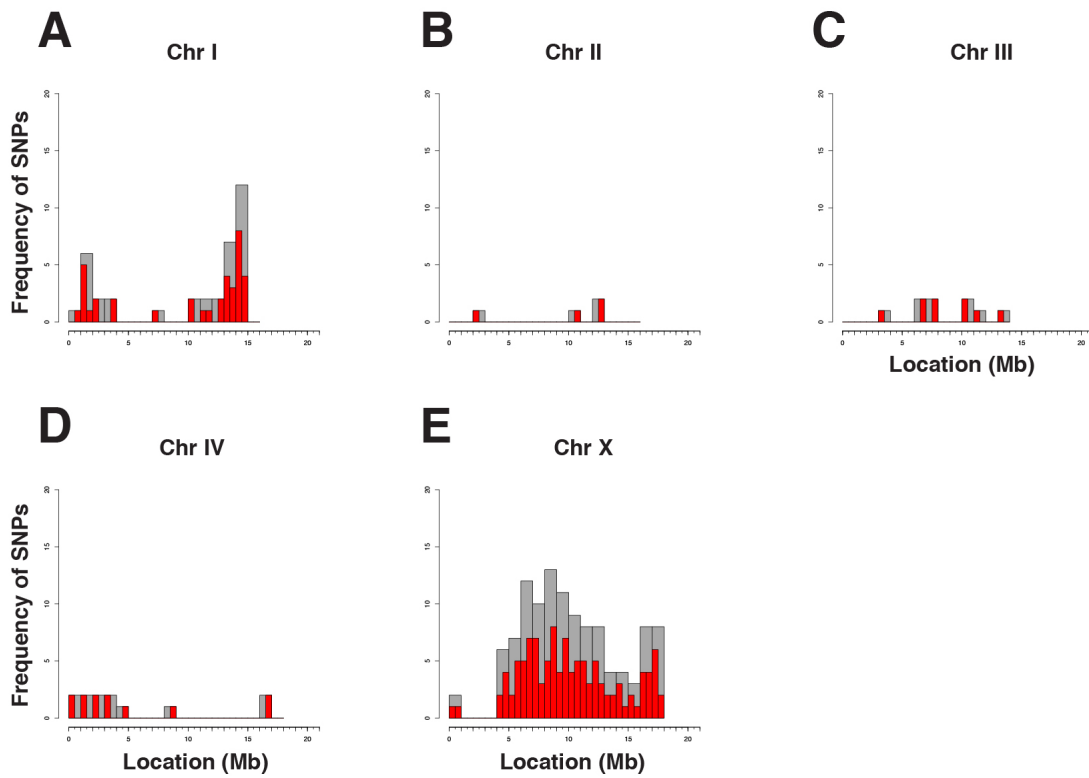
*db1219*



**Appendix 2.5 EMS-induced SNPs plots for chromosomes unlinked to *db1219***

**(A-E)** Plots show the frequency of SNPs generated by EMS mutagenesis over the length of chromosomes. Chromosomes with no clear cluster are shown.

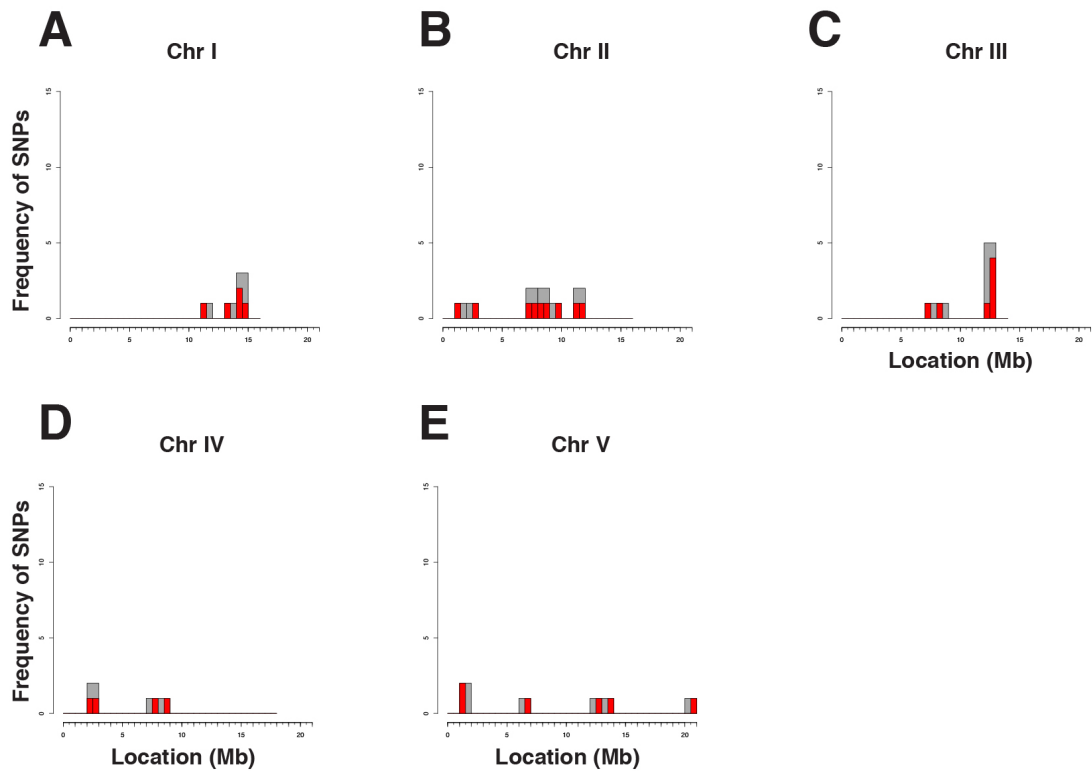
*db1220*



**Appendix 2.6 EMS-induced SNPs plots for chromosomes unlinked to *db1220***

**(A-E)** Plots show the frequency of SNPs generated by EMS mutagenesis over the length of chromosomes. Chromosomes with no clear cluster are shown.

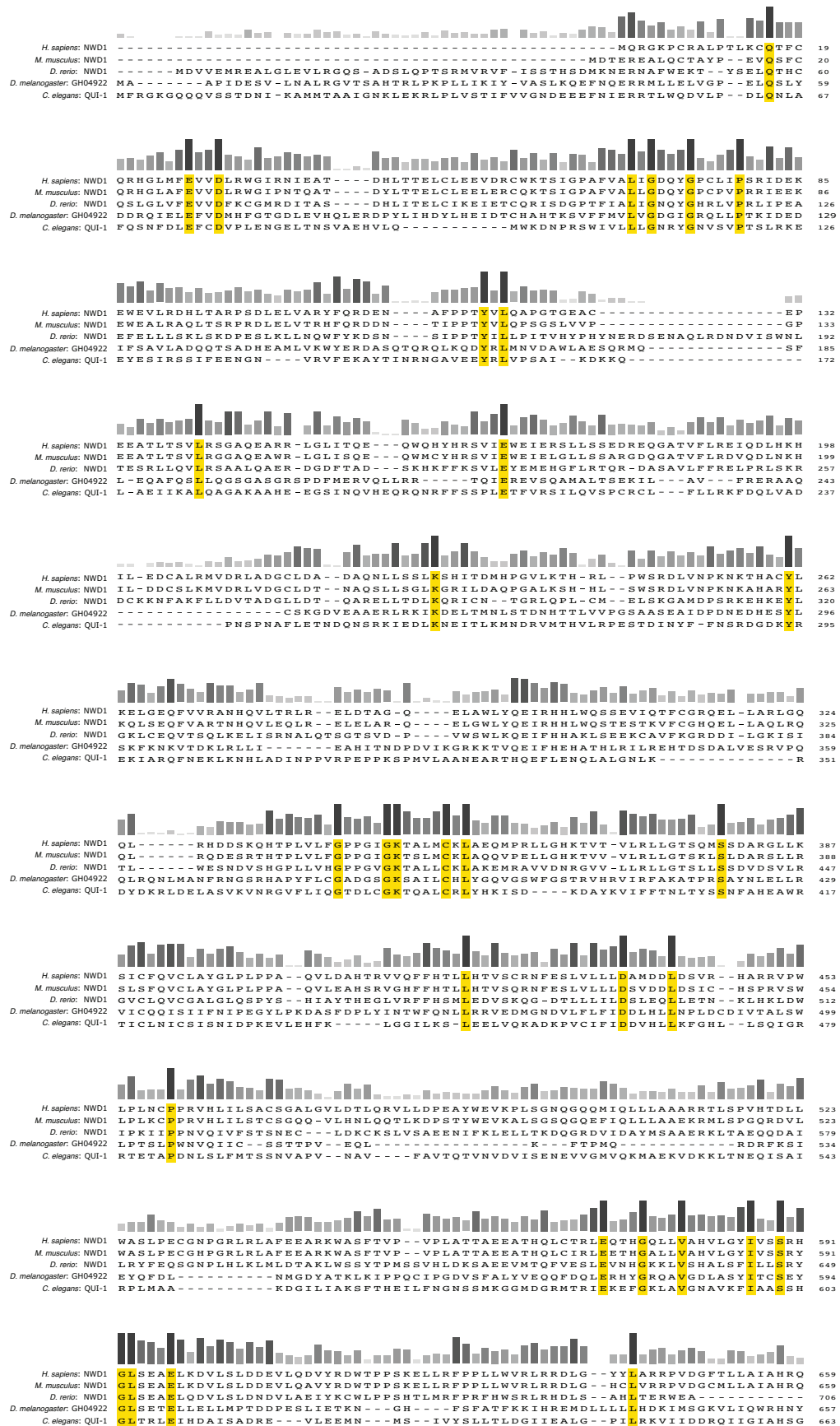
*db1221*

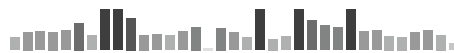


**Appendix 2.7 EMS-induced SNPs plots for chromosomes unlinked to *db1221***

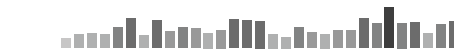
(A-E) Plots show the frequency of SNPs generated by EMS mutagenesis over the length of chromosomes. Chromosomes with no clear cluster are shown.

# Appendix 3 - QUI-1 homology





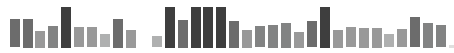
*H. sapiens*: NWD1 LVEVVRER<sup>RY</sup>LSGSR-<sup>AKR</sup>HGV<sup>L</sup>AD<sup>F</sup>FSGTWSQGT-----KKLITLP-----L----- 701  
*M. musculus*: NWD1 LSQVIQVRR<sup>Y</sup>LSGPER-<sup>AKR</sup>HGV<sup>L</sup>A<sup>E</sup>F<sup>F</sup>SGAWSQGT-----KKLITLP-----L----- 701  
*D. rerio*: NWD1 -AELVRRR<sup>Y</sup>LSRDVK-<sup>ADM</sup>HTI<sup>L</sup>A<sup>E</sup>Y<sup>F</sup>SGQWSKGO-----LRPILLP-----S----- 747  
*D. melanogaster*: GH04922 CASVAKRR<sup>Y</sup>M-DVQTRSL<sup>H</sup>CE<sup>L</sup>AN<sup>L</sup>F<sup>F</sup>PODEDESTLENESENRSSEKSVISLKD<sup>R</sup>REK<sup>D</sup>SL<sup>S</sup>AVS<sup>A</sup>V<sup>A</sup> 726  
*C. elegans*: QUI-1 LISWLRN<sup>RY</sup>LTSSQDIRSA<sup>H</sup>LO<sup>L</sup>SD<sup>L</sup>F<sup>F</sup>ADLLID-----NEQS----- 700



*H. sapiens*: NWD1 ---VGKPLNLD<sup>R</sup>KVAPQ<sup>L</sup>PLWFSHTVAN<sup>L</sup>R<sup>K</sup>KLKELPY<sup>H</sup>LLHSGRLEELKQEV<sup>L</sup>LGSM<sup>S</sup>WISCRGISGGIED 767  
*M. musculus*: NWD1 ---VGKPLNLD<sup>R</sup>KVAPQ<sup>L</sup>PLWFSSTVAN<sup>L</sup>R<sup>K</sup>KLTEL<sup>P</sup>F<sup>H</sup>LLHAGRLEELKQEV<sup>L</sup>GNM<sup>S</sup>WISCRGISGGIEV 767  
*D. rerio*: NWD1 ---LSAPLNAD<sup>R</sup>KVSPQ<sup>L</sup>PLWSEELAN<sup>L</sup>R<sup>K</sup>IHEL<sup>P</sup>F<sup>H</sup>LLHAGK<sup>W</sup>DEL<sup>R</sup>QSV<sup>L</sup>LGSL<sup>D</sup>WL<sup>C</sup>CKT<sup>L</sup>QCGV<sup>S</sup>C 813  
*D. melanogaster*: GH04922 GRKSSSTH<sup>H</sup>ND<sup>D</sup>TSTFY<sup>N</sup>PIA-<sup>ADV</sup>YS<sup>M</sup>H<sup>R</sup>HVEES<sup>W</sup>H<sup>L</sup>MRSD<sup>D</sup>TTR<sup>F</sup>KQIA<sup>V</sup>CN<sup>F</sup>DF<sup>L</sup>LA<sup>A</sup>VQ<sup>T</sup>VS<sup>I</sup>SY 795  
*C. elegans*: QUI-1 -----PRHEIAYQ<sup>S</sup>FS<sup>G</sup>IG<sup>I</sup>K<sup>R</sup>D<sup>N</sup>G<sup>S</sup>PN<sup>F</sup>R<sup>L</sup>RLL<sup>W</sup>Y<sup>H</sup>CLHSG<sup>N</sup>L<sup>D</sup>R<sup>L</sup>KEL<sup>S</sup>LC<sup>H</sup>PEY<sup>V</sup>D<sup>V</sup>Y<sup>T</sup>R<sup>F</sup>G<sup>I</sup>SH 764

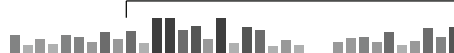


*H. sapiens*: NWD1 LDDDFDL<sup>C</sup>APH<sup>L</sup>DSPEV<sup>L</sup>RVREAL<sup>Q</sup>LC<sup>R</sup>PAVELR--GMERS<sup>L</sup>LY<sup>T</sup>ELLAR<sup>L</sup>HFF---ATSH<sup>P</sup>ALV<sup>G</sup>QL<sup>C</sup>Q 832  
*M. musculus*: NWD1 LDDDFDM<sup>C</sup>APH<sup>M</sup>NSPEV<sup>D</sup>LVREA<sup>I</sup>QL<sup>C</sup>GP<sup>A</sup>VELR--GLEK<sup>S</sup>VLY<sup>T</sup>ELLAR<sup>L</sup>LF---AASH<sup>P</sup>AMIG<sup>Q</sup>LC<sup>Q</sup> 832  
*D. rerio*: NWD1 VIQDLT<sup>L</sup>CTD<sup>L</sup>TD<sup>C</sup>PEI<sup>Q</sup>LL<sup>K</sup>ET<sup>F</sup>LL<sup>L</sup>KL<sup>S</sup>DF<sup>S</sup>DGR<sup>V</sup>DP<sup>S</sup>LL<sup>V</sup>TEI<sup>F</sup>AR<sup>L</sup>QGL---ADH<sup>P</sup>SMIG<sup>Q</sup>LC<sup>S</sup> 880  
*D. melanogaster*: GH04922 LRCLIE<sup>H</sup>VR<sup>C</sup>YI<sup>L</sup>DR<sup>D</sup>IE<sup>L</sup>IY<sup>T</sup>IR--K-SS<sup>D</sup>VL--TR<sup>D</sup>PM<sup>L</sup>GS<sup>Q</sup>LIS<sup>W</sup>LR<sup>P</sup>ISE<sup>H</sup>DD<sup>D</sup>NS<sup>L</sup>LS<sup>M</sup>TV<sup>R</sup> 860  
*C. elegans*: QUI-1 LLSLYE<sup>C</sup>AT<sup>Q</sup>IL<sup>H</sup>HD<sup>L</sup>Q<sup>V</sup>ISE<sup>Q</sup>VL--VP<sup>A</sup>LV<sup>L</sup>--ARD<sup>S</sup>E<sup>Q</sup>L<sup>A</sup>AE<sup>V</sup>IG<sup>R</sup>L<sup>R</sup>FT---RH<sup>S</sup>H<sup>F</sup>LN<sup>S</sup>LV<sup>D</sup> 827



*H. sapiens*: NWD1 QAQS<sup>W</sup>F<sup>L</sup>CA-<sup>H</sup>V<sup>L</sup>V<sup>P</sup>LGG<sup>F</sup>LQ<sup>P</sup>F<sup>F</sup>GG<sup>P</sup>L<sup>R</sup>AT<sup>L</sup>S--GCH<sup>K</sup>G<sup>I</sup>TAM<sup>A</sup>WG<sup>V</sup>E<sup>K</sup>LL<sup>V</sup>I--GT<sup>Q</sup>D<sup>G</sup>IM<sup>A</sup>V<sup>W</sup>D 896  
*M. musculus*: NWD1 QAQS<sup>W</sup>F<sup>R</sup>AC<sup>P</sup>-Y<sup>F</sup>M<sup>L</sup>V<sup>P</sup>L<sup>A</sup>G<sup>F</sup>LQ<sup>P</sup>F<sup>F</sup>GG<sup>P</sup>L<sup>R</sup>AT<sup>L</sup>T--GCH<sup>K</sup>G<sup>I</sup>TAM<sup>A</sup>W<sup>S</sup>L<sup>E</sup>K<sup>L</sup>LV--GT<sup>Q</sup>D<sup>G</sup>AM<sup>V</sup>V<sup>W</sup>D 896  
*D. rerio*: NWD1 QCN<sup>D</sup>WF<sup>E</sup>YS-<sup>D</sup>LL<sup>V</sup>P<sup>K</sup>CF<sup>E</sup>AG<sup>G</sup>EL<sup>S</sup>TLR--G<sup>F</sup>T<sup>G</sup>V<sup>K</sup>AV<sup>L</sup>C<sup>S</sup>K<sup>R</sup>LL<sup>A</sup>--GS<sup>E</sup>D<sup>L</sup>I<sup>V</sup>WS 948  
*D. melanogaster*: GH04922 SAT<sup>A</sup>W<sup>C</sup>D<sup>G</sup>YA-<sup>V</sup>EL<sup>L</sup>V<sup>P</sup>L<sup>T</sup>GW<sup>L</sup>PA<sup>L</sup>PL<sup>S</sup>Q<sup>I</sup>RT<sup>M</sup>T<sup>V</sup>SG<sup>T</sup>GC<sup>I</sup>RA<sup>V</sup>W<sup>L</sup>AP<sup>S</sup>K<sup>O</sup>HL<sup>L</sup>--AT<sup>S</sup>G<sup>D</sup>V<sup>Q</sup>W<sup>H</sup> 925  
*C. elegans*: QUI-1 QAMS<sup>W</sup>V<sup>D</sup>LY<sup>N</sup>RO<sup>L</sup>LL<sup>V</sup>P<sup>L</sup>TC<sup>W</sup>IS<sup>P</sup>PA<sup>T</sup>K<sup>V</sup>CR<sup>S</sup>F<sup>T</sup>L<sup>K</sup>D<sup>W</sup>K<sup>P</sup>GN<sup>T</sup>V<sup>L</sup>TL<sup>S</sup>AN<sup>H</sup>Q<sup>Y</sup>IL<sup>S</sup>GN<sup>S</sup>Q<sup>S</sup>D<sup>F</sup>G<sup>V</sup>IY<sup>A</sup>Y<sup>H</sup> 897

WD40 repeat domain



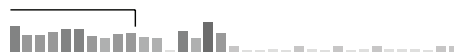
*H. sapiens*: NWD1 ME<sup>F</sup>Q<sup>H</sup>VI<sup>H</sup>ML<sup>T</sup>CH<sup>T</sup>GE<sup>V</sup>RC<sup>V</sup>KIF--AK<sup>G</sup>T<sup>L</sup>AN<sup>S</sup>AS<sup>K</sup>D<sup>Y</sup>T<sup>L</sup>HL<sup>W</sup>N<sup>L</sup>LS<sup>G</sup>Q<sup>E</sup>K<sup>F</sup>TI<sup>W</sup>D<sup>G</sup>S<sup>K</sup>NP<sup>A</sup>EP<sup>Q</sup>I<sup>W</sup>N<sup>L</sup> 964  
*M. musculus*: NWD1 VE<sup>F</sup>Q<sup>Q</sup>V<sup>H</sup>VL<sup>M</sup>CH<sup>T</sup>AE<sup>V</sup>K<sup>C</sup>VR<sup>V</sup>F--AQ<sup>G</sup>T<sup>L</sup>AN<sup>S</sup>AS<sup>K</sup>D<sup>H</sup>T<sup>L</sup>RL<sup>W</sup>N<sup>L</sup>LS<sup>G</sup>Q<sup>E</sup>K<sup>F</sup>TI<sup>W</sup>D<sup>G</sup>S<sup>K</sup>NP<sup>T</sup>EP<sup>Q</sup>S<sup>W</sup>D<sup>L</sup> 964  
*D. rerio*: NWD1 L<sup>N</sup>N<sup>L</sup>Q<sup>L</sup>PL<sup>H</sup>TL<sup>S</sup>CH<sup>T</sup>K<sup>A</sup>G<sup>V</sup>L<sup>S</sup>L<sup>K</sup>L<sup>T</sup>--D<sup>K</sup>T<sup>N</sup>CL<sup>L</sup>ST<sup>G</sup>L<sup>D</sup>GT<sup>L</sup>RR<sup>K</sup>W<sup>C</sup>L<sup>S</sup>G<sup>L</sup>Q<sup>F</sup>C<sup>I</sup>T<sup>A</sup>D<sup>V</sup>SV<sup>O</sup>TH<sup>S</sup>PT--HI 1010  
*D. melanogaster*: GH04922 I<sup>M</sup>SN<sup>S</sup>LD<sup>H</sup>IF<sup>K</sup>CH<sup>T</sup>AA<sup>V</sup>T<sup>C</sup>LL<sup>V</sup>AP<sup>S</sup>D<sup>S</sup>ELL<sup>T</sup>GS<sup>E</sup>D<sup>A</sup>T<sup>V</sup>L<sup>W</sup>V<sup>W</sup>H<sup>V</sup>GL<sup>R</sup>RR<sup>A</sup>H<sup>I</sup>KA<sup>N</sup>HA<sup>T</sup>A--PI<sup>T</sup>G<sup>V</sup>A 991  
*C. elegans*: QUI-1 I<sup>A</sup>SE<sup>Q</sup>L<sup>I</sup>G<sup>T</sup>FK<sup>H</sup>TA<sup>A</sup>V<sup>T</sup>CL<sup>S</sup>S--ND<sup>S</sup>SL<sup>F</sup>V<sup>S</sup>T<sup>S</sup>FD<sup>K</sup>T<sup>V</sup>N<sup>V</sup>W<sup>V</sup>FS<sup>Q</sup>ST<sup>P</sup>T<sup>M</sup>SL<sup>T</sup>-H<sup>H</sup>TA--K<sup>V</sup>T<sup>C</sup>AI 960

WD40 repeat domain

WD40 repeat domain



*H. sapiens*: NWD1 HV<sup>D</sup>E<sup>A</sup>H<sup>K</sup>V<sup>V</sup>YS<sup>A</sup>SG<sup>S</sup>K<sup>I</sup>NA<sup>W</sup>N<sup>L</sup>ET<sup>A</sup>EP<sup>V</sup>PH<sup>L</sup>GD<sup>A</sup>-----SD<sup>P</sup>W<sup>M</sup>CM<sup>A</sup>V<sup>L</sup>AS<sup>O</sup>AT<sup>L</sup>LL<sup>T</sup>V<sup>S</sup>RD<sup>G</sup>V<sup>S</sup>LV<sup>W</sup> 1027  
*M. musculus*: NWD1 HV<sup>D</sup>ERN<sup>N</sup>V<sup>V</sup>YS<sup>T</sup>SG<sup>A</sup>R<sup>I</sup>N<sup>M</sup>W<sup>N</sup>L<sup>E</sup>T<sup>S</sup>KL<sup>V</sup>FC<sup>I</sup>TD<sup>G</sup>V-----SD<sup>P</sup>W<sup>V</sup>CV<sup>A</sup>LL<sup>A</sup>AO<sup>G</sup>LL<sup>L</sup>AK<sup>G</sup>GS<sup>O</sup>W<sup>S</sup>LV<sup>W</sup> 1027  
*D. rerio*: NWD1 HM<sup>N</sup>EE<sup>R</sup>K<sup>I</sup>I<sup>T</sup>NP<sup>S</sup>S<sup>Q</sup>V<sup>K</sup>AW<sup>D</sup>L<sup>E</sup>T<sup>A</sup>EP<sup>L</sup>F<sup>E</sup>LT<sup>A</sup>IG<sup>S</sup>V<sup>L</sup>G<sup>I</sup>VE<sup>D</sup>E<sup>L</sup>AC<sup>I</sup>CS-----E<sup>A</sup>IL<sup>C</sup>F<sup>Y</sup> 1068  
*D. melanogaster*: GH04922 AG<sup>A</sup>NN<sup>T</sup>L<sup>I</sup>I<sup>S</sup>SS<sup>E</sup>DA<sup>S</sup>IA<sup>I</sup>T<sup>D</sup>L<sup>A</sup>SG<sup>K</sup>L<sup>R</sup>HR<sup>I</sup>TH<sup>R</sup>RG<sup>P</sup>V<sup>S</sup>G<sup>I</sup>V<sup>V</sup>-----AG<sup>A</sup>CD<sup>V</sup>L<sup>I</sup>SG<sup>G</sup>L<sup>D</sup>R<sup>T</sup>CV<sup>W</sup> 1053  
*C. elegans*: QUI-1 L<sup>T</sup>SD<sup>D</sup>Q<sup>Y</sup>L<sup>L</sup>TA<sup>S</sup>AD<sup>S</sup>SA<sup>K</sup>M<sup>I</sup>K<sup>L</sup>ET<sup>G</sup>EV<sup>M</sup>RS<sup>F</sup>ND<sup>H</sup>T<sup>G</sup>SV<sup>S</sup>LV<sup>L</sup>QL-----T<sup>S</sup>NN<sup>Q</sup>F<sup>L</sup>IT<sup>G</sup>SG<sup>D</sup>F<sup>V</sup>V<sup>Q</sup>M<sup>W</sup> 1022



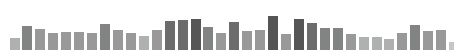
*H. sapiens*: NWD1 SS<sup>A</sup>T<sup>C</sup>K<sup>L</sup>Q<sup>G</sup>K<sup>O</sup>H-M<sup>S</sup>SI-----K<sup>E</sup>T<sup>P</sup>TC<sup>A</sup>VS<sup>V</sup>O-K<sup>O</sup>C 1058  
*M. musculus*: NWD1 SS<sup>A</sup>M<sup>G</sup>K<sup>L</sup>Q<sup>E</sup>K<sup>K</sup>H-M<sup>S</sup>SI-----K<sup>E</sup>BT<sup>P</sup>TC<sup>A</sup>VS<sup>I</sup>O-S<sup>R</sup>A 1058  
*D. rerio*: NWD1 DI<sup>S</sup>T<sup>G</sup>T<sup>Q</sup>T<sup>S</sup>Q<sup>T</sup>LL<sup>P</sup>YS<sup>A</sup>-----G<sup>H</sup>NN<sup>I</sup>T<sup>C</sup>CL<sup>T</sup>L-K<sup>H</sup>S 1100  
*D. melanogaster*: GH04922 LD<sup>N</sup>FT<sup>L</sup>LN<sup>T</sup>MO-M<sup>T</sup>SA<sup>V</sup>L<sup>R</sup>ID<sup>I</sup>SW<sup>N</sup>S<sup>V</sup>FL<sup>L</sup>AL<sup>C</sup>ED<sup>N</sup>AL<sup>V</sup>VRT<sup>L</sup>AT<sup>G</sup>K<sup>E</sup>L<sup>H</sup>TL<sup>K</sup>G<sup>H</sup>K<sup>I</sup>R<sup>S</sup>I<sup>G</sup>K<sup>D</sup>SO 1122  
*C. elegans*: QUI-1 DV<sup>T</sup>NG<sup>K</sup>C<sup>I</sup>SR<sup>M</sup>GL<sup>M</sup>AP<sup>V</sup>ST<sup>L</sup>AI<sup>T</sup>SN<sup>D</sup>AF<sup>V</sup>V<sup>V</sup>ACE<sup>D</sup>ET<sup>L</sup>K<sup>V</sup>F<sup>S</sup>T<sup>V</sup>GG<sup>Q</sup>EL<sup>H</sup>EL<sup>M</sup>G<sup>H</sup>E<sup>G</sup>K<sup>V</sup>NS<sup>L</sup>V<sup>C</sup>A<sup>Q</sup>DD<sup>C</sup> 1092



*H. sapiens*: NWD1 KL<sup>V</sup>TC<sup>F</sup>SN<sup>G</sup>S<sup>I</sup>SL<sup>V</sup>SS<sup>K</sup>GR<sup>L</sup>LE<sup>K</sup>---L-D<sup>A</sup>V<sup>R</sup>L<sup>V</sup>VS<sup>E</sup>DES<sup>L</sup>A<sup>A</sup>GF<sup>G</sup>RS<sup>V</sup>RI<sup>F</sup>L<sup>A</sup>DS<sup>R</sup>G----- 1116  
*M. musculus*: NWD1 RL<sup>V</sup>AG<sup>F</sup>SS<sup>G</sup>S<sup>I</sup>AL<sup>V</sup>S<sup>A</sup>GED<sup>R</sup>LE<sup>K</sup>---L-D<sup>E</sup>AV<sup>G</sup>L<sup>V</sup>VS<sup>E</sup>DD<sup>S</sup>L<sup>L</sup>V<sup>A</sup>GF<sup>G</sup>RF<sup>V</sup>RI<sup>F</sup>L<sup>A</sup>DS<sup>O</sup>G----- 1116  
*D. rerio*: NWD1 K<sup>L</sup>I<sup>L</sup>AF<sup>G</sup>ES<sup>R</sup>LR<sup>H</sup>SV<sup>W</sup>SH<sup>E</sup>MS<sup>E</sup>VID---L-D<sup>S</sup>PAL<sup>F</sup>L<sup>R</sup>TS<sup>E</sup>DE<sup>K</sup>LL<sup>L</sup>AG<sup>C</sup>DR<sup>T</sup>L<sup>C</sup>FL<sup>V</sup>L<sup>T</sup>LS----- 1158  
*D. melanogaster*: GH04922 RC<sup>V</sup>VG<sup>C</sup>DD<sup>T</sup>R<sup>A</sup>L<sup>I</sup>Y<sup>D</sup>M<sup>H</sup>AG<sup>K</sup>L<sup>V</sup>RS<sup>L</sup>PP-N<sup>D</sup>GP<sup>V</sup>T<sup>A</sup>V<sup>H</sup>AM<sup>D</sup>ND<sup>D</sup>DF<sup>L</sup>V<sup>T</sup>V<sup>G</sup>G<sup>N</sup>K<sup>I</sup>T<sup>F</sup>Y<sup>S</sup>FR<sup>N</sup>E<sup>L</sup>Y<sup>V</sup>NP<sup>Y</sup>SR 1191  
*C. elegans*: QUI-1 Q-L<sup>F</sup>AA<sup>T</sup>RS<sup>K</sup>V<sup>F</sup>C<sup>Y</sup>DI<sup>H</sup>NG<sup>Q</sup>M<sup>I</sup>D<sup>V</sup>LD<sup>T</sup>AO<sup>F</sup>FP<sup>I</sup>C<sup>S</sup>L<sup>K</sup>I<sup>S</sup>SD<sup>N</sup>Y<sup>F</sup>L<sup>I</sup>SP<sup>C</sup>GP<sup>K</sup>V<sup>T</sup>I<sup>W</sup>N<sup>V</sup>T<sup>K</sup>R<sup>N</sup>HD<sup>A</sup>HD<sup>V</sup>-- 1159



*H. sapiens*: NWD1 -----FRR<sup>F</sup>MA<sup>N</sup>D<sup>L</sup>E<sup>H</sup>E<sup>D</sup>M<sup>V</sup> 1131  
*M. musculus*: NWD1 -----FRR<sup>F</sup>MA<sup>S</sup>D<sup>L</sup>E<sup>H</sup>E<sup>D</sup>M<sup>V</sup> 1131  
*D. rerio*: NWD1 -----MH<sup>K</sup>V--LD<sup>L</sup>Q<sup>H</sup>DA<sup>S</sup>I 1171  
*D. melanogaster*: GH04922 H<sup>P</sup>RR<sup>K</sup>RS<sup>L</sup>K<sup>R</sup>HA<sup>Q</sup>A<sup>Q</sup>RS<sup>P</sup>ST<sup>T</sup>LP<sup>P</sup>I<sup>T</sup>CF<sup>D</sup>LS<sup>R</sup>DS<sup>Q</sup>MA<sup>I</sup>AS<sup>G</sup>R<sup>H</sup>V<sup>H</sup>LM<sup>R</sup>-INT<sup>P</sup>E<sup>Y</sup>QC--T<sup>L</sup>E<sup>G</sup>H<sup>T</sup>AG<sup>V</sup> 1257  
*C. elegans*: QUI-1 HA<sup>D</sup>KE-----G<sup>F</sup>L<sup>T</sup>AV<sup>A</sup>LS<sup>N</sup>DD<sup>K</sup>YA<sup>A</sup>C--G<sup>T</sup>NN<sup>G</sup>I<sup>V</sup>AL<sup>W</sup>D<sup>L</sup>EV<sup>C</sup>Q<sup>C</sup>V<sup>F</sup>T<sup>T</sup>I<sup>Q</sup>N<sup>K</sup>G<sup>D</sup>P<sup>I</sup> 1210



*H. sapiens*: NWD1 E<sup>T</sup>A<sup>V</sup>F<sup>G</sup>T<sup>E</sup>NN<sup>L</sup>I<sup>T</sup>GS<sup>L</sup>D<sup>A</sup>L<sup>I</sup>Q<sup>V</sup>NS<sup>L</sup>SE<sup>Q</sup>GT<sup>L</sup>LD<sup>L</sup>Z<sup>L</sup>EG<sup>V</sup>G<sup>A</sup>P<sup>V</sup>SL<sup>L</sup>A-RG<sup>A</sup>L<sup>V</sup>AS<sup>A</sup>SP<sup>Q</sup>SS<sup>S</sup>FK<sup>V</sup>W<sup>D</sup>LS 1200  
*M. musculus*: NWD1 E<sup>T</sup>AV<sup>L</sup>GP<sup>E</sup>NN<sup>L</sup>I<sup>T</sup>GS<sup>R</sup>D<sup>A</sup>L<sup>I</sup>Q<sup>V</sup>NS<sup>L</sup>SE<sup>Q</sup>GT<sup>L</sup>LL<sup>N</sup>V<sup>L</sup>EG<sup>V</sup>G<sup>A</sup>P<sup>V</sup>SL<sup>L</sup>V-RG<sup>T</sup>L<sup>V</sup>VS<sup>A</sup>SR<sup>K</sup>SS<sup>S</sup>FK<sup>V</sup>W<sup>D</sup>DL<sup>K</sup> 1200  
*D. rerio*: NWD1 LC<sup>A</sup>VS<sup>N</sup>SE<sup>G</sup>SE<sup>I</sup>IT<sup>S</sup>A<sup>Q</sup>DR<sup>I</sup>IR<sup>V</sup>WS<sup>V</sup>TT-GAL<sup>L</sup>D<sup>W</sup>I<sup>G</sup>VM<sup>D</sup>SS<sup>V</sup>SL<sup>A</sup>-VH<sup>O</sup>R<sup>F</sup>I<sup>S</sup>AS<sup>V</sup>I<sup>N</sup>Q<sup>L</sup>K<sup>V</sup>W<sup>Q</sup>LD 1239  
*D. melanogaster*: GH04922 S<sup>C</sup>L<sup>K</sup>F<sup>A</sup>P<sup>N</sup>GE<sup>F</sup>L<sup>A</sup>T<sup>G</sup>SE<sup>D</sup>R<sup>L</sup>V<sup>H</sup>I<sup>W</sup>N<sup>L</sup>AL<sup>G</sup>-E<sup>I</sup>C<sup>N</sup>S<sup>F</sup>K<sup>G</sup>H<sup>T</sup>AP<sup>V</sup>V<sup>K</sup>V<sup>V</sup>LV<sup>M</sup>DS<sup>L</sup>RV<sup>I</sup>ST<sup>D</sup>R<sup>S</sup>M<sup>L</sup>L<sup>V</sup>W<sup>M</sup>HA<sup>Q</sup> 1326  
*C. elegans*: QUI-1 T<sup>C</sup>R<sup>I</sup>YS<sup>V</sup>DS<sup>Q</sup>Y<sup>C</sup>IS<sup>G</sup>NO<sup>A</sup>GC<sup>I</sup>L<sup>I</sup>LD<sup>A</sup>Q<sup>N</sup>G-V<sup>V</sup>RE<sup>L</sup>FM<sup>H</sup>SS<sup>E</sup>V<sup>L</sup>S<sup>I</sup>MS<sup>L</sup>V-H<sup>N</sup>K<sup>M</sup>IS<sup>C</sup>DI<sup>Q</sup>G<sup>M</sup>I<sup>W</sup>EL<sup>F</sup> 1278

WD40 repeat domain



*H. sapiens*: NWD1 DA<sup>H</sup>RS<sup>R</sup>V<sup>P</sup>AP<sup>F</sup>LD<sup>R</sup>T<sup>G</sup>L<sup>T</sup>AV<sup>S</sup>H<sup>N</sup>GS<sup>Y</sup>V<sup>Y</sup>FP<sup>K</sup>I<sup>G</sup>D<sup>N</sup>K<sup>N</sup>K<sup>V</sup>T<sup>I</sup>W<sup>D</sup>LA<sup>E</sup>GE<sup>E</sup>---Q<sup>D</sup>SL<sup>D</sup>T<sup>S</sup>SE<sup>I</sup>IR<sup>C</sup>LE<sup>V</sup>AE<sup>Q</sup>R 1267  
*M. musculus*: NWD1 S<sup>T</sup>KK<sup>L</sup>QS<sup>P</sup>TP<sup>F</sup>LD<sup>R</sup>T<sup>G</sup>L<sup>A</sup>AV<sup>S</sup>H<sup>H</sup>GS<sup>F</sup>V<sup>Y</sup>FP<sup>K</sup>V<sup>G</sup>D<sup>N</sup>K<sup>N</sup>K<sup>V</sup>T<sup>I</sup>W<sup>D</sup>LA<sup>E</sup>GE<sup>E</sup>---Q<sup>D</sup>CL<sup>D</sup>T<sup>S</sup>NE<sup>V</sup>RC<sup>L</sup>EV<sup>A</sup>E<sup>Q</sup>A 1267  
*D. rerio*: NWD1 H<sup>N</sup>T<sup>L</sup>HR<sup>N</sup>KS<sup>F</sup>IP<sup>A</sup>Y<sup>C</sup>PL<sup>A</sup>VL<sup>S</sup>SK<sup>D</sup>GD<sup>T</sup>V<sup>F</sup>V<sup>K</sup>E<sup>G</sup>N<sup>K</sup>TE<sup>V</sup>F<sup>T</sup>W<sup>S</sup>C<sup>S</sup>E<sup>G</sup>L<sup>Q</sup>---L<sup>D</sup>SM<sup>D</sup>V<sup>S</sup>SE<sup>V</sup>CV<sup>C</sup>MEL<sup>A</sup>Q<sup>Q</sup>K 1306  
*D. melanogaster*: GH04922 S<sup>G</sup>N<sup>L</sup>L<sup>Q</sup>T---IQ<sup>G</sup>PY<sup>K</sup>LS<sup>V</sup>T<sup>N</sup>N<sup>M</sup>RF<sup>A</sup>V<sup>S</sup>T<sup>N</sup>GD<sup>N</sup>T<sup>L</sup>K<sup>I</sup>W<sup>S</sup>L<sup>T</sup>Q<sup>E</sup>D---K<sup>Y</sup>SV<sup>S</sup>H<sup>S</sup>DE<sup>I</sup>TC<sup>F</sup>E<sup>I</sup>S<sup>A</sup>DS 1388  
*C. elegans*: QUI-1 G<sup>D</sup>DD<sup>T</sup>PE<sup>M</sup>V<sup>A</sup>-T<sup>G</sup>V<sup>K</sup>PP<sup>I</sup>F<sup>V</sup>PP<sup>T</sup>GR<sup>I</sup>M<sup>V</sup>G<sup>H</sup>C<sup>S</sup>LS<sup>N</sup>K<sup>E</sup>M<sup>K</sup>I<sup>W</sup>AF<sup>P</sup>EE<sup>G</sup>PP<sup>V</sup>TR<sup>A</sup>KL<sup>S</sup>H<sup>S</sup>DE<sup>I</sup>TC<sup>F</sup>AT<sup>S</sup>PK<sup>G</sup> 1347



## Appendix 4 - Neuropeptides expressed in AQR, PQR and URX

gene name	tpm
<b>Insulin-like peptides</b>	
<i>daf-28</i>	10.68
<i>ins-18</i>	102.55
<i>ins-19</i>	9.32
<i>ins-24</i>	6.43
<i>ins-25</i>	12.59
<i>ins-26</i>	8.00
<i>ins-27</i>	43.52
<i>ins-29</i>	158.85
<i>ins-3</i>	1312.29
<i>ins-33</i>	6.71
<i>ins-4</i>	33.22
<i>ins-6</i>	10.98
<b>FMRFamide Peptide</b>	
<i>flp-1</i>	32.64
<i>flp-11</i>	689.25
<i>flp-12</i>	91.72
<i>flp-13</i>	8.27
<i>flp-14</i>	18840.46
<i>flp-15</i>	3383.21
<i>flp-16</i>	43.35
<i>flp-17</i>	5.44
<i>flp-19</i>	7244.73
<i>flp-2</i>	34.87
<i>flp-20</i>	23.43
<i>flp-21</i>	107.13
<i>flp-22</i>	26.37
<i>flp-24</i>	10.32
<i>flp-27</i>	19.14
<i>flp-28</i>	30.83

gene name	tpm
<i>flp-3</i>	16.02
<i>flp-32</i>	8.82
<i>flp-34</i>	7.43
<i>flp-4</i>	16.45
<i>flp-5</i>	2359.02
<i>flp-6</i>	56.04
<i>flp-7</i>	99.91
<i>flp-8</i>	255192.09
<i>flp-9</i>	7310.90
<b>Neuropeptide-like protein</b>	
<i>nlp-1</i>	199.18
<i>nlp-10</i>	16.58
<i>nlp-11</i>	754.12
<i>nlp-13</i>	9.19
<i>nlp-14</i>	58.69
<i>nlp-15</i>	78.68
<i>nlp-16</i>	15.07
<i>nlp-18</i>	67.63
<i>nlp-20</i>	5.01
<i>nlp-21</i>	3582.86
<i>nlp-24</i>	8.37
<i>nlp-27</i>	52.95
<i>nlp-28</i>	12.23
<i>nlp-3</i>	16.53
<i>nlp-33</i>	38.36
<i>nlp-36</i>	16.70
<i>nlp-40</i>	18.60
<i>nlp-41</i>	26.91
<i>nlp-43</i>	955.09
<i>nlp-45</i>	12.93
<i>nlp-46</i>	27.90

gene name	tpm
<i>nlp-47</i>	231.86
<i>nlp-50</i>	4427.65
<i>nlp-54/trh-1</i>	8.63
<i>nlp-56</i>	30.16
<i>nlp-57</i>	386.56
<i>nlp-58</i>	8.91
<i>nlp-59</i>	91.45
<i>nlp-63</i>	13.05
<i>nlp-64</i>	14.26
<i>nlp-65/msrp-7</i>	23.99
<i>nlp-66</i>	303.74
<i>nlp-7</i>	26.11
<i>nlp-71</i>	22.52
<i>nlp-73</i>	23.81
<i>nlp-74/pdf-1</i>	808.33
<i>nlp-76</i>	10.55
<i>nlp-77</i>	143.39
<i>nlp-80</i>	90.97

## Appendix 5 - Neuropeptide receptors expressed in AQR, PQR and URX

Gene name	tpm
<b>Neuropeptide Y(npr)/RFamide receptors group</b>	
<i>npr-1</i>	37.95
<i>npr-2</i>	103.12
<i>npr-3</i>	19.31
<i>npr-8</i>	7.82
<i>npr-10</i>	25.20
<i>npr-12</i>	72.29
<i>npr-13</i>	6.64
<i>npr-5</i>	7.24
<i>npr-6</i>	42.48
<i>frpr-2</i>	9.81
<i>frpr-3</i>	9.03
<i>frpr-6</i>	60.39
<i>frpr-17</i>	8.20
<i>frpr-19</i>	9.09
<i>daf-37</i>	6.03
<b>Somatostatin and galanin-like receptors group</b>	
<i>npr-16</i>	210.25
<i>npr-17</i>	61.95
<i>npr-18</i>	81.91
<i>npr-25</i>	23.11
<i>npr-26</i>	298.61
<i>npr-29</i>	34.51
<i>npr-32</i>	10.32

Gene name	tpm
<b>Tachykinin (Neurokinin) receptor-like group</b>	
<i>tkr-1</i>	22.12
<i>npr-15</i>	5.94
<i>npr-21</i>	34.54
<i>npr-22</i>	5.49
<b>Gastrin/Cholecystokinin (CCK)-like receptors group</b>	
<i>ckr-1</i>	7.89
<i>ckr-2</i>	11.29
<b>Gonadotropin releasing hormone, oxytocin, vasopressin-like receptors group</b>	
<i>gnrr-2</i>	60.10
<i>daf-38</i>	49.45
<b>Neurotensin, neuromedin U, growth hormone secretagogue, thyrotropin releasing hormone (TRH)-like receptors group</b>	
<i>nmur-1</i>	32.36
<i>dmsr-1</i>	63.21
<i>egl-6</i>	105.92
<i>spr-2</i>	41.74

<b>Gene name</b>	<b>tpm</b>
<i>spr-3</i>	28.08
<i>frpr-7</i>	22.38
<i>aexr-3</i>	5.63
<i>npr-19</i>	54.34
<b>Class B/Secretin Family of GPCRs</b>	
lat-1	18.69
pdfr-1	93.84
<b>Insulin/IGF receptor- like proteins</b>	
daf-2	14.20

## Appendix 6 -Strain list

Strain code	Genotype	Notes
AX522	<i>wrt-6 (db102) X</i>	
AX523	<i>db103</i>	
AX524	<i>qui-1 (db104) IV</i>	
AX532	<i>db107</i>	
AX538	<i>dgk-1 (db106) X; fig-1 (db1239) V</i>	
AX540	<i>npr-1( db108) X</i>	
AX1177	<i>flp-21 (pk1601); npr-1 (db64) X</i>	
AX1178	<i>flp-21 (pk1601); npr-1 (db68) X</i>	
AX1258	<i>flp-21 (pk1601); npr-1 (db1223) X</i>	
AX1287	<i>flp-21 (pk1601); db1219</i>	
AX1289	<i>flp-21 (pk1601); npr-1 (1224) X</i>	
AX1290	<i>flp-21 (pk1601); db1220 V</i>	
AX1292	<i>flp-21 (pk1601); db1221</i>	
AX1293	<i>flp-21 (pk1601); npr-1 (db1247) X</i>	
AX1294	<i>flp-21 (pk1601); npr-1 (db1222) X</i>	
AX1888	<i>npr-1(ad609) X; ials25[gcy-37p:gfp; unc-119(+)]</i>	
AX6545	<i>db107 ox4</i>	
AX6548	<i>db1219 ox4</i>	
AX6552	<i>dgk-1 (db106) X ox4</i>	
AX6758	<i>db1220 V ox4</i>	
AX6946	<i>dgk-1 (db106) dbEx1017 [dgk-1 fosmid; unc-122p:gfp]</i>	
AX6950	<i>db1221 ox4</i>	
AX6954	<i>qui-1 (db104) IV ox4</i>	
AX7164	<i>qui-1 (db104) IV; dbEx1062[fosmid qui-1; unc-122p:gfp]</i>	
AX7169	<i>wrt-6 (db102) X ox4</i>	
AX7176	<i>fig-1 (db1239) AX538 ox4 not dgk-1</i>	

Strain code	Genotype	Notes
AX7246	<i>qui-1 (db104) IV; Ex[sra-6p:qui-1; unc-122p:gfp]</i>	Original line was a kind gift from Sengupta Lab
AX7247	<i>qui-1 (db104) IV; Ex[ sre-1(delta)p:qui-1; unc-122p:gfp]</i>	Original line was a kind gift from Sengupta Lab
AX7248	<i>qui-1 (db104) IV; Ex[sra-6p;qui-1; sre-1(delta)p:qui-1; unc-122p:gfp]</i>	Original line was a kind gift from Sengupta Lab
AX7249	<i>qui-1 (db104) IV; Ex[qui-1 gDNA; unc-122p:gfp]</i>	Original line was a kind gift from Sengupta Lab
AX7287	<i>qui-1 (db104) IV; ftIs25[srh-220p:daf-28-mCherry; myo-2p:gfp; unc-122p:gfp]</i>	
AX7288	<i>ftIs25[srh-220p:daf-28-mCherry; myo-2p:gfp; unc-122p:gfp]</i>	Original line was a kind gift from Ashrafi Lab
AX7290	<i>bbs-7 (n1606) III; ftIs25[srh-220p:daf-28-mCherry; myo-2p:gfp; unc-122p:gfp]</i>	
AX7356	<i>wrt-6 (db102) X; ftIs25[srh-200p:daf-28-mCherry; myo-2p:gfp; unc-122p:gfp]</i>	
AX7357	<i>fig-1 (db1239) V; ftIs25[srh-200p:daf-28-mCherry; myo-2p:gfp; unc-122p:gfp]</i>	
AX7367	<i>qui-1 (db104) IV; ftIs25[srh-200p:daf-28-mCherry; myo-2p:gfp; unc-122p:gfp]; Ex[deltasre-1p:qui-1;unc-122p:gfp]</i>	
AX7383	<i>npr-1 (ad609) X; gcy-36 (db42) X; gcy-35 (ok769) I; ialS25[gcy-37p:gfp; unc-119(+)]</i>	
AX7460	<i>wrt-6 (db102) X; dbEx1081[ wrt-6 fosmid; unc-122p:gfp]</i>	
AX7461	<i>fig-1 (db1239) V; dbEx1082[ fig-1 fosmid; unc-122p:gfp]</i>	
AX7468	<i>npr-1(ad609) X; lin-15(n765ts) X; qui-1(db104) IV; dbEx [ncs-1p:Cre; flp-21p:LoxPSTOPLoxP:npr-1(215V):SL2-gfp; lin-15(+)]; ftIs25[srh-220p:daf-28-mCherry; myo-2p:gfp; unc-122p:gfp]</i>	
AX7477	<i>unc-13 (e51) I; ftIs25[srh-200p:daf-28-mCherry; myo-2p:gfp; unc-122p:gfp]</i>	
AX7478	<i>unc-13 (e51) I; qui-1 (db104) IV; ftIs25[srh-220p:daf-28-mCherry; myo-2p:gfp; unc-122p:gfp]</i>	
AX7499	<i>gcy-35(ok769) I; qui-1(db104) IV; ftIs25[srh-220p:daf-28-mCherry; myo-2p:gfp; unc-122p:gfp]</i>	
AX7500	<i>npr-1(ad609) X; lin-15(n765ts) X; dbEx[ncs-1p:Cre; flp-21-:LoxPSTOPLoxP:npr-1(215V):SL2gfp; lin-15(+)]; ftIs25[srh-220p:daf-28-mCherry; myo-2p:gfp; unc-122p:gfp]</i>	
AX7501	<i>npr-1(ad609) X; lin-15(n765ts) X; ftIs25[srh-220p:daf-28-mCherry; myo-2p:gfp; unc-122p:gfp]</i>	
AX7505	<i>qui-1(db104) IV; daf-7(e1372) III</i>	
	<i>dbEx614[gcy-37p::YC2.60::unc-54 3' UTR; unc-122p:rfp]</i>	

Strain code	Genotype	Notes
	<i>db107; dbEx614[gcy-37p::YC2.60::unc-54 3' UTR; unc-122p:rfp]</i>	
	<i>db1221; dbEx614[gcy-37p::YC2.60::unc-54 3' UTR; unc-122p:rfp]</i>	
	<i>dgk-1 (db106) X; dbEx614[gcy-37p::YC2.60::unc-54 3' UTR; unc-122p:rfp]</i>	
	<i>dbEx637[ncs-1p::Cre; pflp-21::loxPstoploxP::YC2.60 unc-122p:rfp]</i>	
	<i>dgk-1 (db106) X; dbEx637[ncs-1p::Cre; pflp-21::loxPstoploxP::YC2.60 unc-122p:rfp]</i>	
	<i>db1220 V; dbEx637[ncs-1p::Cre; pflp-21::loxPstoploxP::YC2.60 unc-122p:rfp]</i>	
	<i>db1221; dbEx637[ncs-1p::Cre; pflp-21::loxPstoploxP::YC2.60 unc-122p:rfp]</i>	
	<i>db107; dbEx637[ncs-1p::Cre; pflp-21::loxPstoploxP::YC2.60 unc-122p:rfp]</i>	
	<i>db1220; dbEx614[gcy-37p::YC2.60::unc-54 3' UTR; unc-122p:rfp]</i>	
	<i>qui-1 (db104) IV; dbEx637[ncs-1p::Cre; pflp-21::loxPstoploxP::YC2.60 unc-122p:rfp]</i>	
	<i>qui-1 (db104) IV; dbEx614[gcy-37p::YC2.60::unc-54 3' UTR; unc-122p:rfp]</i>	
	<i>wrt-6 (db102) X; dbEx614[gcy-37p::YC2.60::unc-54 3' UTR; unc-122p:rfp]</i>	
	<i>fig-1 (db1239) V; dbEx614[gcy-37p::YC2.60::unc-54 3' UTR; unc-122p:rfp]</i>	
	<i>wrt-6 (db102) X; dbEx637[ncs-1p::Cre; pflp-21::loxPstoploxP::YC2.60 unc-122p:rfp]</i>	
	<i>fig-1 (db1239) V; dbEx637[ncs-1p::Cre; pflp-21::loxPstoploxP::YC2.60 unc-122p:rfp]</i>	
MX52	<i>bbs-8(nx77)V</i>	
VC1569	<i>bbs-2(ok2053) IV</i>	
VC837	<i>bbs-1(ok1111) I</i>	
VC1168	<i>bbs-2(gk544) IV</i>	
VC1062	<i>bbs-9(gk471) I.</i>	
MT3645	<i>osm-12(n1606) III</i>	
CB1372	<i>daf-7(e1372) III</i>	

